Molecular and functional characterization of the *swiss-cheese* and *olk* mutants in *Drosophila melanogaster*

Two approaches to killing neurons

Dissertation zur Erlangung des naturwissenschaftlichen Doktorgrades der bayerischen Julius-Maximilians-Universität Würzburg

vorgelegt von:

Alexandre Bettencourt da Cruz

aus München

Würzburg, 2006

Eingereicht am: .....

Mitglieder der Promotionskommission:

Vorsitzender: Prof. Dr. Martin Müller

Gutachter : Prof Dr. Erich Buchner

Gutachter: Prof. Dr. Doris Kretzschmar

Tag des Promotionskolloquiums: .....

Doktorurkunde ausgehändigt am: .....

Erklärung gemäß §4 der Promotionsordnung für die Fakultät für Biologie der Bayrischen Julius-Maximilians-Universität Würzburg vom 15. März 1999:

Hiermit erkläre ich, daß ich die vorliegende Dissertation selbstständig angefertigt habe und keine anderen Hilfsmittel als die angegebenen angewandt habe. Alle aus der Literatur entnommenen Stellen und Abbildungen sind als solche kenntlich gemacht.

Die Dissertation wurde weder vollständig noch teilweise an einer anderen Fakultät vorgelegt.

Portland, den 27. Februar 2006

Alexandre Bettencourt da Cruz

Contents

ZUSAMMENFASSUNG **6**

SUMMARY **9**

INTRODUCTION **11**

swiss cheese (sws) 12

The Drosophila sws mutant *12*

The vertebrate SWS orthologue NTE *14*

Structure and function of SWS *15*

The serine esterase domain 15

The cAMP binding and protein interaction domain 16

Transmembrane domains 16

Organophosphate induced delayed neuropathy (OPIDN) *17*

Intoxication of NTE as cause for OPIDN 17

The aging reaction 18

olk 20

MAP1B *21*

futsch *22*

The olk mutant *22*

MATERIAL & METHODS **24**

Material 24

Fly strains *24*

sws-alleles *25*

Antibodies *25*

Primer *25*

Plasmid vectors *28*

Yeast two hybrid *28*

Methods 29

Molecular standard methods *29*

Site-directed mutagenesis *29*

Sequencing *29*

Fusion protein expression & antibody production *29*

Lipid and sterol content measurements *29*

Histological methods *29*

Paraffin sections 30

Cryostat sections 30

Immunohistochemistry 30

X-Gal stainings 30

Creation of transgenic Drosophila flies *30*

RESULTS **31**

A- sws 31

A.1- Production of a Drosophila SWS antibody *31*

A.1.1- Specificity of the α-SWS antibody on histological sections 32

A.1.2- Specificity of the α-SWS antibody on western blots 34

A.2- Expression pattern *34*

A.2.1- Subcellular localization 37

A.3- Interaction of PKA-C3 with SWS *38*

A.3.1- Yeast two hybrid screens 38

A.3.1.1- Proteins identified 40

A.3.2- Genetic interactions 42

A.3.2.1- Genetic interactions with Deficiencies in the pka-c3 region 42

A.3.2.2- Deletion mutant for pka-c3 ... 42
A.3.2.3- Genetic interaction using a UAS-pka-c3 construct ... 43
A.4- Analysis of functional domains of the SWS protein ... 44
A.4.1- The wt SWS construct ... 45
A.4.2- The protein interaction domain ... 47
A.4.2.1- Overexpression of SWS-R^{133}A ... 48
A.4.3- The cAMP binding domain ... 48
A.4.3.1- Overexpression of SWS-G^{557}Q ... 50
A.4.4- Esterase independent function of SWS ... 51
A.4.4.1- Function of the 80 N-terminal amino acids ... 51
A.4.4.1.1- Mutation of the catalytic site serine ... 53
A.4.4.1.2- Combination of the Δaa1-80 deletion and S^{985}D mutation (SWSΔ1-80/ S^{985}D) ... 54
A.4.4.2- Detailed analysis of the functional domains in the 80 N-terminal amino acids ... 56
A.4.4.2.1- Deletion of the first TM (SWSΔ33-55) ... 57
A.4.4.2.2- Combination of the Δaa33-55 deletion and S^{985}D mutation (SWSΔ33-55/ S^{985}D) ... 57
A.4.4.2.3- Deletion of the first 35 amino acids (SWSΔ1-35) ... 58
A.4.4.2.4- Combination of the Δaa1-35 deletion and S^{985}D mutation (SWSΔ1-35/ S^{985}D) ... 60
A.5- Influence of SWS on the lipid metabolism ... 60
A.5.1- Lipid and sterol measurements ... 60
A.5.2- Genetic interaction with enzymes catalyzing transacylations ... 62
B- olk ... 64
B.1- The olk phenotype ... 64
B.1.1- Anatomical defects in specific brain areas ... 64
B.1.2- Selective degeneration of projection neurons ... 66
B.1.3- Olfactory memory defects in the *olk* mutant ... 67
B.2- Molecular characterization of the olk mutant ... 69
B.2.1- Mapping and identification of the *olk* mutation ... 69
B.2.2- Genomic sequencing of the mutant *futsch* gene ... 70
B.2.3- Western blot analysis of the *olk* mutant ... 71
B.3- Alterations in the cytoskeletal structure of olk mutants ... 72
B.3.1- Tubulin organization differences between *olk* and wt ... 72
B.3.2- Upregulation of tubulin in *olk* ... 73
B.3.3- Reduced rate of transport in *olk* mutants ... 75
B.4- Interactions of futsch with other genes ... 77
B.4.1- Expression pattern of *futsch* ... 77
B.4.2- Interaction of *futsch* with *dfmr1* ... 78
B.4.3- Tau has partially overlapping functions with *futsch* ... 80
DISCUSSION ... 81
sws ... 81
Subcellular SWS localization ... 81
Functional domains of SWS ... 81
Physiological function of SWS in vivo ... 84
olk ... 87
BIBLIOGRAPHY ... 91
FIGURES ... 99
ABBREVIATIONS ... 100
ACKNOWLEDGEMENT ... 101
LIST OF PUBLICATIONS ... 103
Publications relevant to this thesis ... 103
Further publications ... 103

Zusammenfassung

In dieser Arbeit werden zwei neurodegenerative Mutanten in *Drosophila* beschrieben. Zum einen drei Allele des *futsch* Gens namens *olk* (*omb-like*). *futsch* wurde bereits als Mikrotubuli assoziertes Protein (MAP) beschrieben und ist als MAP1B Ortholog identifiziert worden. Zum anderen *sws* (*swiss cheese*), eine Serinesterase, deren Funktion im Nervensystem noch unbekannt ist.

In *sws* mutanten Fliegen ist Vakuolisierung im gesamten Gehirn sichtbar, es handelt sich um einen generellen, progressiven, neurodegenerativen Phänotyp. Neuronale Apoptose wie auch multiple Membranhüllen um Gliazellen sind für die *sws* Mutanten charakteristisch. Die biologische Funktion von SWS innerhalb des Nervensystems ist bisher noch nicht geklärt. Vertebraten, die für das *sws* Ortholog NTE (neuropathy target esterase) mutant sind, zeigen einen ähnlichen Phänotyp wie *sws* mutante Fliegen. Auch Vergiftung von NTE mit Organophosphaten kann zu axonaler Degeneration führen. Dabei ist jedoch die Inhibition von NTE nicht ausreichend um die Axondegeneration hervorzurufen. Eine weitere Reaktion, die sogenannte "Aging reaction" is notwendig um die paralysierende Wirkung auszulösen. Eine These besagt, dass NTE eine zweite, von der Esterasefunktion unabhängige Funktion ("Nicht-Esterase" Funktion) besitzt, die diese Wirkung auslöst.

Zur Aufklärung der physiologischen Funktion von SWS wurden verschiedene transgene Fliegenlinien etabliert. Diese produzieren verschiedene, mutierte Formen des SWS Proteins, dessen Expression mit Hilfe des GAL4/ UAS Systems genau gesteuert werden kann. Diese Methode erlaubt eine eingehende Untersuchung einzelner Proteindomänen, die in den jeweiligen Konstrukten verändert waren. Insbesondere die Charakterisierung der möglichen "Nicht-Esterase" Funktion war von Interesse. Eine bereits beschriebene mutante Form des SWS Proteins, dem die ersten 80 Aminosäuren fehlen (SWSΔ1-80), zeigte einen dominanten degenerativen Effekt. Die Überexpression von SWSΔ1-80 führt, wie auch die Vergiftung mit bestimmten Organophosphaten, zur Degeneration der betroffenen Zellen und wurde deshalb als Modell für Organophosphatvergiftung herangezogen. Es konnte gezeigt werden, dass dieses

Konstrukt auch dann einen schädlichen Effekt zeigt, wenn die katalytische Serinesterasefähigkeit durch Mutation entfernt wurde. Dies deutet die Möglichkeit an, dass SWS eine, von der Esteraseaktivität unhabhängige, Funktion ausüben kann.

Ein Vergleich des Lipidgehalts von *sws* Mutanten mit wt und SWS überexprimierenden Fliegen gab wertvolle Hinweise auf eine mögliche biologische Funktion von SWS. Der Gehalt an Phosphatidylcholin, ein Hauptbestandteil von Zellmembranen, scheint in *sws* Mutanten erhöht zu sein, während es in SWS überexprimierenden Fliegen in geringeren Mengen zu finden ist. Dies weist darauf hin, dass SWS an der Phosphatidylcholinregulation beteiligt sein könnte.

Der in dieser Arbeit hergestellte α-SWS Antikörper ermöglichte eine genauere intrazelluläre Lokalisation des SWS Proteins. Doppelfärbungen mit einem ER (Endoplasmatisches Retikulum) Marker zeigen, dass ein grosser Anteil von SWS im ER zu finden ist. Dies stimmt mit den kürzlich veröffentlichten Ergebnisse zur Lokalisation von SWS/ NTE in Hefe- und Mauszellen überein.

Die *olk* Mutante zeigt ebenfalls progressive Neurodegeneration, die Effekte sind jedoch lokaler, insbesondere das olfaktorische System und die Pilzkörper sind betroffen. Die Projektionsneurone (PN) degenerieren in dieser Mutante innerhalb von etwa 20 Tagen. Noch vor der histologisch sichtbaren Degeneration ist bereits ein Verhaltensphänotyp erkennbar, der sich in schlechter, olfaktorischen Lernleistung äussert. Projektionsneurone verbinden die Antennalloben und die Pilzkörper, die als "Lernzentren" gelten, daher entspricht ein Lerndefekt den Erwartungen.

Die drei *olk* Mutanten (olk^{1-3}) wurden durch Komplementationstests mit dem publizierten $futsch^{N94}$ Allel als weitere *futsch* Allele identifiziert. In olk^{1} zeigte die Sequenzierung der kodierenden Sequenz eine Mutation, die frühzeitig zu einem Stopcodon im Protein führt.

Die Degenerationserscheinungen in der Mutanten sind vermutlich auf Defekte im Mikrotubulinetzwek und axonalen Transport zurück zu führen. In histologischen Gehirnschnitten sind Veränderungen im Zytoskelett zu beobachten und Western Blots deuten auf einen erhöhten Tubulingehalt in der olk^{1} Mutante hin. Für die Entwicklung von

Axonen und Dendriten ist ein intaktes Zytoskelett unentbehrlich. Transportprozesse sind in *olk*^{1} Mutanten ebenso betroffen, insbesondere ist der mitochondriale Transport reduziert.

Das *fragile X mental retardation* Gen (*dfmr1*) interagiert mit der *olk* Mutante, so dass eine *dfmr1*/ *olk*^{1} Doppelmutante einen weniger starken Phänotyp zeigt als die *olk*^{1} Mutante. *tau*, ein weiteres MAP Gen, besitzt ebenso die Fähigkeit den *olk*^{1} Phänotyp partiell zu suprimieren.

Summary

In this thesis two genes involved in causing neurodegenerative phenotypes in *Drosophila* are described. *olk* (*omb-like*), a *futsch* allele, is a micotubule associated protein (MAP) which is homologous to MAP1B and *sws* (swiss cheese) a serine esterase of yet unknown function within the nervous system. The lack of either one of these genes causes progressive neurodegeneration in two different ways.

The *sws* mutant is characterized by general degeneration of the adult nervous system, glial hyperwrapping and neuronal apoptosis. Deletion of NTE (neuropathy target esterase), the SWS homolog in vertebrates, has been shown to cause a similar pattern of progressive neural degeneration in mice. NTE reacts with organophosphates causing axonal degeneration in humans. Inhibition of vertebrate NTE is insufficient to induce paralyzing axonal degeneration, a reaction called "aging reaction" is necessary for the disease to set in. It is hypothesized that a second "non-esterase" function of NTE is responsible for this phenomenon. The biological function of SWS within the nervous system is still unknown.

To characterize the function of this protein several transgenic fly lines expressing different mutated forms of SWS were established. The controlled expression of altered SWS protein with the GAL4/UAS system allowed the analysis of isolated parts of the protein that were altered in the respective constructs. The characterization of a possible non-esterase function was of particular interest in these experiments. One previously described aberrant SWS construct lacking the first 80 amino acids (SWSΔ1-80) showed a deleterious, dominant effect when overexpressed and was used as a model for organophosphate (OP) intoxication. This construct retains part of its detrimental effect even without catalytically active serine esterase function. This strongly suggests that there is another characteristic to SWS that is not defined solely by its serine esterase activity.

Experiments analyzing the lipid contents of *sws* mutant, wildtype (wt) and SWS over-expressing flies gave valuable insights into a possible biological function of SWS. Phosphatidylcholine, a major component of cell membranes, accumulates in *sws*

mutants whereas it is depleted in SWS overexpressing flies. This suggests that SWS is involved in phosphatidylcholine regulation.

The produced α-SWS antibody made it possible to study the intracellular localization of SWS. Images of double stainings with ER (endoplasmic reticulum) markers show that SWS is in great part localized to the ER. This is consistent with findings of SWS/ NTE localization in yeast and mouse cells.

The *olk* mutant also shows progressive neurodegeneration but it is more localized to the olfactory system and mushroom bodies. Regarding specific cell types it seemed that specifically the projection neurons (PNs) are affected. A behavioral phenotype consisting of poor olfactory memory compared to wt is also observed even before histologically visible neurodegeneration sets in. Considering that the projection neurons connect the antennal lobes to the mushroom bodies, widely regarded as the "learning center", this impairment was expected.

Three mutants where identified (olk^{1-3}) by complementation analysis with the previously known $futsch^{N94}$ allele and sequencing of the coding sequence of olk^{1} revealed a nonsense mutation early in the protein.

Consistent with the predicted function of Futsch as a microtubule associated protein (MAP), abnormalities are most likely due to a defective microtubule network and defects in axonal transport. In histological sections a modified cytoskeletal network is observed and western blots confirm a difference in the amount of tubulin present in the olk^{1} mutant versus the wt. The elaboration of neuronal axons and dendrites is dependent on a functional cytoskeleton. Observation of transport processes in primary neural cultures derived from olk^{1} mutant flies also showed a reduction of mitochondrial transport.

Interaction with the *fragile X mental retardation* gene (*dfmr1*) was observed with the *olk* mutant. A *dfmr1*/ olk^{1} double mutant shows an ameliorated phenotype compared to the olk^{1} single mutant. *tau*, another MAP gene, was also shown to be able to partially rescue the olk^{1} mutant.

Introduction

Neurodegenerative diseases in humans often have devastating clinical symptoms including cognitive and memory loss and movement disorders like tremors and ataxia. The continuous loss of the defining characteristics of an individual puts an immense emotional burden on relatives, friends and other caregivers. The risk for acquiring a senile dementia increases with age, the prevalence rate for individuals aged 65 or more is 7% with the risk doubling every five years after age 65 (McDowell 2001). With increasing life expectancy in western society it also takes a heavy toll on society in its entirety as the health care system is jeopardized by rising health care costs. There are more than 600 neurological disorders affecting about 50 million patients per year in the United States alone (Brown et al. 2005). The costs are estimated to be in the billions of dollars, with an estimated $100,000,000,000 per year spend on Alzheimer disease alone in the United States (Meek et al. 1998).

Age is not the only risk factor to be considered in the study of cognitive diseases. Known risk factors also include polymorphisms, oxidative stress and chemical exposure. In our modern society we are exposed to a high variety of substances with unknown toxicity. Unfortunately cures and treatments are rare, while pressure on science to find new ways to fight these diseases increases.

Due to ethical and scientific limitations in studying the human brain and its aging processes, the mechanisms underlying neurodegenerative diseases have mostly been elucidated in animal models before the resulting models were tested in humans. Due to its many advantages *Drosophila* has proven to be an excellent model system for neurodegenerative disease. Benefits of *Drosophila* as model system include a faster time frame due to the shorter life span, flies produce a large number of progeny, many techniques and tools for manipulation of gene expression are already available (Matthews et al. 2005), general anatomy is well known and its genome is sequenced and published (Adams et al. 2000; Myers et al. 2000). Comparisons between eukaryotic genomes indicated that fundamental biological pathways are highly conserved (Rubin et al. 2000), highlighting another important aspect of a good model organism, the ability of transferring acquired results to humans.

Drosophila has been successfully used to model several human neurodegenerative diseases, including Huntington disease, Spinocerebellar ataxia, Fragile X mental retardation, Parkinson disease and Alzheimer disease among others (reviewed in Bilen and Bonini 2005). The Kretzschmar lab took a different approach in trying to clone and characterize neurodegenerative mutants derived from mutagenesis screens in *Drosophila* instead. This approach promises to deliver new findings about the basic mechanisms of neuronal function without prior knowledge of function or identity of previously isolated proteins. Several mutants with a progressive neurodegenerative phenotype have been identified so far.

Several *Drosophila* mutants show strikingly similar neurodegenerative pathology to mammals. The *sws* gene mutant shows a brain phenotype comparable to the mouse orthologue, the NTE mouse mutant (Akassoglou et al. 2004). However, unlike *sws* mutant flies NTE knockout mice die early in embryogenesis apparently because NTE has an essential role in placental development in mammals (Moser et al. 2004). Therefore conditional knockouts were used to study the NTE knockout in mice.

In this work two mutants with a progressive neurodegenerative phenotype, *omb-like* (*olk*) and *swiss cheese* (*sws*) are described. Although progressive neurodegeneration is visible in both these mutants, *sws* shows a general pathology in the entire brain whereas *olk* mutants display a more localized phenotype specifically affecting restricted brain areas and neurons.

swiss cheese (sws)

The *Drosophila sws* mutant

Dsws was originally isolated in a screen for anatomical brain mutants (Heisenberg and Böhl 1979) and later cloned and described by Doris Kretzschmar (Kretzschmar et al. 1997). Few days after eclosion *sws* mutant flies mutant show general, progressive neurodegeneration throughout the brain. After about seven days prominent vacuoles are visible in brain sections of these flies suggesting loss or weakening of these neurons resulting in weak tissue in those spots (Figure 1). In addition to the vacuolar phenotype glial hyperwrapping is characteristic for the *sws* mutant. Dense structures

around neurons of adult fly heads seem to originate from several layers of glial membranes. These structures are already visible at latter stages of pupal development whereas no vacuoles are visible immediately after eclosion. This suggests that *sws* is not essential in neurogenesis or *Drosophila* development in general, but is necessary for the maintenance of postmitotic cells (Kretzschmar et al. 1997).

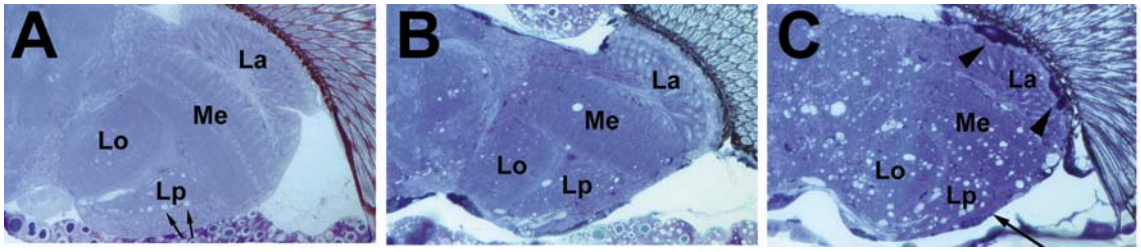

Figure 1: *sws* mutant phenotype

Progression of brain degeneration is *sws* flies. (A-C) Vacuolization and darkly stained structures (arrowheads in C) increase with advancing age. These are accompanied by a thinning of the cortex (long arrow in C). (A) wild type, age 20 d (arrows indicate white areas in the lobula plate that are not vacuoles but cross-sections of giant fibers). (B) sws^1 5 d old. (C) sws^1 20 d old. (A-C) One micrometer horizontal plastic head sections stained with toluidine blue. (modified; from Kretzschmar et al. 1997).

The two different aspects of the *sws* mutant have been shown to be dependent on the autonomous requirement of SWS in neurons as well as glial cells (Muhlig-Versen et al. 2005). The progressive neural degeneration causing vacuoles in widespread areas of the brain is rescuable by providing wild-type SWS-protein to the neurons. On the other hand glial hyperwrapping can be remedied by driving the rescue construct in glial cells. Both of these phenomena are independent of each other and rescue of one does not influence the other (Figure 13).

Further evidence for the local requirement of SWS was provided by mosaic analysis. Flies carrying heterozygous and hemizygous *sws* mutant cells display the *sws* phenotype only in the *sws* hemizygous areas of the brain. This suggests that SWS is not a diffusible factor with a long-range effect but a cell autonomous or short range protein (Kretzschmar et al. 1997).

Six Alleles of the *Drosophila sws* gene have been described and for three of these, *sws*^{1}, *sws*^{4} and *sws*^{5}, the mutation has been documented on a molecular level (Kretzschmar et al. 1997). All of the alleles show a reduced lifespan ranging from three to ten days (50% survival time) compared to 15 d for wt at 29 °C. Another allele originally identified as an olfactory mutant called *olfE* (Hasan 1990) does not show a neurodegenerative or olfactory phenotype when heterozygous over *sws*^{1} or *sws*^{2}. Two transcription units have been identified for *sws*. Either the shorter transcript is responsible for the olfactory effect only or they are two complementing alleles of the same gene locus. For most purposes in this work the *sws*^{1} allele was used. This allele has a C to A mutation at position 1124 of the ORF creating a stop-codon instead of a serine (TCG→TAG). This causes the protein to be truncated after 374 of the 1425 amino acids (aa) present in the wt protein. Presumably a truncated protein of about a fourth of the original length is synthesized. The predicted catalytic site of SWS is at aa position 985 and not present in *sws*^{1}. Unlike wt, homogenates of *sws*^{1} mutant shows no in vitro catalytic activity in a standard in vitro assay (Johnson 1977; Muhlig-Versen 2001).

Examination of the type of cell death in cells affected by lack of SWS revealed that characteristic signs of apoptotic cell death (DNA fragmentation made visible by TUNEL staining) increased progressively. This seems to apply to neurons and glia. The loss of glial cells was made visible by a glia specific enhancer trap line (rC56), which specifically expresses *lacZ* in most glial cells. The expression of this marker is lost during aging of adult flies indicating a loss or dysfunction of glial cells (Kretzschmar et al. 1997).

The vertebrate SWS orthologue NTE

Using the sequence information acquired from the cloning of the *sws* gene, its mouse orthologue was identified soon afterwards (Moser et al. 2000). Results of the cloning of the human NTE have also been published (Glynn et al. 1999). The sequencing of genomes of several other organisms showed that NTE seems to be highly conserved and orthologues are present in a variety of other species, including nematodes and yeast. A much shorter protein which shares only the catalytic domain is found in E. coli.

Plants appear to be free of SWS orthologues, however patatins, plant proteins with phospholipase activity, have homology to the catalytic domain of NTE (Lush et al. 1998).

Mouse NTE is capable of substituting for DSWS in vivo when used in transgenic constructs to rescue the phenotype of the *sws*^{1} mutant. The rescue was virtually identical to the use of *Dsws* (Muhlig-Versen et al. 2005). This indicates that *sws* and vertebrate NTE are not only conserved at a sequence level, but are also similar in their catalytical and biological properties. Reports of NTE knockout mice state that total loss of NTE is lethal at embryonic day nine (Winrow et al. 2003). However this effect was due to failed placental development. Histological analysis indicated that NTE is essential for the development of the labyrinth layer and secondary giant cells in mice (Moser et al. 2004). A neuron specific knockout showed a neurodegenerative phenotype which strongly resembled the *sws* phenotype in flies. Lack of NTE in neuronal tissues leads to prominent neuronal pathology in the hippocampus, thalamus and cerebellum. Disruption of the endoplasmic reticulum (ER), vacuolization of nerve cell bodies and abnormal reticular aggregates can also be observed (Akassoglou et al. 2004).

Structure and function of SWS

Sequence analysis of SWS suggested that it contains a serine esterase domain, a cAMP binding domain, a protein interaction domain and four transmembrane domains (TM).

The serine esterase domain

The sequence G-X-S-X-G has been described as a consensus sequence for serine esterases. This sequence is present in the amino acids G^{983} through G^{987}, making SWS a member of the very large class of serine hydrolase enzymes, which include esterases, phospholipases, amidases, peptidases and proteases. The reaction mechanism of all these enzymes involves a nucleophilic serine residue, S^{985} for SWS, that forms a covalent intermediate with the acyl moiety of the substrate which is rapidly

hydrolyzed. Interestingly the active site serine lies in a predicted TM suggesting that a hydrophilic pouch is formed to perform the hydrolization reaction.

Martin Johnson defined NTE as the proportion of the esterase activity which could be inhibited by preincubating the brain homogenate with those OPs which induce delayed neuropathy (Johnson 1969). Based on this definition an assay was developed to assess the NTE activity in vitro. By measuring rate of phenyl valerate esterase activity that is resistant to inhibition by paraoxon, but sensitive to mipafox the NTE activity can be measured according to the above definition (Johnson 1977).

The cAMP binding and protein interaction domain

Comparison of SWS to the cAMP binding and protein interaction domain of *protein kinase A* (*pka*) showed similarities between both (Figure 15).

Protein kinases play a major role in the integration of signaling networks in eukaryotic cells. The activity of the catalytic (C) subunit is regulated by a set of four different regulatory (R) subunit isoforms forming a tetramer. In the Type I holoenzyme binding between the catalytic and the regulatory subunit, RIα is primarily mediated by the protein interaction site, also called the pseudo substrate site because it binds to the catalytic site. The secondary site of interaction referred to as a peripheral docking site is comprised of residues in the cAMP binding domain A (Herberg et al. 1994). The holoenzyme is catalytically inactive and is activated by dissociation of the regulatory subunit allowing the catalytic subunit to unfold its kinase activity. The cAMP binding module found in the regulatory domains allows cells to translate an extracellular signal into a biological response.

Transmembrane domains

The TMpred structural analysis program (Hofmann and Stoffel 1993) predicts four TMs for SWS. Comparing the scores of each of the TMs to each other shows that the first TM is the most likely to act as a TM in vivo whereas TM2 is the least likely to fulfill that function. This pattern of TM prediction is also found in other species, for example the human and murine NTE as well as the *C. elegans* orthologue.

However experiments done with the mouse NTE on microsomes showed that most of the protein is cytoplasmic. Exposure of SWS to Proteinase K digestion in microsomes resulted in no detectable fragments in a western blot (Li et al. 2003). This excludes long intraluminal fragments that would have been visible in the western blot. The second predicted TM being far away from both, the first and the third TM, contradicts this model, the third and forth do not because they are very close to each other. The protected fragment would be too small to be seen in a western blot. The first TM would also not be detectable because it is very close to the N-terminus.

The DSWS might be different and these experiments on the mouse orthologue were performed on microsomes and might differ from the results in vivo. Nevertheless the working model for this thesis assumes that SWS harbors three TMs, for historical reasons labeled TM1, TM3 and TM4 (Figure 4).

Organophosphate induced delayed neuropathy (OPIDN)

In 1930, a strange new paralytic plague with symptoms similar to poliomyelitis began to be reported in the American South and Midwest. Usually the symptoms would progress over a time period of several weeks, from the lower to the upper extremities and closer to the body. Drs. E. Miles and W. H. Goldfain were the first to associate this disease to the consumption of Jamaica Ginger (hence the symptoms were also described as "Ginger Paralysis") contaminated with the OP tri-ortho-crescyl-phosphate (TOCP) (Segel 2002). Jamaica Ginger was popular at the time as a covert way of drinking alcohol during prohibition. The number of affected individuals was somewhere between 35,000 and 100,000 (Smith et al. 1930; Segel 2002). Epidemics of paralysis occurred in Marocco (Smith and Spalding 1959) and Sri Lanka (Senanayake 1981) that were also traced back to TOCP exposure.

Intoxication of NTE as cause for OPIDN

NTE was identified as the target molecule for TOCP (Johnson 1969). The resulting paralysis was shown to be independent of acetylcholine esterase (AChE) inhibition (reviewed in Jamal 1997) and termed organophosphate induced delayed neuropathy

(OPIDN). In humans clinical symptoms are visible between one and three weeks after intoxication starting with leg weakness and progressing to a flaccid paralysis of the limbs. The effect is reversible as long as the central nervous system is not affected (Triebig 1990).

Adult chickens appear to be especially sensitive to the development of OPIDN by TOCP intoxication. Leg weakness becomes apparent 8-10 days after administration of TOCP, by age 14-16 days, the birds are severely paralyzed. Histopathological examination reveals degeneration of distal regions of long axons in the spinal cord and peripheral nerves (Cavanagh 1954). Similar clinical symptoms can be observed in several other animals upon dosing with TOCP, for example cats (Cavanagh and Patangia 1965) and pigs, however most rodents that research was conducted on, do not develop OPIDN upon intoxication (reviewed in Glynn 2000).

The aging reaction

OPs inhibit esterases by acting as pseudo-substrates and covalently binding to the active site serine. The resulting organophosphorylated intermediate, unlike the endogenous substrate, is hydrolyzed very slowly thereby preventing the enzyme from catalyzing further substrate molecules (Figure 2).

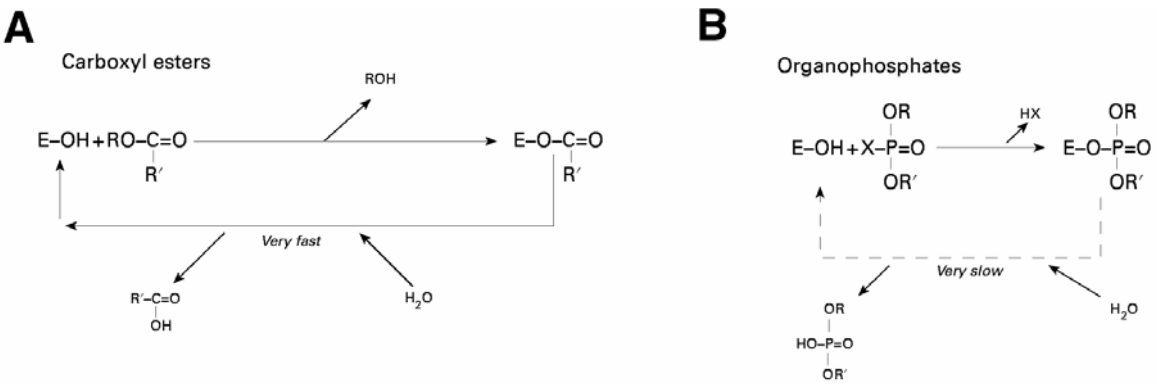

Figure 2: Reaction mechanism of serine esterases
(A) Carboxyl esters bind covalently to the nucleophilic active site serine, thereby creating an intermediate enzyme-substrate complex. This is rapidly hydrolyzed restoring the functional enzyme. (B) OPs bind to the same nucleophilic enzyme but the intermediate complex cannot easily be hydrolyzed thereby inhibiting the enzyme.

Initiation of OPIDN requires the concerted inhibition of more than 70% of neural NTE (Johnson 1982). However not all organophosphates that inhibit NTE lead to OPIDN. Inhibiting the NTE activity of chickens by more than 80% will still not lead to OPIDN with certain OPs (Petroianu et al. 2001). Predosing birds with these non-neuropathic OPs actually protected them from the effects of neuropathic OPs administered afterwards. A second reaction after the binding of certain neuropathic OPs is the so called "aging" reaction which is a critical event in the development of OPIDN. Classically the aging has been considered to involve side-group loss from the phosphorylated NTE, rendering the enzyme refractory to reactivation (Johnson 1982; Glynn 2000). A negative charge remains at the active site serine and a side-group is transferred to another site of the enzyme known as site Z in the case of some neuropathic OPs (Williams 1983). However recent results suggest that this intramolecular transfer of the side group is not defining of the aging reaction as it does not happen in aging of a shortened version of NTE intoxicated with mipafox, a neuropathic OP. Instead a proton loss at the catalytic site occurs rendering a negative charge in the active site serine, a phenomenon also observed in classical aging (Kropp et al. 2004).

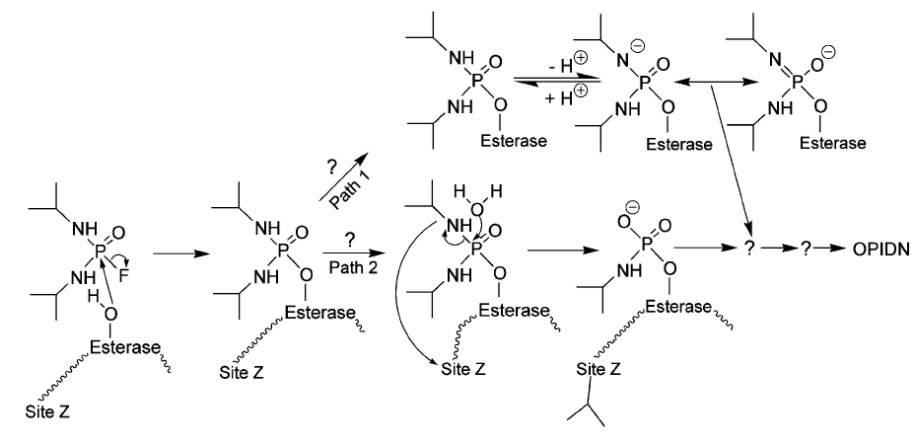

Figure 3: Alternative mechanisms for the aging reaction

Path 2 shows the classical aging mechanism involving an intramolecular group transfer to site Z, leaving a negative charge at the active site serine of the esterase. Path 1 describes the findings of intoxication with Mipafox. No intramolecular reorganization is observed, however a proton loss again leads to a negative charge at the catalytic site.

olk

The cytoskeleton is the major intracellular framework for neuronal morphology and is required in development and maintenance of the neuron. In order to transform an immature neuroblast into a mature neuron, cytoplasmatic extensions (axon and dendrites) which make synaptic contacts with other cells, are formed. One factor in achieving cell polarity is the rearrangement of the cytoskeleton in certain regions of the cell by regionally selective stabilization of microtubules (Kirschner and Mitchison 1986a; Kirschner and Mitchison 1986b). The balance between unorganized tubulin and polymerized microtubules capable of forming networks is regulated by several microtubule-associated proteins (MAPs), which bind to tubulin to stabilize it and link microtubules to other components of the cytoskeleton. Some of the best studied MAPs are MAP1A, MAP1B, MAP2, tau, doublecortin and LIS1. Tau and MAP1B, as well as other MAPs, are able to form several different isoforms by alternative splicing (Himmler 1989; Kutschera et al. 1998).

Several human neurodegenerative disorders have been found to involve the presence of abnormal protein aggregates in neurons and glia, and abnormalities in the neuronal cytoskeleton. Aggregates of tau are found in a range of disorders that have collectively been named "tauopathies". These are characterized by filamentous inclusions consisting of hyperphosphorylated tau. However, for most disorders it remains unclear if MAP aggregates are cause or effect of the neurodegenerative pathology (reviewed in Brandt 2001).

The discovery of a pathogenic set of mutations in the tau gene in a disease called "frontotemporal dementia with parkinsonism linked to chromosome 17 (FTDP-17)" confirmed the central role of MAPs in neurodegenerative disorders (Foster et al. 1997; Hutton et al. 1998; Poorkaj et al. 1998; Spillantini et al. 1998). Although proving in principle that abnormal MAPs can cause neurodegeneration few other inheritable forms of pathogenic MAP mutations have been reported. Mutations in intermediate fibers (IF) have been reported to cause hereditary forms of Charcot-Marie-Tooth disease (CMT) (Mersiyanova et al. 2000; De Jonghe et al. 2001) and amyotrophic lateral sclerosis (ALS) (Figlewicz et al. 1994).

Interestingly the loss of TAU protein in mice produces only subtle axonal defects, apparently because TAU function can be partially assumed by other MAPs (Harada et al. 1994). This suggests that the severe neurological defects observed in FTDP-17 are not due to loss of function of tau. However, overexpression of tau in *Drosophila* led to severe axonal defects, neurodegeneration and (in combination with hyper-phosphorylation) a neurofibrillary pathology (Williams et al. 2000; Wittmann et al. 2001; Jackson et al. 2002).

MAP1B

MAP1B is the first MAP to be expressed in the nervous system during development (Tucker et al. 1988; Tucker et al. 1989). Two further proteins were found to be associated with MAP1B, light chain 1 (LC1) and light chain 3 (LC3) (Kuznetsov et al. 1986; Mann and Hammarback 1994). MAP1B and LC1 are transcribed as a single mRNA and translated as a polyprotein, which is proteolytically cleaved to form the mature MAP1B and LC1 (Hammarback et al. 1991).

Phosphorylation of MAP1B appears to have a major role in modifying its role in neuronal development (reviewed in Gonzalez-Billault et al. 2004). Two modes of phosphorylation (mode I and mode II) have been identified (Avila et al. 1994). Mode I is mainly present in the distal part of the axon, whereas mode II is present in all subcellular domains of the neuron, including the axon and the somatodentritic compartment (Ulloa et al. 1994).

Four mouse mutants of MAP1B have been reported independently from each other (Edelmann et al. 1996; Takei et al. 1997; Gonzalez-Billault et al. 2000; Meixner et al. 2000). Although slightly conflicting results have been reported for these mutants the consensus is that true null mutants are homozygous lethal and display abnormalities in their nervous system. These studies indicate that like tau, MAP1B may be particularly important for the formation and maintenance of a functional nervous system.

Compensation effects for loss of MAP1B have been described in hippocampal cells that showed more MAP2 bound to microtubules in the absence of MAP1B (Gonzalez-Billault et al. 2001). Studies with double knockouts of MAP1B and MAP2 suggested

synergistic effects in laminin-enhanced neurite outgrowth (Teng et al. 2001). Redundancies have also been reported for tau and MAP1B during laminin enhanced axonal growth (DiTella et al. 1996).

futsch

In *Drosophila*, a MAP1 orthologue is encoded by the *futsch* gene (Hummel et al. 2000). Futsch is a protein of predicted 5327 amino acids with strong homology to vertebrate MAP1B at its N-and C-termini, plus a large middle portion that contains 66 direct repeats similar to repeats found in neurofilaments. Futsch is expressed in many neurons in the fly CNS, whereas in vitro experiments have revealed that it binds microtubules (Roos et al. 2000). Notably, a loss-of function *futsch* allele produces defects in axonal and dendritic growth in the embryonic nervous system (Hummel et al. 2000), whereas hypomorphic viable alleles show disruption of synaptic microtubule organization, reduction in bouton number and an increase in bouton size at the neuromuscular junction (Roos et al. 2000). These phenotypes are partially rescued by expression of a shortened Futsch protein containing only the conserved N-terminus. Together, these results suggest that Futsch is required to regulate microtubule architecture, thereby controlling growth cone function and synapse formation. Whether this protein also regulates neuronal structure and function in the postembryonic nervous system (as has been suggested for vertebrate MAP1B) has remained unexplored.

The *olk* mutant

In this thesis three new, viable alleles of *futsch*, named *omb-like*$^{1-3}$ (*olk*$^{1-3}$) were characterized (Bettencourt da Cruz et al. 2005). These mutants were isolated in a screen for mutants with defects in the morphology of the adult brain performed in the laboratory of M. Heisenberg. Histological sections of these mutants` brains lack the characteristic reduced silver staining associated with organized axonal bundles and fiber tracts. This abnormality led to the mutant's name because as in the mutant *optomotor-blind* (*omb*) the giant fibers of the lobula plate are not discernible in silver

stained or autofluorescent sections. Nevertheless as shown in the results section the *olk* mutants were identified as *futsch* alleles.

Material & Methods

Material

Fly strains

Genotype	Comment	Source	Reference
wt Canton S	Wild-type flies Canton special	stock collection	(Lindsley and Zimm 1992)
w^{1118}	White mutant	Stock collection	(Lindsley and Zimm 1992)
w/FM7a; D/TM3Sb	White mutant, balanced on the 1st and 3rd chromosome	Stock collection	
w; CyO/Sco; D/TM3Sb	White mutant, balanced on the 2nd and 3rd chromosome	stock collection	
p{w^+Δ2-3} Sb/TM3Tb	stable source of transposase	stock collection	(Robertson et al. 1988)
sws$^{1/2/4-6}$	*sws* mutant alleles	D. Kretzschmar	(Kretzschmar et al. 1997)
w; p{*elav*-Gal4/TM3Sb}	neuronal GAL4 expression line	Bloomington	
w; p{*loco*-Gal4}	glial GAL4 expression line	C. Klämbt	
w; p{GMR-Gal4}	retinal GAL4 expression line	M. Freeman	
w; p{actin-Gal4}	ubiquitous GAL4 expression line	Bloomington	
w; p{UAS-DSWS}	*sws*-cDNA under upstream activating sequence control	M. Mühlig-Versen	(Muhlig-Versen 2001)
w; p{UAS-SWSΔ1-80}	*sws*-cDNA lacking first 80 aa under upstream activating sequence control	M. Mühlig-Versen	(Muhlig-Versen 2001)
w; p{UAS-SWS^{S985D}}	*sws*-cDNA under upstream activating sequence control	M. Mühlig-Versen	(Muhlig-Versen 2001)
olk$^{1-3}$	new *futsch* alleles that cause neural degeneration	M. Heisenberg	(Bettencourt da Cruz et al. 2005)
w; p{UAS-SWSΔ1-35}	*sws*-cDNA lacking aa 1-35 under upstream activating sequence control	this thesis	
w; p{UAS-SWS^{S985D} Δ1-35}	*sws*-cDNA with mutated catalytic center and lacking aa 1-35 under upstream activating sequence control	this thesis	
w; p{UAS-SWS^{S985D} Δ33-55}	*sws*-cDNA lacking aa 33-55 under upstream activating sequence control	this thesis	
w; p{UAS-SWS^{S985D} Δ33-55}	*sws*-cDNA with mutated catalytic center and lacking aa 33-55 under upstream activating sequence control	this thesis	
w; p{UAS-SWS^{R129A}}	*sws*-cDNA with mutated putative protein interaction domain under upstream activating sequence control	this thesis	

Genotype	Comment	Source	Reference
w; p{UAS-SWS^{G553Q}}	*sws*-cDNA with mutated putative cAMP interaction domain under upstream activating sequence control	this thesis	

Stocks were maintained and raised on standard cornmeal food (Guo et al. 1996) in a 14-10h light- dark cycle at 25°C and 60% relative humidity.

sws-alleles

Allele	Mutation
sws^{1} (*sws*^{151})	S^{375}Amber
sws^{2} (*sws*^{1509})	unknown
sws^{4} (*sws*^{1600})	G^{958}D
sws^{5} (*sws*^{1680})	G^{648}R
sws^{6}(*sws*^{KS43})	unknown

Antibodies

Antibody	organism	Antigen	source	dilution
22C10	mouse	*Drosophila* Futsch	S. Benzer	1: 50
α-tubulin	mouse	tubulin	Sigma	1: 5,000
α-*sws*	rabbit	*Drosophila* SWS	this thesis	1: 1,000
α-HA	mouse	epitope of the influenza hemagglutinin	Cell signaling technology	1: 1,000
α-mouse	goat (HRP-linked)	mouse IgG	Amersham	1: 1,000
α-rabbit	donkey (HRP-linked)	rabbit Ig	Amersham	1: 1,000
α-mouse	goat (IRDye 800)	mouse IgG	Rockland	1: 1,000
α-rabbit	goat (IRDye 700DX)	rabbit IgG	Rockland	1: 1,000

Primer

Custom primers were obtained from Sigma-Genosys and Operon.

Name	SEQUENCE (5`-> 3`)	Bp	Cut sites
sws fwd1 mut inter	GGATA CTCCA GCTGA GGGCG GATAA TATGC CGCTA G	36	
sws rev1 mut inter	CTAGC GGCAT ATTAT CCGCC CTCAG CTGGA GTATC C	36	
sws fwd2 mut cAMP	GCATC CCGGC GAAAT CGTTG AAGGA CTGGC CATGC	35	

Name	SEQUENCE (5`-> 3`)	Bp	Cut sites
sws rev2 mut cAMP	GCATG GCCAG TCCTT CAACG ATTTC GCCGG GATGC	35	
sws fwd3 (2hybrid)	CGCGG ATCCG TTTGC GTTTG CGCGA CGAG	29	BamH I
sws rev3 (2hybrid)	CGCGA GCTCC GACTC GCCCT TCCTG ACC	28	Sac I
sws rev4 (2hybrid)	CGCGA GCTCT CTTAT CCTGC TTGGC CCGC	29	Sac I
sws fwd5 HA	CGCGA ATTCA TGTAC CCCTA CGATG TGCCC GATTA CGCCA TGGAT GTCCT GGAAA TGCTG CGCGC GAGC	69	EcoR I
sws rev5 HA	CGCCT CGAGC TAGGC GTAAT CGGGC ACATC GTAGG GGTAG TTTTT GGTTT CGTTA TTCGG GCTAC TTC	68	Xho I
sws fwd6	AAACG AATGG CACGT TTGCG TTTGC G	26	
sws rev6	CGTTG CTGTG ATCTG CTTGG AGAC	24	
sws fwd7 HA	ATCGC GAATT CATGT ACCCC TACGA TGTGC CCGAT TACGC CGTGT ACATG TATTT CGCCC TGGTA ATGAT GAGCC	75	
sws fwd8 (2hybrid)	CGCGT CGACA ATGGA TGTCC TGGAA ATGCT GCG	33	Sal I
sws rev8 (2hybrid)	CGAGC GGCCG CCTAG TTTTT GGTTT CGTTA TTCGG G	36	Not I
sws fwd12	GTTGT TGTTG CTGCT GCTGG CGCTG	25	
sws rev12	CACGC ACGCA CACGA AAACG CACTG	25	
sws rev13	GCCGC CCTGA CCGTG ATTTG TTTAC G	26	
sws rev14	CCTCG CGTCC TCTCG CTCTC GCAC	24	
sws fwd15	CGCGA ATTCG GTGTT CCAGG ACAAT CCGGA CG	32	EcoR I
sws rev15	CGCGC GGCCG CCCAA ACTTA CTGGT AAATA GCTGC TCG	38	Not I
sws fwd16	CGCTC TAGAG TGTTC CAGGA CAATC CGGAC G	31	Xba I
sws rev16	CGCCT CGAGC CCAAA CTTAC TGGTA AATAG CTGCT CG	37	Xho I
sws fwd17	CGCGC GGCCG CGTAG TCAAA AAGCTCC CGATT TG	32	Not I
sws rev17	CGCCT CGAGC ATGCC AGCAA TGATA AGTCG GTGGG TG	37	Xho I
sws fwd18	GCCCC AAAAT TGCCG ACACT CGTGT AG	27	
sws rev18	GAGCC GAAAT AAACG CGCAT TTTGC	25	
sws fwd19	CGCCT GCAGG AGGAG ACAAT CGAGG GCAGC GATAG AG	37	Pst I
sws rev19	CGCCT GCAGC CTTCT CGCGA AACGC ATGAC AGCAC G	36	Pst I
sws met eco (DK)	ATGAA TTCAT GGATG TCCTG GAAAT GCTG	29	EcoR I
sws1 (DK)	GACAG CGTAG AGAGT CATTG G	21	
swsR1 (DK)	CACGG TGCGC ATCTC TAGCG G	21	
sws2 (DK)	CAAGC GTCGT GCTGT CATGC G	21	
swsR2 (DK)	CAAAG CGGTG AACAG TACGC G	21	
sws3 (DK)	AAATC GGTGG TCATT CGTCT G	21	
swsR3 (DK)	GTGTC TGTAG ACACG AGTGC G	21	
sws4 (DK)	GGCAA CCTAT CCACG CGTCG CAG	23	
swsR4 (DK)	AGACG GCGTA CTACT CCGTT GC	22	

Name	SEQUENCE (5`-> 3`)	Bp	Cut sites
sws5 (DK)	AATAG CCTTC ATCCG ACGAG CAG	23	
swsR5 (DK)	GGCAC CAGGG CCACC GTG	18	
sws6 (DK)	GATGC AGACG CGCTC GGGCA GCGGG G	26	
swsR6 (DK)	CCGCT TGACG CAGAG CACAT GG	22	
sws7 (DK)	GCTCG TCCTG CTATA TCCGG	20	
swsR7 (DK)	CGTAA CGCCA CAGAG ATCCA TTGGT GTG	28	
sws8 (DK)	GACAC TTTCG GGGAC GTGAG	20	
sws9 (DK)	GATCA CATCG ATGTT CTCCG	20	
swsR9 (DK)	GTGAA GGGAT TCCAT TTCTT G	21	
swsR10 (DK)	ATCCG TATTC AGTGT GGTCG G	21	
swsR10b (DK)	TCTTG TACTT ATCGA TCGGC GG	22	
sws11 (DK)	TACGC CGTGA ATACC GCGG	21	
sws11-2 (DK)	AGATC GTGTG CCGTC TGCCG G	21	
swsR11 (DK)	TGAGT ATATA GCCAC GCTTC G	21	
swsR11b (DK)	TTGAT GATTG AGTAG TTGCG G	21	
swsR11PST (DK)	ATCTG CAGTT GATGA TTGAG TAGTT GCGG	29	Pst I
sws-TM1rev (DK)	TACTG CAGTG GCCCG CGTGG CATCCT GATTG CTCTG G	36	
sws-TM2for (DK)	ATGGT ACCAG AATTC GAGGC CAGTG CGTAT ACCAT TCGAT CG	42	
sws-TM4for (DK)	ATGGT ACCAG AATTC CGTAA TATCA CCACG GTAAC CCAGA AG	42	
mNTE fwd1	GCAAC CGGTA TCGAT GGAGG CCCCA CTG	28	Age I/ Cla I
mNTE rev1	CGCAC CGGTG TGGCA TCTGC GACTG AGCTG GG	32	Age I
mNTE fwd2	GCACT CGAGA TGGAG GCCCC ACTGC AAACC	30	Xho I
mNTE rev2	CGCCCGCGGT CAGGC ATCTG CGACT GAGCT	30	Sac II
m-sws8 (MMV-fwd)	ATCTC GAGGT CTGAG GCAGC GGGCA GAAAA CTAGG GG	37	Xho I
m-sws9 (MMV-fwd)	CAATC GATGG AGGCC CCACT GCAAA CCGGA ATGGT G	36	Cla I
m-sws10 (MMV-rev)	TGCTT CTAAG GATGT GGGCT TCACG GG	27	
T7uni*	GTAAT ACGAC TCACT ATAGG GCG	23	
T3rev*	AATTA ACCCT CACTA AAGGG	20	
SV40*	TACCT TAGAG CTTTA AATCT CTGTA GG	27	
Hsp70*	GCGCT TCGTC TACGG AGCGA C	21	
sos 5`	CCAAG ACCAG GTACC ATG	18	
sos 3`	GCCAG GGTTT TCCCA GT	17	
myr 5`	ACTAC TAGCA GCTGT AATAC	20	
myr 3`	CGTGA ATGTA AGCGT GACAT	20	
olk fwd11 (2 hybrid)	CGCGG ATCCA TATGT CGGAC GAAGG CGGCC	30	BamH I
olk rev11 (2 hybrid)	CGAGC GGCCG CGGCG CCGGC GTCCT GACTG TCC	33	Not I
olk fwd12 (2hybrid)	CGCGG ATCCA GGACA GTCAG GACGC CGGCG	30	BamH I
olk rev12 (2hybrid)	CGCGA GCTCC CCACG CTGGT CTTGA GGACT CC	32	Sac I

Name	SEQUENCE (5`-> 3`)	Bp	Cut sites
olk fwd13 (2hybrid)	CGCGG ATCCA GGAGT CCTCA AGACC AGCGT GGG	33	BamH I
olk rev13 (2hybrid)	CGCGA GCTCG GGGCA GACTG AGGTC AGCAA TGG	33	Sac I
olk fwd14 (2hybrid)	CGAGC GGCCG CCCAT TGCTG ACCTC AGTCT GCC	33	Not I
olk rev14 (2hybrid)	CGAGC GGCCG CCTAG AACTC TAGGC GGTAG GCC	33	Not I
pka-c3 fwd1	GACCC TTGCA CGGAA TCCGT CTC	23	
pka-c3 rev1	CGGGC TGTAA ATTAG CAAAG CG	22	
pka-c3 rev2	CGTAC GCGTT CGAAA TGTTT GGAC	24	
pka-c3 fwd3	CCTCG GCTGG TTAAT TAAAC GACC	24	
pka-c3 rev3	CGGGA AAGGG GTTAC ACTTG CCG	23	
pka-c3 fwd4	CCGGA AACGG AAGCG GCAAC ACG	23	
pka-c3 rev4	CGCTG CTGCT CCTGC TCCGG ATCCT CC	22	
pka-c3 fwd5	CCGCA GGCGA GGATT GCGAC AGC	23	
pka-c3 rev5	GGCGC GGGAC CTTAA CATCA ATC	23	
tau fwd1	CCCAA CCACC ACCCA CAGAC ACGCC CC	27	
tau rev1	GACCT TGCCC GAGAG CAGAA ACCC	24	
tau fwd2	AACGA ACCGA AACAT GTTTA AACC	24	
tau rev2	TCAGA TTCAG TTTCA GATAC AGCTC G	26	
tau fwd3	GGCAA CAGCG CTTTC CATCC ATGTG TTCCC G	31	
tau rev3	GGATC GTGGC AATCA AGCGC CCTTG TAGCG C	31	
tau fwd4	GATTT GTGCA ATCCG ATACG CATTC ACG	28	
tau fwd5	GCGAC CAGTG AAAAC CAAAA ACCAA ACCC	29	
tau rev5	CAGGG TGTAA ATAAA TCGTG AGAAT G	26	
tau rev6	GCATC TAGGT TTCTA TACAA AAGCA CAC	28	
tau fwd7	CCGTT CGATC GATAT TTTGA CTTTG GC	26	
tau rev7	GGACT TGGCG TTCCA CTGCA ACTTT G	26	
tau fwd8	CTGTA CGTTG CCGGT GCCGG TGCTA C	26	
tau rev8	CTAGA TATCA TACGT AACTA CTTTG AGC	28	
tau fwd9	GCGCC TTCAC CCAAT CTGAA GGCGG TACGC	30	

Plasmid vectors

Name	Source	Comment
pBluescript SK (+/-)	Stratagene	Cloning vector
pSos	Stratagene	Yeast two hybrid vector
pGEM-T easy	Promega	PCR cloning vector
pUAST	Brand and Perimon	*Drosophila* transformation vector
pUCπΔ(2-3)	*Drosophila* genome resource center	non-integrating transposase source
pQE80-82L	Stratagene	Protein expression vector

Yeast two hybrid

The CytoTrap system from Stratagene Catalog #217438 was used to perform Two-Hybrid-Screens. The cDNA library was isolated from adult *Drosophila*.

Methods

Molecular standard methods

Unless otherwise stated all molecular biology methods were performed according to protocols described by Ausubel and Coworkers (Ausubel et al. 1988).

Site-directed mutagenesis

Specific bases were exchanged according to the instructions provided by the Quick-Change Site-directed mutagenesis kit from Stratagene (Catalog #200518/9).

Sequencing

All sequencing was performed in the Vollum sequencing core of the Oregon Health and Science University using methods, instruments and protocols developed by ABI Prism.

Fusion protein expression & antibody production

The QiaExpressionist kit from Qiagen was used to express and purify a HIS-tagged fusion protein. The resulting fusion protein was send to David's Biotechnologie, Regensburg to immunize rabbits.

Lipid and sterol content measurements

Lipid and sterol measurements were performed by Karin Athenstaedt (Institut für Biochemie und Lebensmittelchemie, Technische Universität Graz, 8010 Graz, Austria) according to the procedure described previously in (Muhlig-Versen et al. 2005)

Histological methods

Histological methods need to be adapted specifically to the performed experiment, therefore in this section a more general description is provided. More detailed information can be found in the description part of the corresponding experiments.

Paraffin sections

Paraffin section were prepared according to protocol 112 in Ashburners *Drosophila* manual (Ashburner 1989) except for usage of increasing concentrations of ethanol (70, 80, 90 and 100%) instead of absolute ethanol for all wash steps.

Cryostat sections

Immunohistochemistry

Immunohistochemistry was performed according to protocol 115 in Ashburners *Drosophila* manual (Ashburner 1989).

X-Gal stainings

Immunohistochemistry was performed according to protocol 74 “alternate procedure” in Ashburners *Drosophila* manual (Ashburner 1989).

Creation of transgenic *Drosophila* flies

Transformations were performed by the Model systems genomics unit of Duke university, NC and Rainbow transgenic flies, Inc., CA.

Results

A- sws

A.1- Production of a *Drosophila* SWS antibody

SWS-Antibody production has proven to be a challenging endeavor. Great difficulties had already been experienced in obtaining a chicken NTE antibody (Paul Glynn, personal communication)(Glynn 1997) and earlier attempts to create antibodies to DSWS by peptide- and DNA immunization have failed (Muhlig-Versen 2001).

One possible explanation for this might be low immunoreactivity of the SWS protein. SWS shows a high degree of conservation among a broad range of species, including *Drosophila*, mouse and humans. The sequences of the mouse NTE and *Drosophila* SWS are 41% identical over the entire length of the protein, however there are sites of higher conservation in certain critical domains (Lush et al. 1998). Therefore production of mice antibodies against a peptide that is so similar to their endogenous protein might be inhibited by the same mechanisms that suppress autoimmunization.

Another possibility is that the short peptides did not form an immunoreactive tertiary structure. A longer part of the SWS protein or even the full length product would be necessary for the production of a usable antibody.

The more common approach to inject full length protein into a host animal had so far been unusable because it was impossible to isolate enough protein to immunize an animal. NTE is known to be firmly associated with microsomal membranes and appears to be an integral membrane protein (Davis and Richardson 1987; Ruffer-Turner et al. 1992). Purification of this protein has proven to be extremely difficult, presumably because of its membrane anchoring.

Comparisons of hydrophobicity blots predicted four TMs in the SWS protein and in most of its orthologues, the most N-terminal one being the most prominent one. Recent results suggest that in NTE only the first TM actually anchors the protein to the membrane (Li et al. 2003). Although the working model for this thesis generally assumes that SWS harbors three TMs (see introduction), for historical reasons labeled

TM1, TM3 and TM4 (Figure 4), for the design of the antigen all four potential TMs were considered.

To avoid the problems arising in trying to purify a protein with TMs, it was decided to use a fragment of SWS to obtain an immunogenic product. Determination of TMs is an important aspect in the design of the antigen as TMs might interfere with the purification of the protein by accumulation in the bacterial cell membrane. The fragment that was chosen to produce the protein was located immediately C-terminal to the predicted transmembrane domain 1 up to TM2 (Figure 4). In order to be able to purify the protein more easily a His-tag was fused to the N-terminus of the protein fragment. This fusion protein was expressed with the QiaExpressionist vector pQE82L in a bacterial system to obtain immunoreactive material.

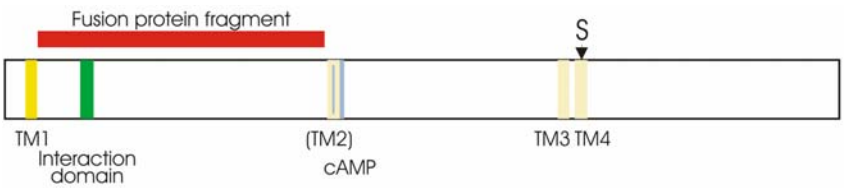

Figure 4: SWS protein with the designated fusion protein fragment

The diagram of the SWS protein shows the location of the fragment used for immunization with the His-tag fusion protein. Recent data suggest that the predicted transmembrane domain 1 (yellow) acts as a TM in vivo, whereas predicted TMs 2, 3 and 4 (light yellow) might not span the membrane in vivo. The fusion protein fragment includes the domain with similarities with the interaction domain of PKA (green) but not the cAMP binding domain (blue). The “S” marks the catalytically active serine.

A.1.1- Specificity of the α-SWS antibody on histological sections

The resulting antibody was examined closely to make sure it specifically recognized SWS. Histological means to test an antibody include staining of brain section on overexpressing flies. With the UAS-GAL4 system it is possible to control the expression of cloned proteins in specific areas. If the isolated antibody is specific to SWS it should show an increase in the areas where SWS is overexpressed. While α-SWS antibody staining in wt flies is moderate (Figure 5A), stainings in flies overexpressing SWS

protein with the glial specific driver *loco,* showed a higher signal in glial cells (Figure 5B). Conversely in combination with retinal specific GMR driver, strong and specific staining in the eye was observed (Figure 5C and D). The now available α-SWS antibody showed a high specificity for SWS in histological sections.

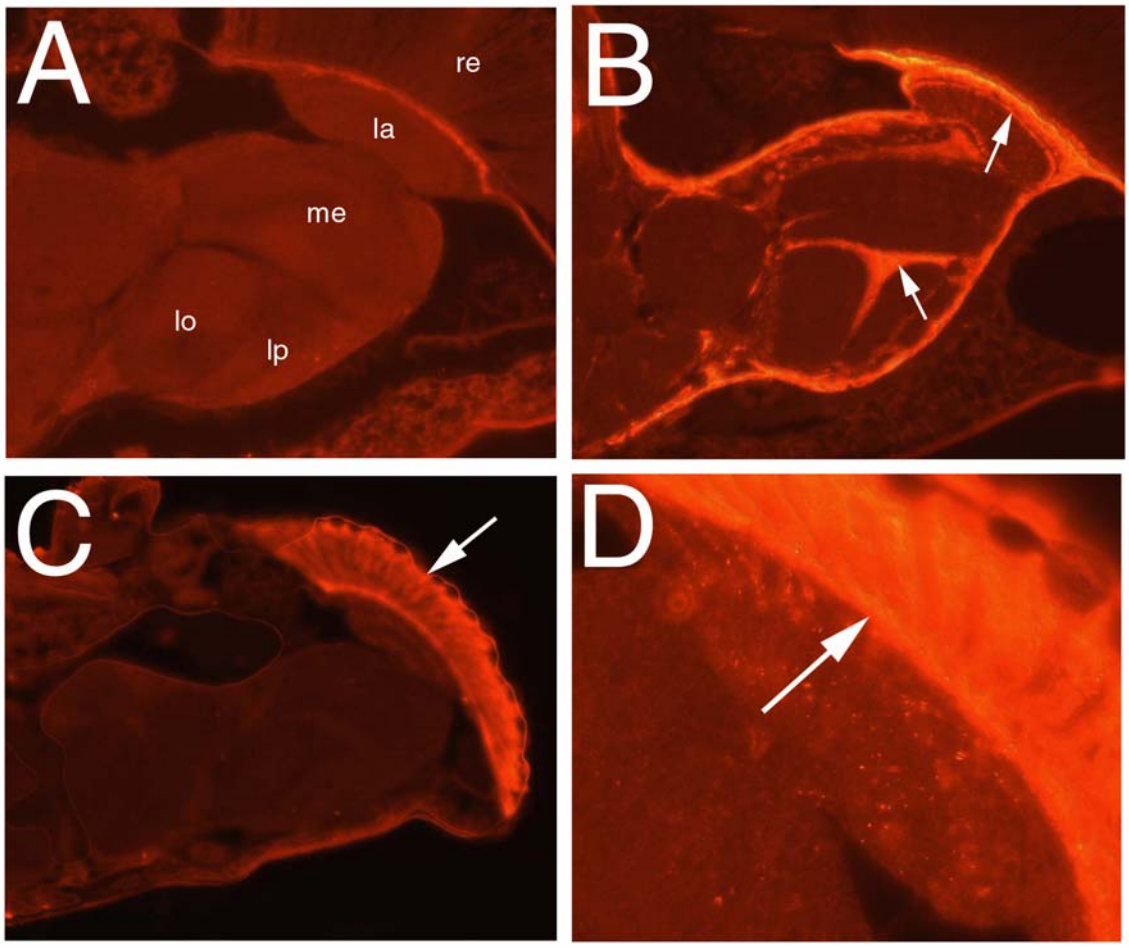

Figure 5: α-SWS antibody staining on SWS overexpressing flies

Paraffin sections stained with α-SWS antibody. (A) wild-type, (B) *loco*-GAL4/ UAS-DSWS and (C) GMR-GAL4/ UAS-DSWS. (D) Magnification of (C). The areas of more intense staining with α-SWS (arrows) are consistent with the areas where the glia specific loco driver (B) and the retinal specific GMR driver (C and D) are known to drive expression. This strongly suggests that this α-SWS antibody is specific for the SWS protein.
re: retina; la: lamina; me: medulla; lo: lobula; lp: lobula plate.

A.1.2- Specificity of the α-SWS antibody on western blots

In Western blots the α-SWS antibody detects a band of the 160 kDa, the computed size of the SWS protein. Differences between flies mutant for *sws*, flies overexpressing SWS and wt flies are easily visible. In wt flies there is a clear signal at about 160 kDa when five fly heads are loaded. This signal is much more intense in flies that had a transgenic SWS expressing construct under the control of the glial *loco* driver even though only one head was loaded onto this lane. In the *sws* mutants sws^1 and sws^5 no signal could be detected (Figure 6). sws^1 could still produce a shorter truncated version of SWS that harbors the antigen, however a shortened version was not visible on the blot. sws^5 is a point mutation resulting in an arginine instead of a glycine at position 648 ($G^{648}R$). This mutant might still produce a full length product. The reason why the products of sws^1 and sws^5 are not seen might be because the mutation makes the product unstable. A high turnover rate would make the concentration of the SWS protein too low to be detected. The modification of the protein might also change the conformation of the protein thereby making it unrecognizable to the α-SWS antibody. The mutation of sws^6 is not known, no nucleic acid substitution has been found in the coding region. The total amount of protein seems to be the same in this mutant as in the wt, but nothing can be said about the spatial expression of the protein in this mutant. Regulation in the wrong cell compartments might lead to depletion in essential regions without showing a difference in the band intensity.

A.2- Expression pattern

The expression pattern of the *sws* mRNA has previously been determined by in situ hybridization experiments. The results suggested that SWS was expressed in neurons in the adult brain cortex, but no mRNA could be found in the glial cells of the neuropil (Kretzschmar et al. 1997). However, analysis of lines expressing *lacZ* in glial cells suggested that although epithelial glia seems to be unaffected, other glial cells degenerate in *sws* mutants (Kretzschmar et al. 1997).

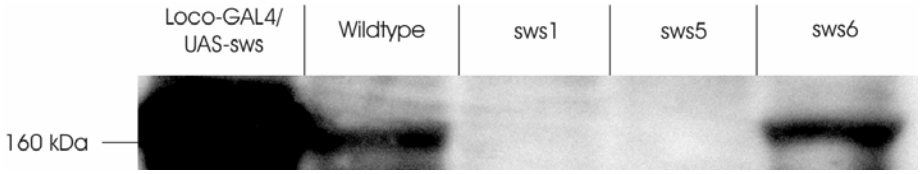

Figure 6: Western blot of *sws* overexpressing, wild-type and sws deficient flies

Western blot performed with the α-SWS antibody. The first lane was loaded with the head extract of one fly head overexpressing SWS under the control of the *loco* enhancer, the second lane contained five homogenized wild-type fly heads, the following lanes contained five fly heads each from sws^1, sws^5 and sws^6 flies respectively. As expected a lot more gene product is found in the overexpressing flies compared to wild-type. sws^1 and sws^5 mutants have no visible gene product. In the case of sws^1 the truncated protein is not visible although the antibody epitope is still present, perhaps because of a destabilization of the truncated product. sws^6 is an unknown mutation and seems to be present in amounts comparable to wild-type however disturbed spatial distribution might render it non-funtional.

Rescue experiments showed that SWS is endogenously required in neural cell as well as glia. SWS driven by neuronal drivers will rescue only the neuronal degenerative phenotype, conversely glial expression of SWS in the mutant will only rescue the glial hyperwrapping pathology (Muhlig-Versen et al. 2005).

Antibody stainings reveal that SWS is widely expressed in neurons shortly after eclosion (Figure 7A and B) but shows a more restricted pattern with increasing age. Specific subsets of neurons are expressing more SWS if twelve day old flies are observed (Figure 7C). This change of expression to a more specific subset of neurons is also seen in the aging mouse brain (Moser et al. 2000).

To determine whether SWS is expressed in the glia an antibody against the glial marker *repo* was used (Xiong et al. 1994). This showed that DSWS is expressed in some but not all glial cells. SWS is coexpressed with repo in the interface glia but not in the neuropil glial cells (Figure 7D and E). This is consistent with the previous results obtained by in situ hybridization (Kretzschmar et al. 1997) and the pattern of glial degeneration.

A closer look at the optic system revealed no detectable DSWS in the epithelial glia of the lamina and the giant glia at the optic chiasm. However DSWS was detectable in the fenestrated and satellite glia in the lamina cortex and the medulla glia at the cortex-neuropil interface (Figure 7F). There was no expression found in the giant glia.

Due to the fact that rescue experiments showed that SWS is endogenously required not only in neurons but also in the glial cells, it was expected that SWS can be found in the glia of wt flies. This was confirmed by the antibody staining made possible by the α-SWS antibody.

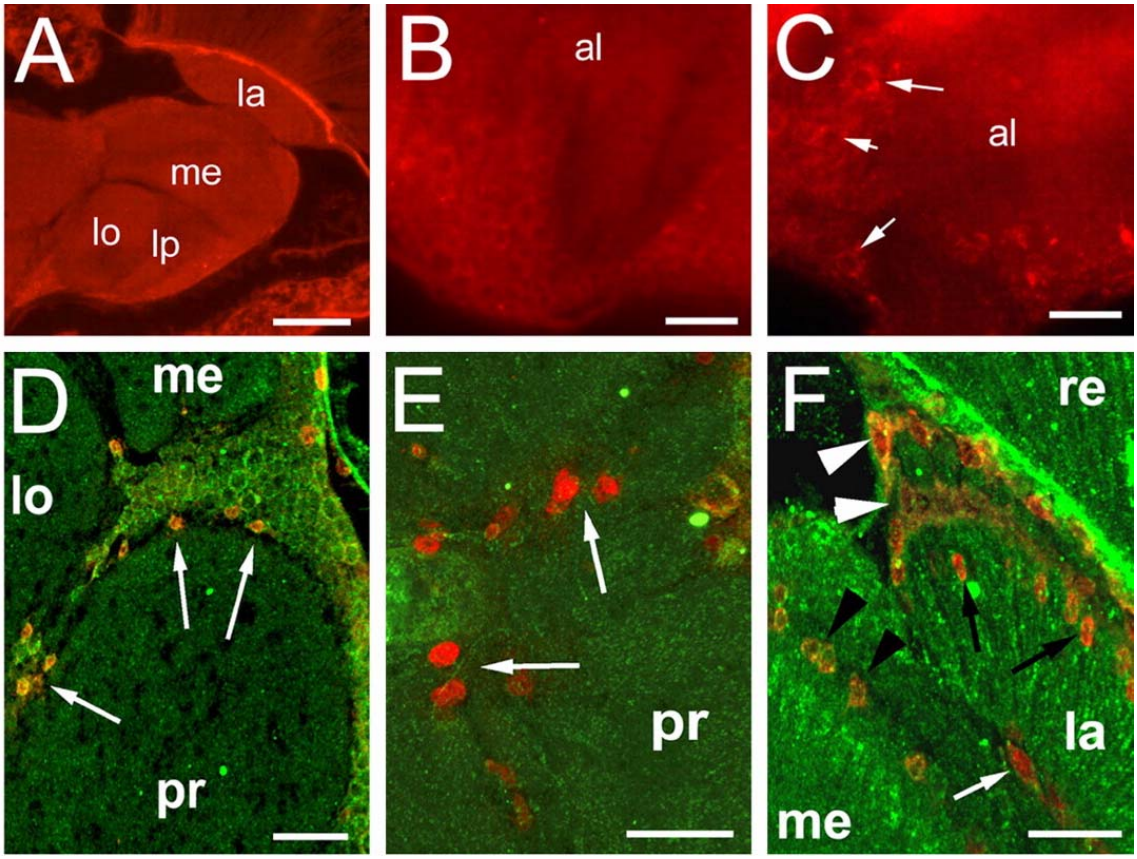

Figure 7: Expression pattern of DSWS

(A and B) In a 1-d-old wild type DSWS is expressed in most or all neurons. (C) In 12-d-old flies the pattern becomes more restricted with some neurons (arrows) containing higher levels of protein (compare with B). (D-F) Double staining with anti-DSWS (green) and the glia-specific protein REPO (red) reveals expression in interface glia at the border of the neuropil and cortex (D, arrows) but not in the neuropil glia (E, arrows) of the protocerebrum. (F) In the optic system DSWS was not detected in the epithelial glia of the lamina (black arrows) and the giant glia at the optic chiasm (white arrow). In contrast DSWS is expressed in the fenestrated and satellite glia in the lamina cortex (white arrowheads) and the medulla glia (black arrow-heads) at the cortex-neuropil interface.

Horizontal cryosections from heads were used. la: Lamina, me: medulla, lo: lobula, lp: lobula plate, al: antennal lobe, pr: protocerebrum, n: nucleus, re: retina. Scale bars: A, 50 µm; B, C, 10 µm; D-F, 20 µm;

A.2.1- Subcellular localization

In higher magnifications of the cortex area the α-SWS-Antibody localizes to round structures that appear to be vesicles suggesting SWS could be an ER bound protein (Figure 8A). The specific localization becomes even more apparent when over-expression lines are analyzed (Figure 8B). SWS/ NTE has also been localized to the ER in hippocampal neurons in cell culture (Akassoglou et al. 2004) and COS cells (Li et al. 2003). To address this question in *Drosophila* a double staining with α-SWS antibody (Figure 9A) and the α-Grp78 (an ER marker) antibody (Figure 9B) was performed. Colocalization of the SWS and Grp78 can be found as well as SWS protein in vesicles that are not part of the ER (Figure 9C). This finding confirms that SWS resides in the ER, although it is also found in structures not marked by the ER specific antibody. These structures can be other vesicles budding off from the ER.

This is consistent with the finding that purified SWS will not show any catalytic activity in vitro unless it is associated with membrane vesicles suggesting it has to be integrated into a membrane to unfold its function (Atkins and Glynn 2000).

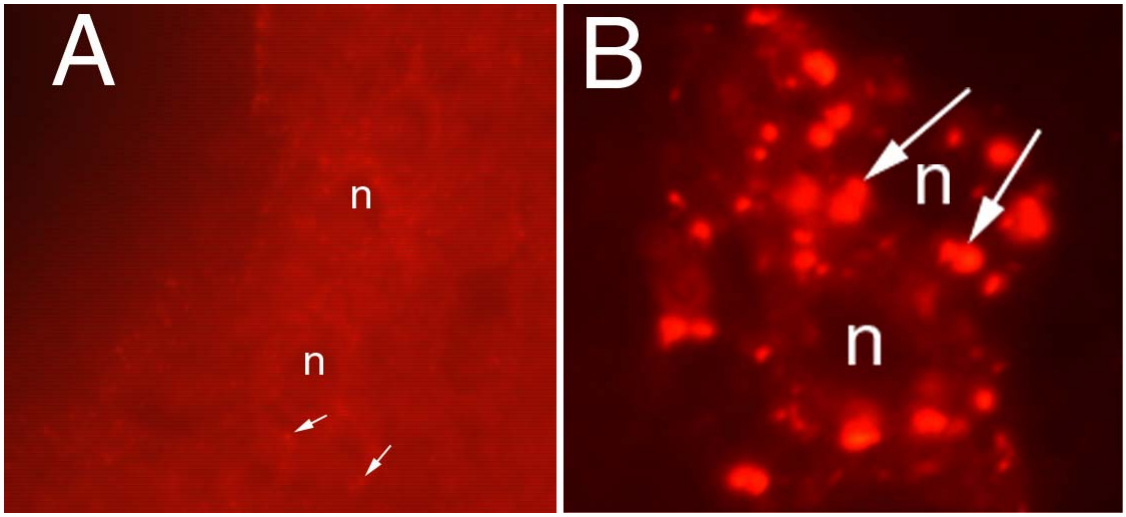

Figure 8: Vesicles in higher magnification α-SWS stainings
(A) Magnification from cortex region in wt and (B) *elav*-driven UAS-DSWS flies. Paraffin sections were used and stained with α-SWS antibody. Localization to round structures is visible in wildtype (A) but becomes very prominent in flies with higher levels of SWS (B) (arrows). n: nucleus

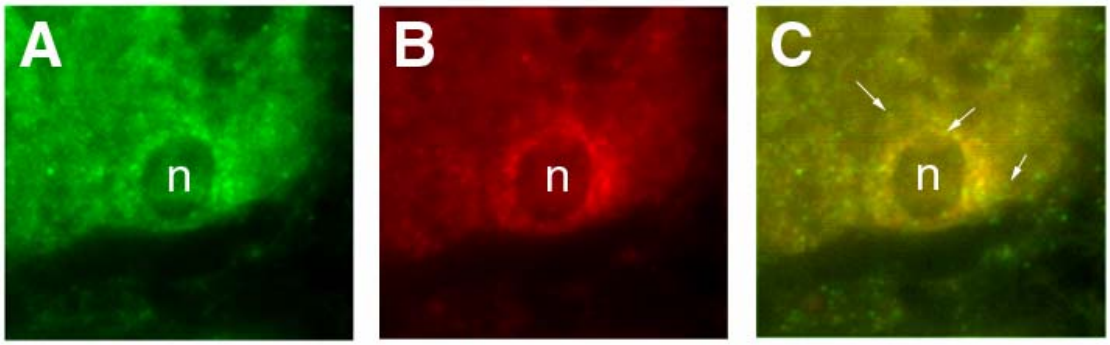

Figure 9: Double staining with α-SWS and ER-marker

(A) The SWS protein (green) is found in the cytoplasm of neurons and appears to be localized in vesicles (shown in the cortex of the central brain). (B) Grp78 is used as a marker for the ER (red). (C) SWS and Grp78 colocalize (yellow) suggesting that most of the SWS protein localizes to the ER and only some SWS protein is found in other vesicular structures (arrows). Horizontal cryosections from heads were used. n: nucleus.

A.3- Interaction of PKA-C3 with SWS

In this work interaction of SWS with PKA-C3 is observed with several different methods. The first hints for a possible connection were found by sequence analysis revealing a region in SWS that shows similarity to the protein binding domain of PKA-R (Figure 15A), which mediates the binding of the regulatory to the catalytic subunit of PKA. A yeast two hybrid screen was then performed in order to confirm this hypothetical interaction in the yeast model system (A.3.1- Yeast two hybrid screens, page 38). PKA-C3 was isolated out of several screens performed with SWS and SWS fragments as bait. To test interaction in vivo in *Drosophila sws*-mutants were crossed with deficiencies covering the *pka-c3* locus (A.3.2- Genetic interactions, page 42), as well as flies carrying a transgenic UAS-PKA-C3 construct under the control of several drivers for GAL4 (A.3.2.3- Genetic interaction using a UAS-pka-c3 construct, page 43).

A.3.1- Yeast two hybrid screens

In a classical two-hybrid screen the bait and the target protein will enter the nucleus of a yeast cell and activate a reporter construct within the nucleus. This will allow to identify a yeast colony and identify the target protein, thereby demonstrating an interaction within the yeast nucleus. This is not necessarily identical with the conditions

found within the natural environment of the protein which usually is in the cells of other species and can be in other compartments of the cell.

In order for the classical approach to function the bait and the target will both have to enter the nucleus before a positive interaction will start the transcription of the reporter gene. Both proteins will have to pass through a membrane and bind to each other in the nuclear environment. For proteins containing transmembrane domains, such as SWS, this might be a hindrance. By using the CytoTrap Two-hybrid-system (Stratagene) to perform this screen this problem can be partially bypassed because the entire interaction takes place in the cytoplasm (Figure 10). The interaction of the bait with the membrane bound target localizes the bait to the membrane. The bait which is fused to hSos, a human RAS activating protein, will indirectly activate the RAS pathway permitting the mutant yeast to grow at the otherwise non-permissive temperature of 37°C, thereby indicating the interaction (For details see CytoTrap Vector Kit Instruction manual, Catalog #217438).

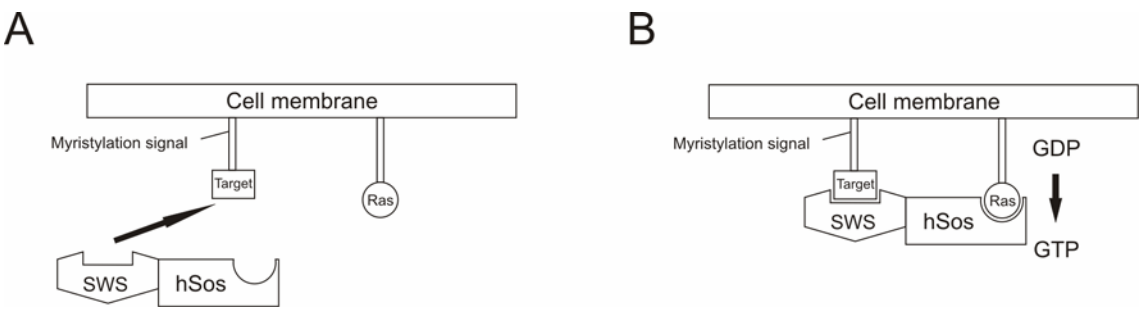

Figure 10: Diagram of the CytoTrap system
(A) SWS fused to hSos (Son of Sevenless) will be used as bait, the cell membrane anchored target proteins are derived from an adult *Drosophila* head library. (B) The bait protein binds to the target, localizing hSos to the membrane. hSos activates RAS by promoting GDP/GTP exchange. Ras activates signaling cascade that permits mutant yeast cdc25H to grow at 37°C.
Modified from The CytoTrap Vector Kit Instruction manual, Catalog #217438.

However to exclude any complication with membrane association, in addition to the full length protein, two fragments that contained no part of any predicted transmembrane domain were chosen to act as bait. Both of these fragments contained the protein interaction region as predicted from sequence similarity from the regulatory subunit of

PKA. The longer fragment contained amino acids 60-544, the smaller amino acids 60-241 (Figure 11), referred to as long and short fragment respectively.

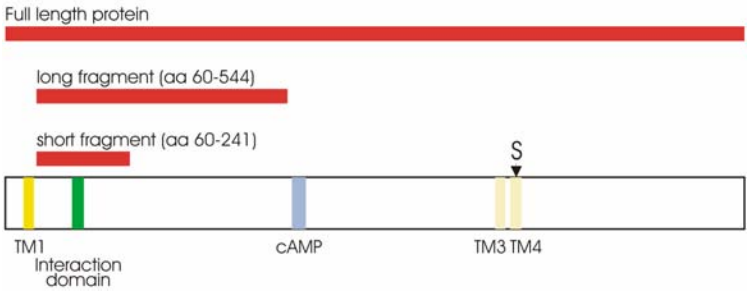

Figure 11: Fragments used as yeast two hybrid bait

The diagram of the SWS protein shows the location of the fragments used as bait in the yeast two hybrid screens (red). The fusion protein fragment includes the domain with similarities with the interaction domain of PKA (green) but not the cAMP binding domain (blue). Recent data suggest that the predicted TM 1 (yellow) acts as a TM in vivo, whereas predicted TMs 3 and 4 (light yellow) might not span the membrane in vivo. The "S" marks the catalytically active serine.

A.3.1.1- Proteins identified

In all the screens it was carefully tested if the bait would produce false positives without real interaction with any target proteins. Specially in the case of the full length protein it is a possibility that the protein attached itself to the cell membrane with its TMs without the need for interaction with the target. None of the fragments or the full length protein had this problem in this system. Also a positive and a negative control were used in every screen as described in the Stratagene manual for the CytoTrap system. Screens were performed with each of the fragments and the full length protein.

The only protein that was found in all screens was PKA-C3 (cAMP dependent protein kinase A, catalytic subunit 3). PKA-C3 showed strong interaction with the long and short fragment as well as the full length protein. PKA acts as tetramer consisting of two regulatory (R) and two catalytic (C) subunits. The regulatory subunits keep the catalytic subunits in an inactive state which turn active as soon as the complex dissociates. The regulatory subunits are bound to the catalytic subunits at a specific region that shows homology to the DSWS protein (Figure 15). Considering that PKA-C3 showed the

strongest interaction overall in the screens using different baits and SWS shows homology to the respective regulatory subunit, efforts were concentrated on this protein.

Other proteins isolated in some of the screens are mentioned below. However, none of these were isolated in the screen with the full length protein as bait and not further investigated in detail at this point.

Hsp22 (Heat shock protein 22) showed an interaction with both, the long and the short fragment. Flies that carry the *sws* mutation and are heterozygous for the deficiency DF(3L)29A6, which uncovers the region where Hsp22 is located, show a worse phenotype than the *sws* mutant by itself. However, in order to function as general chaperones Hsp22 has to bind to proteins in a less specific manner.

Hsc70-4 (Heat shock protein cognate 4) showed medium interaction with the short but not the long fragment. Hsc70-4 encodes an adenosinetriphosphatase (ATPase) involved in neurotransmitter secretion in the mitochondrial inner membrane.

mRpL7-L12 (mitochondrial ribosomal protein L7/L12) showed medium interaction with both the short and the long fragment. It encodes a structural constituent of ribosome involved in protein biosynthesis which is a component of the large ribosomal subunit. Genetic tests with the uncovering deficiency Df(3L)Rdl-2 showed no modification of the *sws* phenotype

lcs (*la costa*) showed medium interaction with the long fragment and strong interaction with the short fragment. lcs contains a leader sequence, a collagen-related repetitive motif, and a serine/ threonine-rich motif found in many different proteins. The La Costa protein is almost totally repetitive, consisting of 24 variant repeats of a collagen-like sequence and 9 copies of a threonine/ serine repeat that is found in diverse human proteins (Miklos et al. 1997; Maleszka et al. 1998).

CG 8223 showed medium interaction with the short fragment and no interaction with the long fragment. This computed gene contains a Tetratricopeptide repeat. Genetic interaction with the deficiency Df(3R)p25 resulted in a slight increase in the amount of holes in the brain.

A.3.2- Genetic interactions

A.3.2.1- Genetic interactions with Deficiencies in the pka-c3 region

Three catalytic subunits have been described for *Drosophila* (C1-3) however a mutant is only available for the C1 subunit. Homozygous mutant *pka-c1* flies die as first instar larvae (Lane and Kalderon 1993). However, a test of sws mutant flies that were also heterozygous mutant for *pka-c1* showed no phenotype discernible from *sws* flies.

Without a mutant for *pka-c3* the best alternative for a genetic interaction presented itself in form of two overlapping deficiencies. Deficiencies Df(3L)brm11 and Df(3L)A27 both span the region of the *pka-c3* gene. The overlap of the two Deficiencies is only about 10-20 kb long as determined by southern blots (Melendez et al. 1995). Although the homozygous mutant *pka-c1* flies are lethal the overlapping deficiencies for *pka-c3* seem to be viable (Melendez et al. 1995). However, flies carrying both the deficiencies and the *sws* mutation could not be produced. Presumably this was due to the low viability of the deficiency stocks themselves.

A small scale test using each deficiency individually over *sws* flies resulted in a worse phenotype than the *sws* phenotype. This confirms an interaction between SWS and PKA-C3. For a statistic approach more sections are needed to determine how much worse these deficiencies make the *sws* phenotype. This project is in progress and the results will be available soon.

A.3.2.2- Deletion mutant for pka-c3

A line with a homozygous viable P-element insertion localized within the second intron of *pka-c3* exists. This intron is almost 6kb long and the coding region starts in the third exon. The P-element is localized about 2.5 kb upstream of the start methionin. Remobilizing P-elements results in deletion to nearby sequences in a fraction of the flies. It is possible to use this method to create a deletion mutant of *pka-c3* (O`Kane and in: Roberts 1998). The distance between the start codon and the P-element is comparatively large for this method. Therefore a large number of jump-out lines have to

be created and tested. A short PCR amplification will reveal if any of the jump-out lines has a deletion in the coding sequence.

Although at least two independent, lethal jump out lines have been isolated neither of them lack any part of the coding sequence of *pka-c3*. Nevertheless these flies were tested over deficiencies Df(3L)brm11 and Df(3L)A27, which uncover the *pka-c3* gene (Melendez et al. 1995). The jump-out lines were viable over the deficiency suggesting the lethal effect is due to a defect in another region. Preliminary results show that the transheterozygous flies show a worse degenerative phenotype than the deficiency over wildtype heterozygotes, therefore the deletion might have an effect on the expression of *pka-c3* that is independent of the cause of lethality. In addition to this deletion line more jump-out lines are currently being analyzed in order to obtain a mutant deleting the 5` end of the coding region.

A.3.2.3- Genetic interaction using a UAS-pka-c3 construct

To further test this genetic interaction the reciprocal experiment was performed with a UAS-*pka-c3* construct. The construct was made by cloning the *pka-c3* cDNA into the pUAST vector that provides the upstream activating sequence (UAS). Expression of this construct was tested by tissue specific expression with the GAL4/ UAS system, which activates the transgenic construct within the fly via the upstream activating sequence, dependent on the presence of GAL4 (Brand and Perrimon 1993).

In the tests with the deficiencies covering *pka-c3* a worse phenotype than *sws* alone was observed, therefore an amelioration of the neurodegenerative phenotype is expected by overexpressing the UAS-*pka-c3* construct in *sws* flies.

When *pka-c3* was overexpressed in a *sws* background in glial cells with the *loco*-GAL4 driver construct a slight improvement of the *sws* phenotype was observed. Expression of UAS-*pka-c3* driven by the neuronal specific elav driver is under way, results will be available soon. Overexpression of PKA-C3 in the eye and glial cells with GMR and *loco* drivers respectively lead to a similar degenerative phenotype as overexpression of SWS does. All these results point to an involvement of PKA and SWS in the same pathway. Assuming sws^1 is a true null mutation this would lead to the conclusion that

pka is downstream of *sws*. However *sws*[1] is a point mutation leading to a nonsense mutation after about a third of the wt gene. This will truncate the protein before the translation of the catalytic site but other function might still be intact in the N-terminal part.

A.4- Analysis of functional domains of the SWS protein

In order to analyze potential interaction domains several constructs mutated in the potential functional domains were designed and tested concerning their properties compared to the wt protein. The ability to rescue the original *sws*[1] phenotype and to cause an overexpression phenotype are two criteria to test the properties of the modified SWS protein.

Several regions of the SWS protein have been identified as potential candidates for functionally important domains. Two sections of SWS show high similarity with the PKA-R protein (Figure 12/ Figure 15). One is responsible for interaction with the catalytic subunits, the other for binding of cAMP. Furthermore previous experiments with SWS lacking the first 80 amino acids of the N-terminus, revealed that there seems to be an important function within that region (Muhlig-Versen 2001). The first 80 amino acids contain a TM (amino acids 35-55) which will be investigated in detail and a short N-terminal sequence (amino acids 1-35)(Figure 12). All these candidate regions were mutated and the modified proteins analyzed in detail.

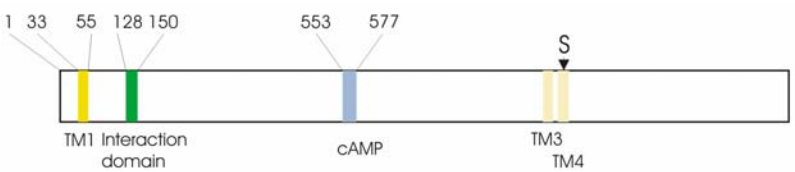

Figure 12: SWS proteins with potential functional domains

Numbering refers to the amino acids of the start and the end of the respective domain. Predicted TM1 (aa 33-55) is yellow, the protein interaction domain (aa 128-150) is green and the cAMP binding domain (amino acids 553-577) is blue. The “S” marks the catalytically active serine, predicted TMs 3 and 4 are kept in light yellow.

A.4.1- The wt SWS construct

Expressed in neuronal or glial cells the wt SWS construct is able to rescue the *sws* phenotype in the respective cells. The expression within these cells is sufficient for the transgenic SWS to assume the function of the lacking endogenous SWS (Figure 13D and E) (Muhlig-Versen et al. 2005).

When this construct is expressed under the control of the Actin driver it becomes lethal. This suggests that there is also a toxic characteristic to the SWS protein.

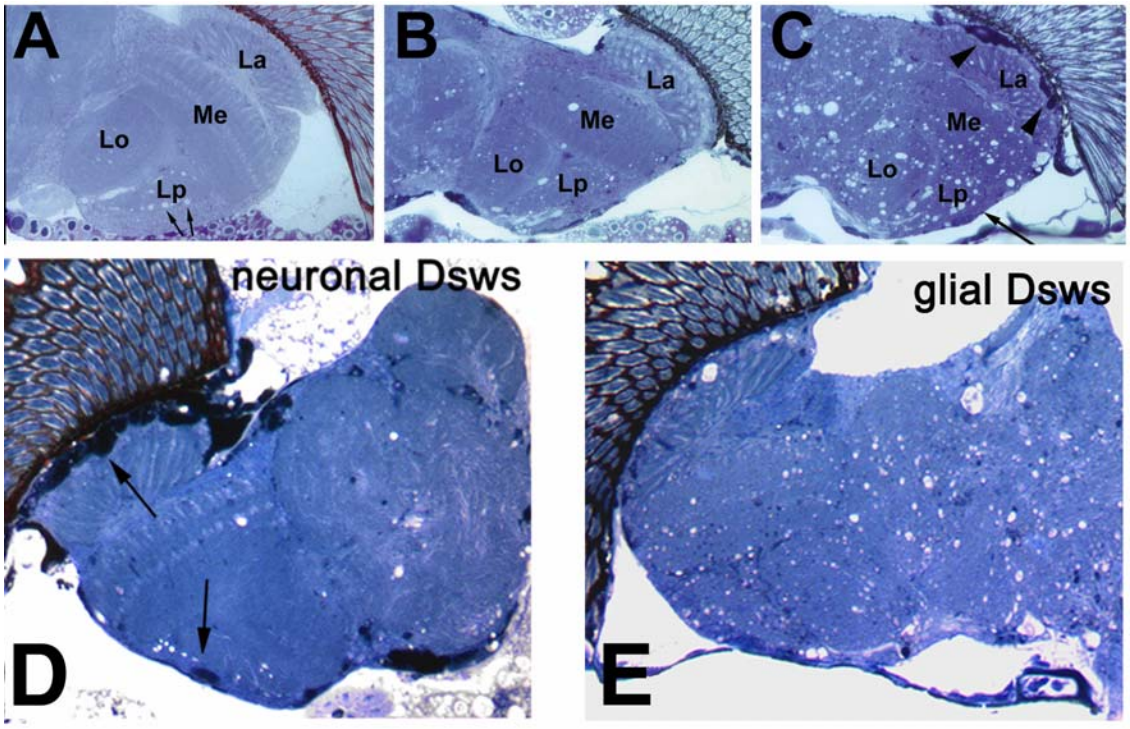

Figure 13: Neurodegeneration in *sws* mutant flies and rescue of *sws* phenotype

(A-C) Vacuolization and darkly stained structures, consisting of hyperwrapped glial membranes, (arrow-heads in C) increase with advancing age. These are accompanied by a thinning of the cortex (long arrow in C). (A) Wild type, age 20 days. (Arrows indicate white areas in the lobula plate that are not vacuoles but cross-sections of giant fibers). (B) sws^1 5 days old. (C) sws^1 20 days old. (D) Expressing the *Drosophila* gene in neurons almost completely inhibits the formation of vacuoles while the glial phenotype still persists (arrows). (E) Conversely expression of DSWS in glia prevents the glial phenotype but not the vacuolization.

1µm horizontal plastic head sections stained with toluidine blue. Re: retina; La: lamina; Me: medulla; Lo: lobula; Lp: lobula plate. Anterior is up.

GMR overexpression in the eye, a tissue where SWS seems to be weakly expressed endogenously if at all, leads to a slight rough eye phenotype (Figure 18B), also suggesting SWS toxicity (Muhlig-Versen et al. 2005). Interestingly *loco* overexpression will lead to lethality with certain insertion lines in a wt background but not in the *sws*[1] background (Muhlig-Versen 2001). Taken together these results suggest that SWS levels have to be carefully regulated in the cell for proper development.

These results from a transgenic yet unaltered SWS product were used as baseline for all the following experiments with transgenically inserted and modified SWS. For most lines overexpression testing with the GMR and Actin drivers was the first indicator for functionality because the eye phenotype is easy to see and Actin lethality is also quickly scored. However, the GMR-GAL4 overexpression lines show a slight rough eye phenotype even when no UAS construct is present. Therefore the experimental lines have to be compared to age matched controls carrying the GMR-GAL4 driver alone (Figure 14). The control flies shown are 14 days old, whereas some of the experimental data show younger flies. As the degeneration is progressive, older control flies can be used. If an interesting result was observed the constructs were also tested under the control of *elav* and *loco* as well as in the *sws* background.

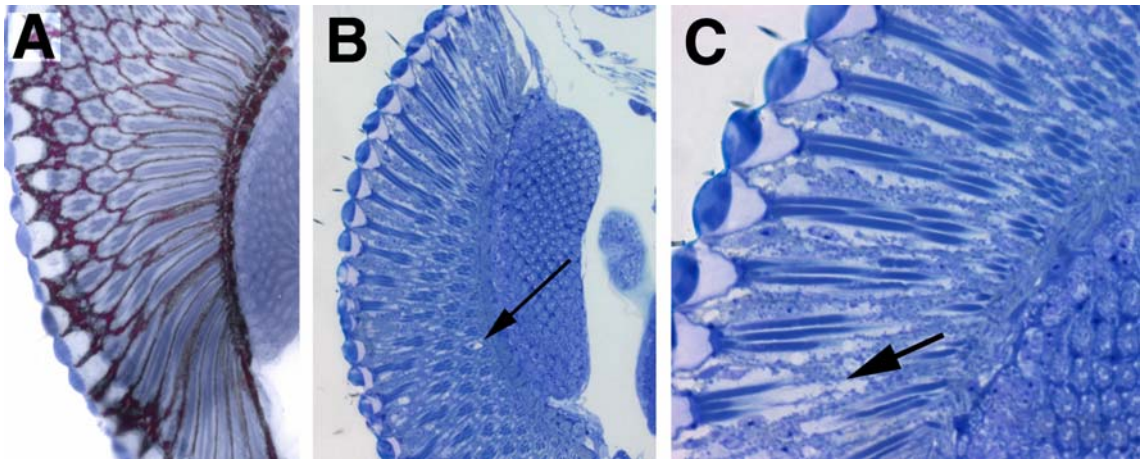

Figure 14: GMR-GAL4 control flies

Semithin plastic sections of (A) wildtype fly, (B and C) 14 d flies carrying the GMR-GAL4 driver but no UAS construct. Slight disorganization can be seen in the eye (arrows). (B) 40x (C) 100x. Experiments performed with constructs driven by the GMR-GAL4 driver have to be compared to these control flies (B and C).

A.4.2- The protein interaction domain

Two regions of SWS show high similarity with the regulatory subunits of *protein kinase A* (*pka*). Aminoacids 128-150 of SWS show high similarity with the protein interaction domain of the regulatory subunit of PKA (PKA-R). The PKA holoenzyme consists of two regulatory subunits and two catalytic subunits. The regulatory subunits have an inhibitory effect on the catalytic subunit. When dissociated from the regulatory subunits the catalytic subunit unfolds its enzymatic activity. The region mediating the binding to the catalytic subunits seems to be conserved between PKA and SWS. Three amino acids are shared by all regulatory subunit isoforms and also SWS (Figure 15A). One aa *sws* has been shown to be essential for binding and severely reduced the interaction when mutated in PKA (Poteet-Smith et al. 1997). By mutating this site at the critical argenine residue to an alanine ($R^{133}A$) a construct without functional binding domain (designated as SWS-$R^{133}A$) was created to study the role of this unit for the overall performance of the SWS protein.

Figure 15: Amino acid line-up of SWS and PKA-RI

Comparison of conserved amino acids between DSWS and the regulatory subunit of PKA. Shown are the sites critical to the binding of (A) the catalytic subunit of PKA and (B) cAMP. The critical residue for each functional domain is shown in red. Identical or similar amino acids are shown in green and marked with the one letter code of the amino acid or a plus sign respectively.

As described earlier for the wt SWS construct the function of the was tested in transgenic flies. If, analogous to the PKA subunits, this region is crucial for SWS binding to another protein, possibly PKA-C3, the ability of SWS-$R^{133}A$ to rescue the sws^1 phenotype and/ or cause an overexpression phenotype might be altered.

However the catalytic domain remains intact in this protein and the binding might represent an independent function SWS assumes in wt.

Alternatively this region might also be involved in the binding of the substrate, in this case a loss of efficient binding should have a similar effect as catalytically less or inactive protein.

A.4.2.1- Overexpression of SWS-R^{133}A

Overexpression of SWS-R^{133}A with the eye specific GMR-driver resulted in moderate degeneration of the eye (Figure 16). It is significantly more severe than the rough eye phenotype observed with the overexpression of the wt SWS construct (Figure 18B). This shows that this region has a physiological function which is altered by the mutation. High amounts of SWS-R^{133}A seem to have a more deleterious effect on eye development than wt SWS.

Interestingly SWS-R^{133}A driven by the Actin driver yields viable flies whereas wt SWS driven by Actin will keep flies from developing to adult stages (Muhlig-Versen 2001). This seems to be contradictory to the GMR overexpression results which suggest that SWS-R^{133}A is more toxic than wt SWS. A possible explanation for this phenomenon is that the genetic background has changed over the years since the experiments with wt SWS have been performed by Max Mühlig-Versen (Muhlig-Versen 2001) compared to these more recent results produced in this thesis. To solve this question some basic experiments with the wt SWS are being repeated to make sure accumulation of attenuating mutations did not change the severity of the degenerative phenotype.

A.4.3- The cAMP binding domain

A second domain within the SWS protein was also identified by similarity to the PKA protein. The PKA holoenzyme dissociates upon binding of cAMP and allows the catalytic subunit to unfold its kinase activity. The region that binds cAMP in PKA-R shows similarities to amino acids 553-574 in SWS (Figure 15B). This indicates that SWS might also be regulated by cAMP.

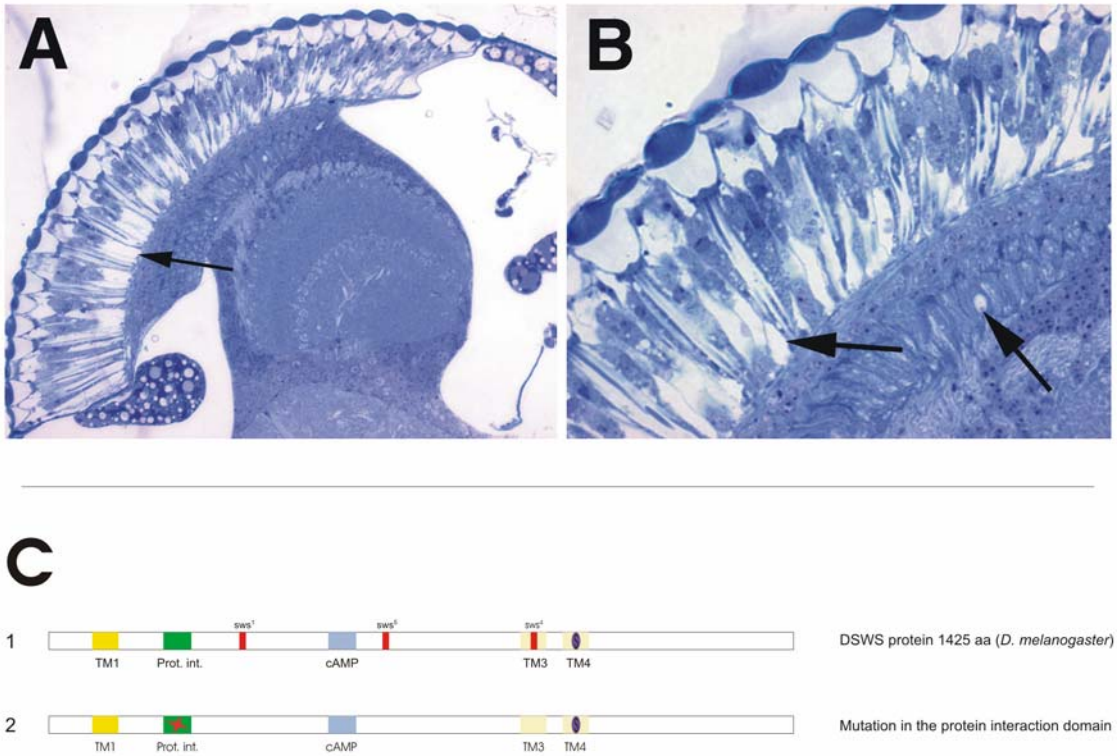

Figure 16: GMR overexpression of SWS-R^{133}A (protein interaction domain mutant)
(A and B) 7 day old GMR-GAL4/ UAS-SWS-R^{133}A flies. Degeneration of the retina and some vacuoles in the lamina are visible (arrows), stronger than in the overexpression of wild-type SWS (Figure 18B) (A) 40x (B) 100x. Compare to Figure 14 for GMR-GAL4 controls. Semi-thin horizontal plastic sections. (C) Map of the wild-type protein (1) and the mutated construct (2).
TM1: transmembrane domain 1 TM3/ TM4: putative transmembrane domains, *sws*$^{1/4/5}$: sites of identified *sws* mutations, S: Catalytic site serine, Prot. int.: Area with homology to the site binding the catalytic subunit of PKA, cAMP: Area with homology to the site binding cAMP in PKA, Star: site of mutation.

Although in vitro testing of NTE activity showed no correlation between cAMP concentration and esterase activity an experiment using the endogenous environment might be more efficient. The in vitro test uses artificial substrates to test the enzymatic activity which might lead to differing results than in an animal. Another limitation of the in vitro assay is that it can only test for the esterase activity. Any other functions would not be noticed, unlike in an experiment involving transgenic flies.

To test whether SWS function is influenced by the cAMP binding site a mutant form of SWS was created that should not be able to bind cAMP anymore. The cAMP domain has an essential glycine necessary for binding of the cyclic nucleotide. Replacing this aa results in loss of response to cAMP (Taylor et al. 1990). A construct replacing this

glycine by a glutamine ($G^{557}Q$) should abolish cAMP responsiveness (Figure 15B). This construct (SWS-$G^{557}Q$) was used to test cAMP responsiveness in the *Drosophila* system.

A.4.3.1- Overexpression of SWS-$G^{557}Q$

Overexpression of SWS-$G^{557}Q$ resulted in very mild eye degeneration in aged flies. However this degeneration was hardly discernable from the defects in flies carrying only the GMR driver (Figure 17A). The GMR driver by itself is known to cause a slight rough eye phenotype. Apparently the overexpression of SWS-$G^{557}Q$ has no effect on the development of the eye, even very old flies show no drastic degeneration phenotype (Figure 17B). This suggests that cAMP binding is necessary for normal activity of SWS because overexpression of wt SWS will lead to more severe eye degeneration (Figure 18B). Therefore the lack of toxicity shown by SWS-$G^{557}Q$ points to a loss of functionality. However further experiments have to be performed with this line, a side by side comparison to age matched GMR-DSWS flies will give a clearer picture of the effect SWS-$G^{557}Q$ has.

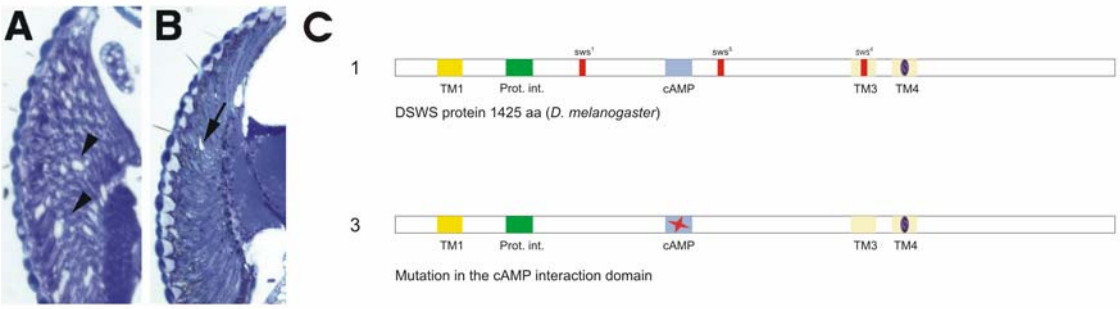

Figure 17: GMR overexpression of SWS-$G^{557}Q$ (cAMP binding domain mutant)

(A) Control fly carrying the GMR-GAL4 driver but no UAS-construct. At this age some retinal degeneration can be observed in the control flies (arrowheads). (B) GMR-GAL4/ UAS-SWS-$G^{557}Q$ flies. Degeneration in the construct carrying flies does not appear to be significantly worse than in the controls, although the flies are very old. (A and B) Semi-thin horizontal sections of 45 day old flies. (C) Map of the wild-type protein (1) and the mutated construct (3). For labeling see Figure 16.

A.4.4- Esterase independent function of SWS

Intoxication of NTE by certain organophosphates can lead to degeneration of nerve cells. However not all OPs that are able to inhibit NTE esterase function are also able to induce neurodegeneration. Only certain organophosphates capable of triggering the so called "aging reaction" result in degeneration of the nerve cells (Johnson 1982). Other "non-neuropathic" organophosphates inhibit the NTE enzyme activity but do not lead to the organophosphate induced delayed neuropathology (Petroianu et al. 2001).

Hypothetically as a result of the aging reaction another yet unknown function (non-esterase function) of the SWS protein could be inhibited. If this function is crucial for the survival of the neural cells, this might explain the neurodegeneration induced by neuropathic OPs but not by non-neuropathic OPs.

An alternative explanation would be a gain-of function induced by neuropathic OPs either of the esterase or non-esterase function which would result in a dominant deleterious effect. Although the esterase function seems to be inhibited in the in vitro test it has to be taken into account that this is an artificial substrate tested outside of a cell (Johnson and Richardson 1983; Atkins and Glynn 2000). Nevertheless it seems highly unlikely that organophosphates, which have been shown to covalently bind to the catalytic center of serine esterases, would actually increase the metabolic rate of SWS.

A.4.4.1- Function of the 80 N-terminal amino acids

Max Mühlig-Versen produced a mutated form of the SWS protein that lacked the first 80 amino acids, but was otherwise identical to the wt SWS (SWSΔ1-80). Under the control of GMR it showed a severe deleterious effect when expressed in the *Drosophila* eye tissue (Figure 18C and D)(Muhlig-Versen 2001). The overexpression of SWSΔ1-80 had a more severe effect than the wt SWS under the control of the same driver. Over-expression of SWSΔ1-80 under Actin control is lethal just as overexpression of wt SWS.

When expressed in the *sws*^{1} background SWSΔ1-80 will shorten the life span of these flies instead of rescuing the phenotype as wt SWS does. Expression of SWSΔ1-80 in

the *sws*[1] background with the *loco* driver is lethal to the host flies (Muhlig-Versen 2001).

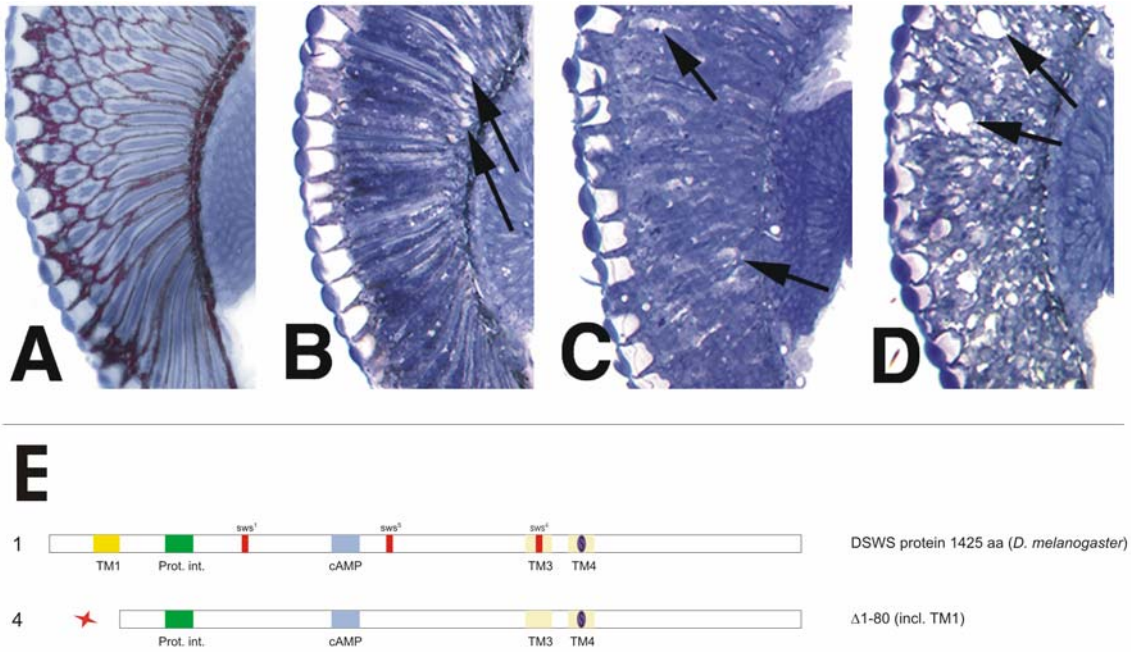

Figure 18: Ectopic expression of wt and mutated SWS in the eye

(A-D) Semi-thin horizontal section from 7 day old flies (A) wild type eye. (B) A 7day old fly that ectopically expresses wild type DSWS in the eye driven by the GMR enhancer reveals moderate degeneration (arrows). (C) Induction of SWSΔ1-80 already causes retinal degeneration in a 1day old animal and cell death, which is dramatically increased in (D) 7day old flies. (E) Map of the wild-type protein (1) and the truncated construct SWSΔ1-80 (4). For labeling see Figure 16. (modified; from Muhlig-Versen 2001)

The intracellular localization of SWSΔ1-80 is different from that of wt SWS. While wt SWS seems to be strongly localized to vesicles (Figure 19A and B) SWSΔ1-80 lost that specificity. It seems to be found in a more diffuse manner throughout the cytoplasm (Figure 19C).

This indicates an important role for the N-terminal part of SWS. It appears that SWSΔ1-80 actually has a dominant negative effect. Possibly this is due to the same non-esterase function that causes the degenerative phenotype in SWS modified by the aging reaction.

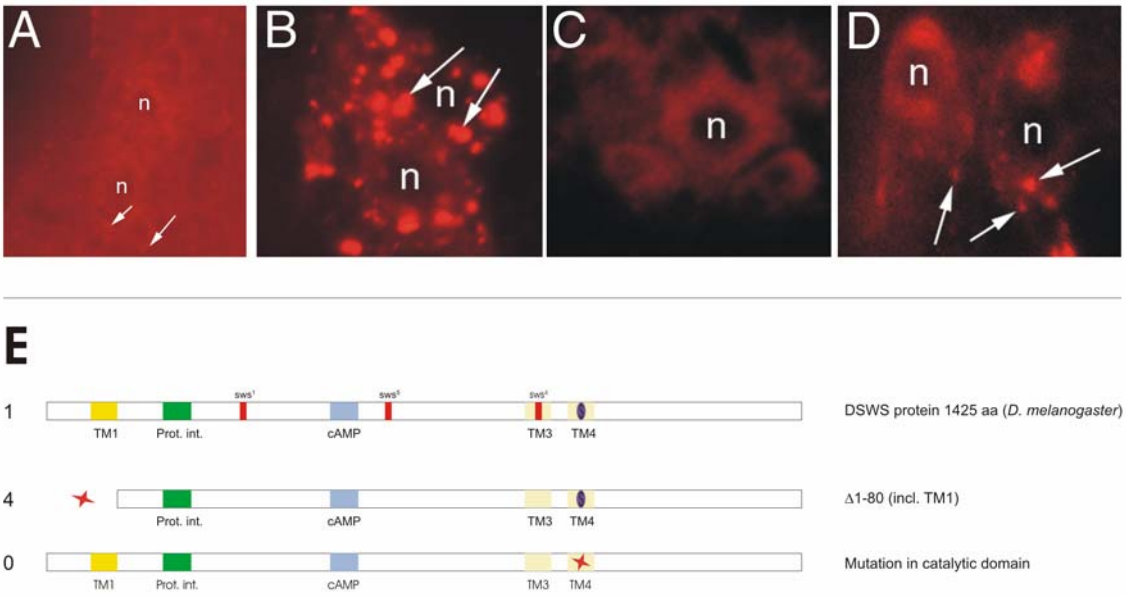

Figure 19: α-SWS stainings on different, overexpressed SWS constructs

Paraffin sections of α-DSWS stained cortex region. (A) wt. (B) *elav*-driven UAS-DSWS, localization to vesicles (arrows) can be observed. (C) *elav*-driven UAS-SWSΔ1-80. Localization to vesicles appears to be lost in this construct. (D) *elav*-driven UAS-SWS-S^{985}D. Localization seems to be more diffuse than in (B). n: nucleus. (E) Map of the wild-type protein (1) and the two mutated constructs (4 and 0). For labeling see Figure 16.

An alternative explanation is that the loss of the first TM (aa33-55) causes the protein to be misslocalized within the cell. As shown earlier (A.2.1- Subcellular localization, p. 37) SWS is localized to vesicles, it is thought that this is in part due to the first TM. However the first 80 aa might also harbor a signaling sequence N-terminally to the first TM that might be responsible for correct intracellular localization.

If the effects of SWSΔ1-80 in fact has similarities to the mechanisms involved in the aging reaction, the in-depth analysis might give us insights into these alternative roles of SWS.

A.4.4.1.1- Mutation of the catalytic site serine

To determine which characteristics of SWS are attributable to the already known esterase function and which might be due to the postulated non-esterase function a construct without any classical esterase function was necessary. In this fashion the influence of the esterase function would be eliminated. A construct produced by Max Mühlig-Versen that has an aspartate instead of a serine in its active site (SWS-S^{985}D)

seems to be functionally inactive in all physiological and enzymatic assays (Muhlig-Versen 2001). Expression of SWS-S^{985}D in the *sws*^{1} background shows no signs of rescue and overexpression in the wt background shows no detrimental effect. The in vitro activity of this construct in a standard assay is severely reduced and points to a total loss of esterase function in this mutant (Muhlig-Versen 2001).

The S^{985}D construct also exhibits some signs of slight cellular misslocalization (Figure 19D). This is slightly surprising considering only one aa is changed. However this aa seems to be in a potential transmembrane domain and therefore could change the charge of this portion of the protein thereby hampering its function as a transmembrane domain. Localization to the cell membrane might be crucial to the function of SWS. In vitro SWS shows no activity unless associate with microsomes (Davis and Richardson 1987; Pope and Padilla 1989).

A.4.4.1.2- Combination of the Δaa1-80 deletion and S^{985}D mutation (SWSΔ1-80/ S^{985}D)

The combination of the Δaa1-80 and the S^{985}D mutation (SWSΔ1-80/ S^{985}D) makes it possible to test if serine esterase activity is involved in the generation of the severely deleterious phenotype observed in SWSΔ1-80. If the deleterious effect can be observed despite the lack of a functional catalytic esterase site a non-esterase function has to be postulated. It is also thinkable that the active site serine is involved in the activation of a non-esterase function. In the aging reaction mechanism an organophosphate binds to the active site serine before the relocation of an alcyl group onto another aa within NTE. Therefore although the serine blockage itself is not sufficient to cause the degenerative effect it is still necessary for the aging reaction.

Overexpression of SWSΔ1-80/ S^{985}D

SWSΔ1-80/ S^{985}D is viable under the control of all used drivers (*elav*, *loco*, GMR and Actin). Driven with the GMR construct SWSΔ1-80/ S^{985}D shows a slightly degenerated eye (Figure 20). which is definitively less deformed than the GMR driven SWSΔ1-80 eye but is not as healthy as the SWS-S^{985}D (Muhlig-Versen 2001). Apparently the deleterious effect is not completely independent of the catalytic site serine, but this

result also shows that there is an additional factor causing an physiological effect in the *Drosophila* eye besides the serine esterase function.

Further analysis of this construct is necessary, specifically plastic sections will give a higher optical resolution of the differences between SWSΔ1-80 and SWSΔ1-80/ S^{985}D. Once again genetic background might play a role and side by side preparation of SWSΔ1-80/ S^{985}D, SWSΔ1-80 and S^{985}D will give a more exact picture.

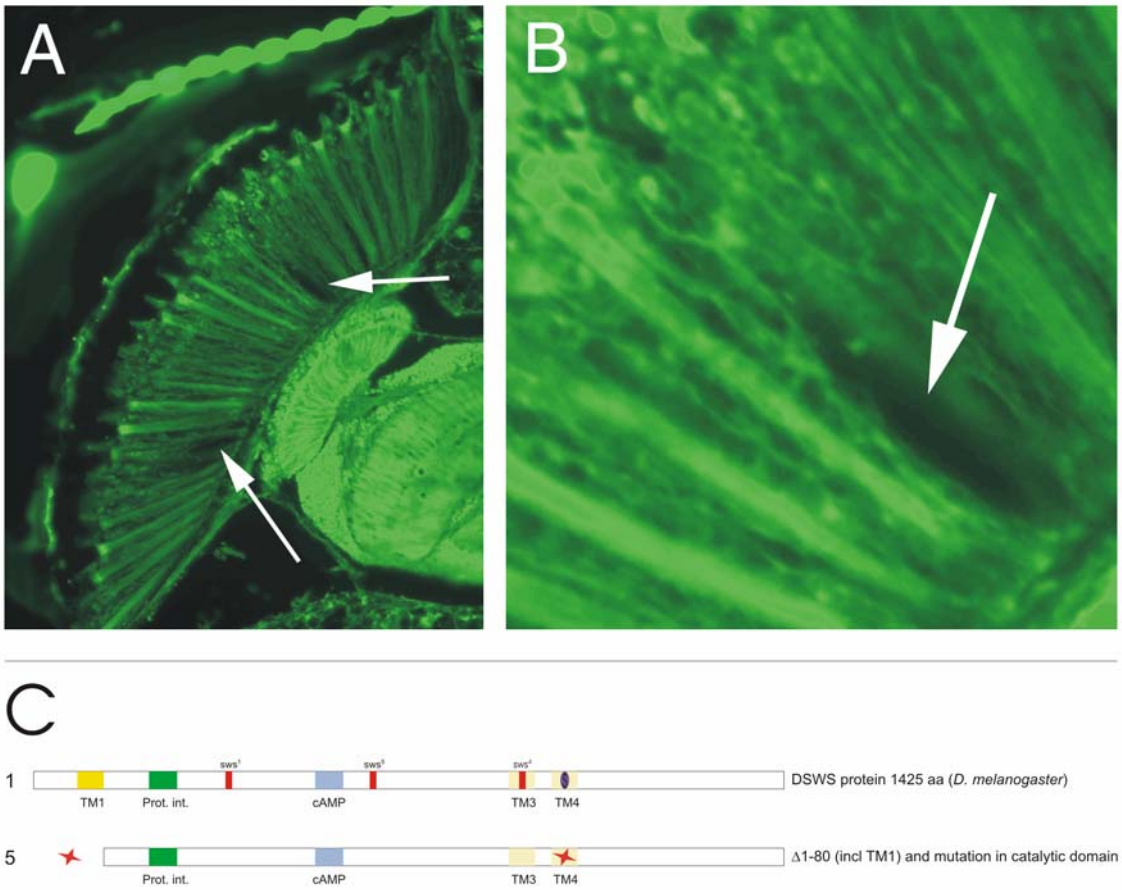

Figure 20: GMR overexpression of SWSΔ1-80/ S^{985}D

(A and B) Paraffin sections of 7 day old GMR-GAL4/ SWSΔ1-80/ S^{985}D flies. Unlike SWS–S^{985}D over-expression of SWSΔ1-80/ S^{985}D shows slight degeneration of the retina (arrows) but less severe than in SWSΔ1-80 (Figure 18C and D). Compare to Figure 14 for GMR-GAL4 controls. (C) Map of the wild-type protein (1) and the mutated construct (5). For labeling see Figure 16.

A.4.4.2- Detailed analysis of the functional domains in the 80 N-terminal amino acids

Deletion constructs from the N-terminal part have shown that the first 80 amino acids harbor one or more important functional domains. Two stretches within that region are striking for a potential function (Figure 12). The most conspicuous is the first TM ranging from amino acids 33-55. The second stretch is the first few amino acids up to the first TM. Typically signaling sequences are found within the first few amino acids. To distinguish between the contribution of each of these domains to the effect of SWSΔ1-80, if any, two individual deletions of these domains were created (Figure 21(6) and (8)). A combination construct yielding a catalytically inactive ($S^{985}D$) form of each of these single deletions was made to determine the non-esterase function of these parts (Figure 21 (7) and (9)).

Figure 21: Map of the SWS Protein and all mutated constructs

Map of the wild-type protein (DSWS) (1) and the mutated constructs created for analysis (4-9). (4) Construct with deletion of amino acids 1-80 (SWSΔ1-80) and (5) an additional point mutation in the catalytic site serine (SWSΔ1-80/ $S^{985}D$). (6) Construct with deletion of amino acids 1-35 (SWSΔ1-35) and (7) an additional point mutation in the catalytic site serine (SWSΔ1-35/ $S^{985}D$). (8) Construct with deletion of amino acids 33-55 (SWSΔ33-55) and (9) an additional point mutation in the catalytic site serine (SWSΔ33-55/ $S^{985}D$).

TM1: transmembrane domain 1 TM3/ TM4: putative transmembrane domains, $sws^{1/4/5}$: sites of identified *sws* mutations, S: Catalytic site serine, Prot. int.: Area with homology to the site binding the catalytic subunit of PKA, cAMP: Area with homology to the site binding cAMP in PKA, Star: site of mutation.

A.4.4.2.1- Deletion of the first TM (SWS∆33-55)

Amino acids 33-55 represent a region that was identified by transmembrane prediction programs to have a high probability of being a transmembrane domain. Three further weaker transmembrane domains were predicted to the C-terminal side of the protein. According to results in the mouse NTE only the first transmembrane domain was confirmed in vivo, however the existence of further TMs was not excluded (Li et al. 2003).

At the first glance the transmembrane domain seems to be the most important part within the first 80 amino acids of the protein. It is thought to anchor the protein to the membrane although it has been shown in the mouse orthologue NTE, that localization is retained even when this transmembrane domain is deleted (Li et al. 2003). Nevertheless Max Mühlig-Versen (2001) has shown that loss of the transmembrane domain and all of the N-terminal portion of the SWS protein will result in a serious deleterious effect (Figure 18C and D) and loss of discrete localization within the cell (Figure 19C).

Overexpression of SWS∆33-55

Overexpression of this construct has a much milder effect than SWS∆1-80 (Figure 22). A mild rough eye phenotype can be seen in 7 day old flies which is comparable to flies carrying the GMR driver alone (Figure 14). Therefore deleting the transmembrane alone is not sufficient to cause the severe degeneration caused by SWS∆1-80.

A.4.4.2.2- Combination of the ∆aa33-55 deletion and $S^{985}D$ mutation (SWS∆33-55/ $S^{985}D$)

SWS∆33-55 did not show any obvious overexpression phenotype compared to control flies carrying the GMR-GAL4 construct alone (Figure 14), therefore it was not expected to see any effect with SWS∆33-55/ $S^{985}D$ either, considering it is the same construct except for lacking the catalytic serine.

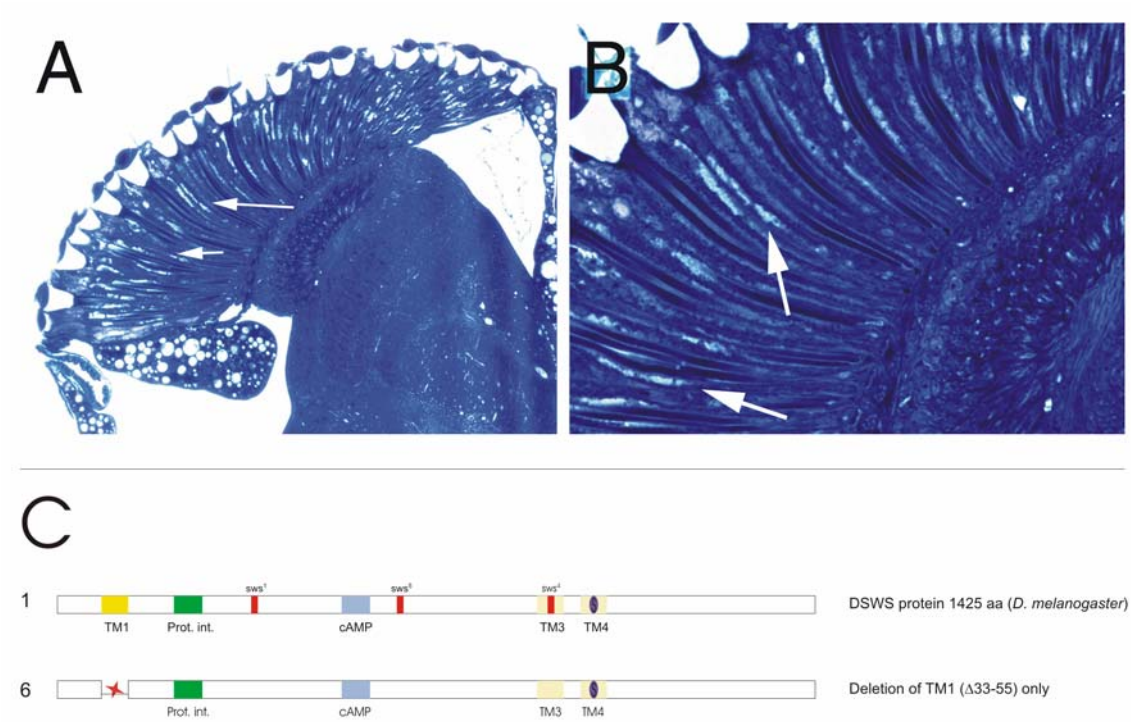

Figure 22: GMR overexpression of SWSΔ33-55

(A and B) Semi-thin horizontal sections of 7 day old GMR/ SWSΔ33-55 flies. (A) 40x, (B) 100x. Degeneration in the eye can be observed (arrows), however the effect is a lot milder than in SWSΔ1-80 (Figure 18D). Apparently deleting the transmembrane is not sufficient to create a strong deleterious effect by itself. Compare to Figure 14 for GMR-GAL4 controls. (C) Map of the wild-type protein (1) and the mutated construct (6). For labeling see Figure 21.

Overexpression of SWSΔ33-55/ $S^{985}D$ revealed only very slight degeneration of the eye. This can be attributed to the fact that GAL4 overexpression by the GMR enhancer itself is unhealthy for the *Drosophila* eye (Figure 14). The construct itself had no additional effect on the rough eye phenotype (Figure 23).

A.4.4.2.3- Deletion of the first 35 amino acids (SWSΔ1-35)

A construct without the first 35 amino acids would reveal if there is an important domain, possibly a signaling sequence, in the N-terminal part of the protein. Considering that SWSΔ33-55 does not show the same deleterious effect as SWSΔ1-80 it seemed likely that there is a relevant functional domain in the first 35 amino acids. Unfortunately when this construct was made a mutation found its way into the PCR product used to produce the N-terminally deleted fragment. As a consequence of this there would have been an undesirable $N^{312}D$ substitution in the construct. It was

decided that this is inadequate and the construct was discarded in favor of a new construct without any mutations. The results of these transgenic flies will be available soon.

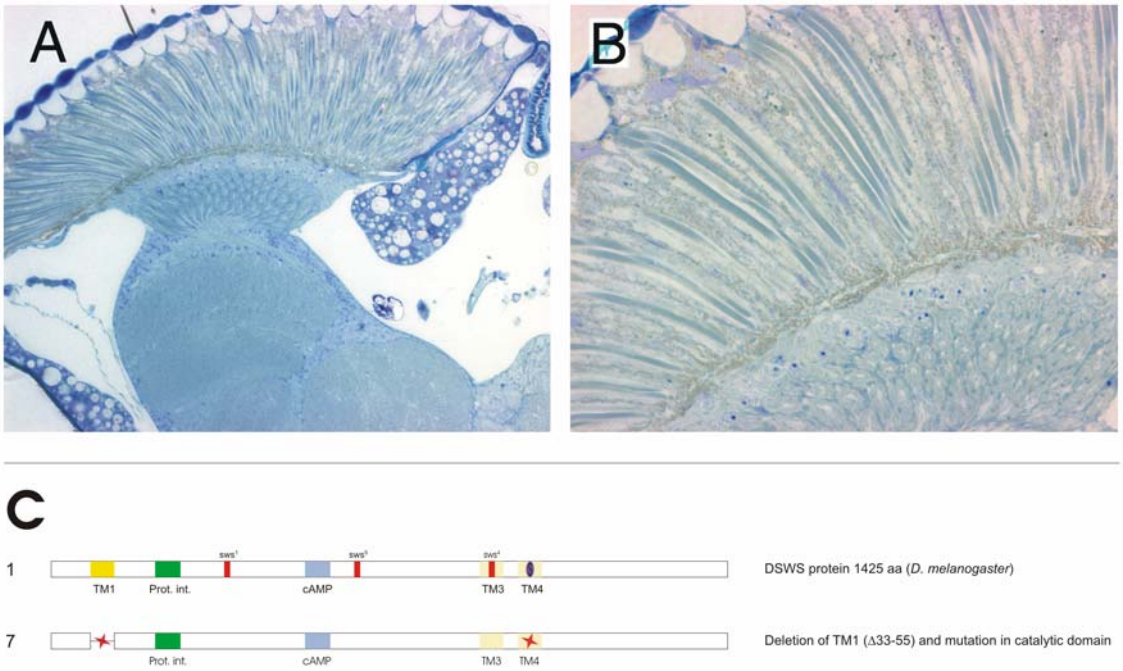

Figure 23: GMR overexpression of SWSΔ33-55/ $S^{985}D$

(A and B) Semi-thin horizontal sections of 14 day old GMR/ SWSΔ33-55/ $S^{985}D$ flies. (A) 40x, (B) 100x. There is almost no degeneration visible in these flies, as expected by comparison with SWSΔ33-55 (Figure 22) and SWS-$S^{985}D$ (Muhlig-Versen 2001). Both of these constructs show no deleterious overexpression phenotype either. Compare to Figure 14 for GMR-GAL4 controls. (C) Map of the wild-type protein (1) and the mutated construct (7). For labeling see Figure 21.

In case SWSΔ1-35 flies show no deleterious effects either, other possibilities have to be considered. One hypothesis is that both areas have to be deleted and only the cumulative effect of both show the same effect as SWSΔ1-80. Another explanation would include the amino acids 55-80 which have not been analyzed yet.

A.4.4.2.4- Combination of the Δaa1-35 deletion and $S^{985}D$ mutation (SWSΔ1-35/ $S^{985}D$)

As mentioned for SWSΔ1-35 (see above) the PCR used to create both, SWSΔ1-35 and SWSΔ1-35/ $S^{985}D$, contained a mutation. Unfortunately in the case of SWSΔ1-35/ $S^{985}D$ this was not noticed until after the transgenic flies were created. For this reason these results have to be observed with caution.

SWSΔ1-35/ $S^{985}D$ was meant to answer the question if the catalytic serine is needed for the deleterious effect observed in SWSΔ1-80. When overexpressed with the GMR driver SWSΔ1-35/ $S^{985}D$ showed no degeneration (data not shown).

However without the results from SWSΔ1-35 the results from SWSΔ1-35/ $S^{985}D$ are hard to interpret if no deleterious effect is seen. It is impossible to say if this is due to SWSΔ1-35 by itself not having an effect or the effect disappearing because of the loss of catalytic activity. In order to draw a final conclusion the results from SWSΔ1-35 have to be included in the analysis of the results.

A.5- Influence of SWS on the lipid metabolism

The SWS protein is known to be a serine esterase and is localized to membranes, probably the ER membrane. The biological function of SWS is not yet known. SWS has motifs shared by serine esterases and has been shown to cleave phenyl valerate (PV) in vitro when associated to microsomes (Johnson 1969; Johnson 1977). Therefore the thought occurred that it might be involved in the lipid metabolism of the cell membrane. It had been shown earlier that human NTE catalyzes the degradation of membrane lipids in vitro (van Tienhoven et al. 2002) and both the human and the yeast orthologue of NTE have been shown to deacetylate phosphatidylcholine (PtdCho) in yeast cells (Zaccheo et al. 2004).

A.5.1- Lipid and sterol measurements

In order to elucidate the endogenous function of the SWS protein in *Drosophila* the lipid content of sws^1 and *sws* overexpressing flies (*elav* driven) was compared to that of wt flies. Flies overexpressing SWS in neurons show a two-fold increase in esterase

activity measured in a standard esterase assay, whereas *sws*[1] flies have an esterase activity level that is within the background noise (Muhlig-Versen 2001).

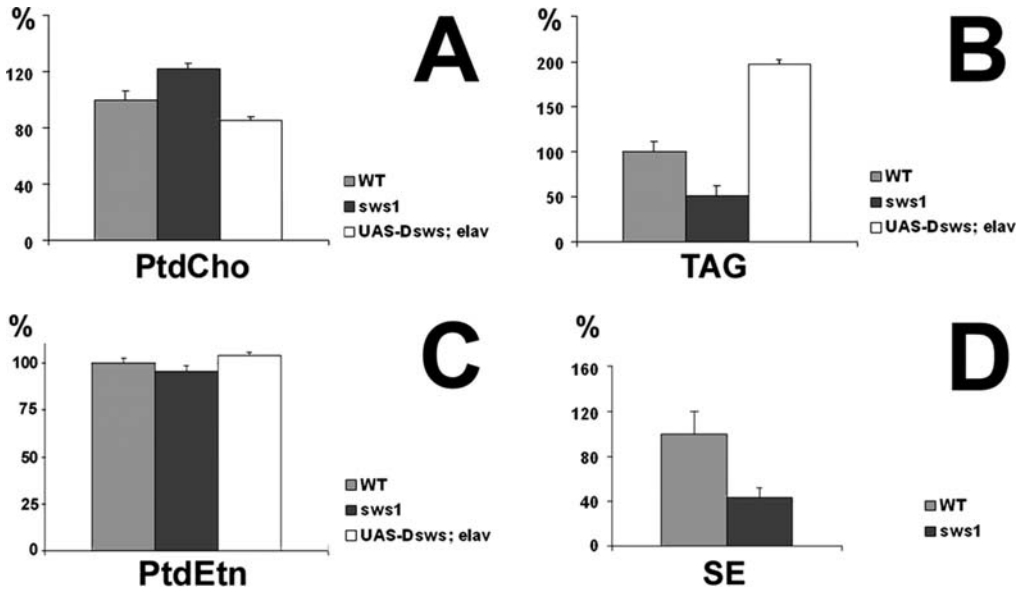

Figure 24: Different lipid content in *sws* deficient and *sws* overexpressing flies

Head homogenates from *sws*[1] mutant flies and flies overexpressing DSWS in neurons were compared with wild-type (WT) controls. (A) Phosphatidylcholine (PtdCho) levels are increased in the mutant and decreased in flies expressing additional SWS. (B) The opposite effect is seen for the levels of Triacylglycerids (TAG). (C) The level of Phosphatidylethanolamine (PtdEtn) is not significantly changed. (D) Also, the level of sterol ester (SE) is reduced in the *sws*[1] mutant. All values are expressed relative to wild type (100%). SEMs are indicated.

In *Drosophila* an increase in phosphatidylcholine was observed in the *sws*[1] mutant, conversely in the overexpression flies phosphatidylcholine levels were reduced compared to wt (Figure 24). Triacylglycerides on the other hand are reduced in *sws*[1] but increased in *elav*-SWS flies. Also sterol esters (SE) are decreased in *sws*[1] flies. Levels of Phosphatidylethanolamine (PtdEtn), which is a reactant that produces phosphatidylcholine by methylation, are not significantly changed in any of the studied genotypes. This result reflects the reaction mechanism of lipid synthesis in mammalian cells. Diacylglycerol is a precursor for phosphatidylcholine and triacylglycerol (TAG), thus inhibition of phosphatidylcholine synthesis results in increased triacylglycerine levels and vice-versa (Allan 2000; Jackowski et al. 2000).

A.5.2- Genetic interaction with enzymes catalyzing transacylations

A model of the potential reaction mechanism resulting from these findings would be that SWS catalyzes the transfer of an acyl group from phosphatidylcholine onto cholesterol resulting in cholesterol ester and lysolecithin (Figure 25). Blocking this reaction would result in an increase in phosphatidylcholine and cholesterol and a decrease in cholesterol esters (a sterol ester) and Lysolecithin (which can be metabolized into triacylglycerol). These results would be consistent with the findings observed except for the increase in cholesterol. However cholesterol is metabolized by a lot of other enzymes therefore the impact of lacking SWS might be absorbed by other cholesterol metabolizing enzymes. Interestingly the enzyme lecithin cholesterol acyltransferase (LCAT) has been shown to catalyze the transfer of an acyl group from PtdCho to cholesterol (Jonas 2000).

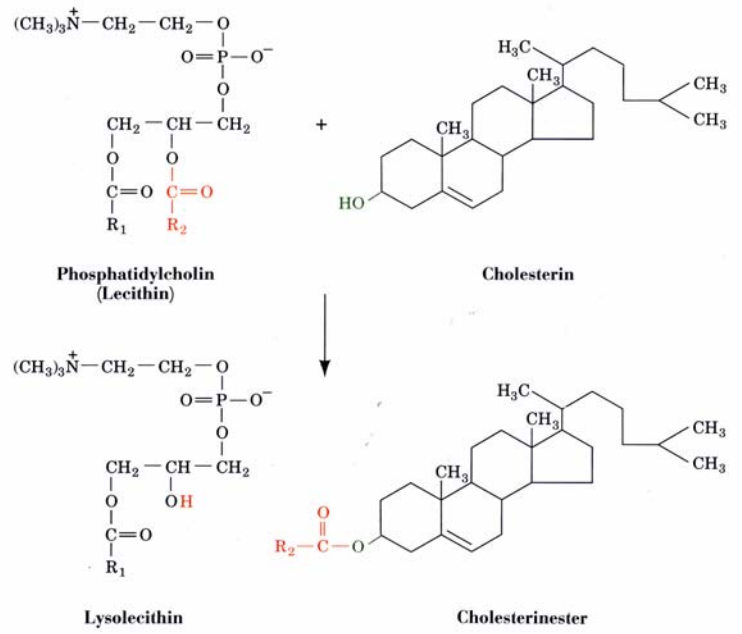

Figure 25: Reaction mechanism of LCAT

The results from the lipid content measurements suggest that SWS could act similarly to LCAT. In *sws*[1] mutants phosphatidylcholine levels are elevated whereas triacylglycerol and sterol esters are reduced and vice versa in flies with additional SWS. Lysolecithin can be metabolized to triacylglycerol, cholesterol esters are sterol esters. Therefore by blocking the LCAT reaction it would be expected to get a similar accumulation as was observed with the blocking of the SWS enzyme.

SWS has no significant homology to LCAT and a *Drosophila* LCAT exists, therefore it appears to be unlikely that SWS catalyzes the LCAT reaction. SWS might indirectly influences the lipid metabolism by regulating LCAT. In this case a double knockout of SWS and LCAT should show a worse phenotype than either of the mutants by itself. Currently *lcat* deficient flies are being crossed to sws^5 to create double mutant flies.

SWS might also catalyze a reaction that involves slightly different reactants in the same pathway. Special consideration has to be given to the fact that LCAT is expressed in different tissues than SWS. SWS is expressed mainly in the central and peripheral nervous system, LCAT has been shown to be greatly expressed in the liver, although smaller amounts can be found in the brain (Collet et al. 1999). SWS could have a similar function in transferring acyl groups from PtdCho to cholesterol in the central nervous system as LCAT does in other tissues.

B- olk

B.1- The *olk* phenotype

B.1.1- Anatomical defects in specific brain areas

olk mutant flies show an unusual organization of axon bundles and fiber tracts in silver stainings. The mutant *omb* (*optomotor-blind*) shows a silver staining phenotype that is virtually identical to *olk*. Hence the name *olk* for *omb-like*. In both fly mutants the giant fibers of the lobula plate are indiscernible (Figure 26).

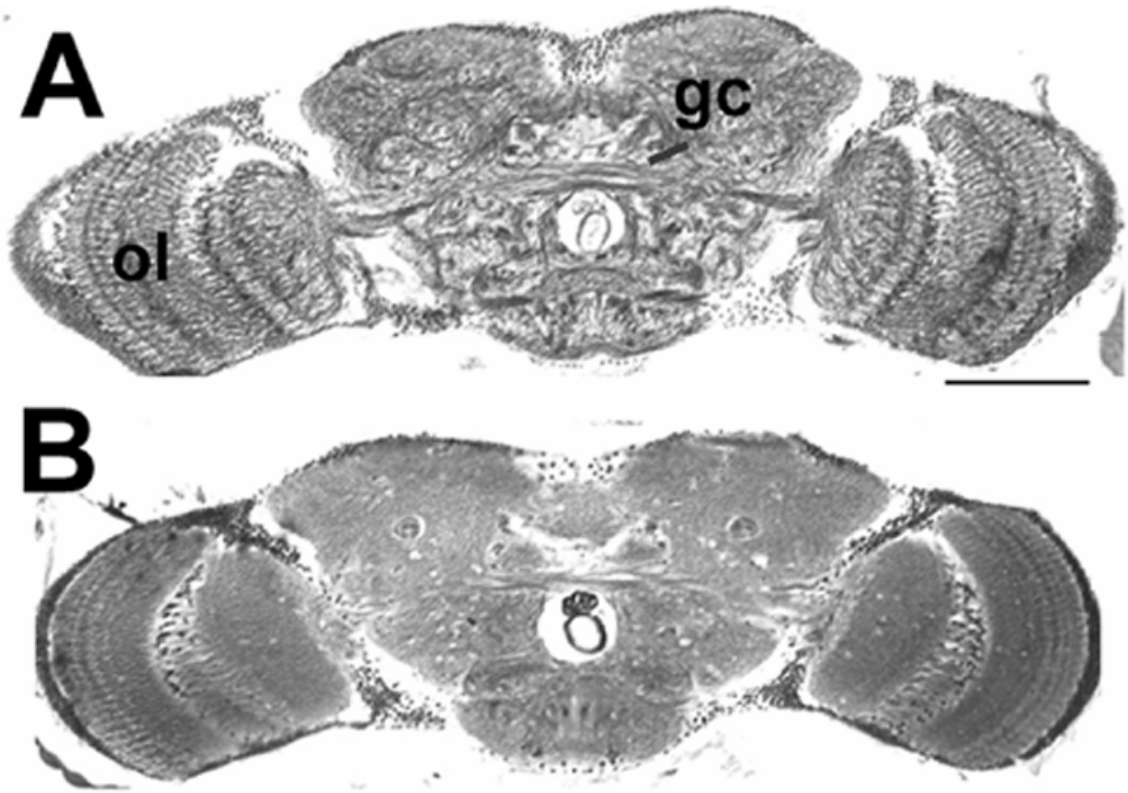

Figure 26: Fiber structure defects visible in silver stainings
(A) Silver staining reveals fibers and axon bundles in a wild-type head section. (B) In *olk*[1] the fibers are much less prominent, revealing a defect in fiber structure in *olk*.

The brain development in *olk* mutant flies seems to be unaffected by this mutation. *olk* flies show no visibly different morphology one day after eclosion from the age matched

wild-type controls. However with increasing age signs of degeneration become apparent in certain areas of the brain such as the calyces (at around 6 d), a substructure of the mushroom bodies, and at later stages (10 d) the antennal lobes and the mechanosensory neuropil of the ventrolateral protocerebrum (Figure 27). The mean size of vacuoles in the mechanosensory neuropil of *olk*^{1} increases from about 2 µm^2 to 11 µm^2 at the age of 8 days to 25 µm^2 in 14 day old *olk*^{1} flies. Conversely the number of flies without any vacuoles decreases dramatically with the progression of age.

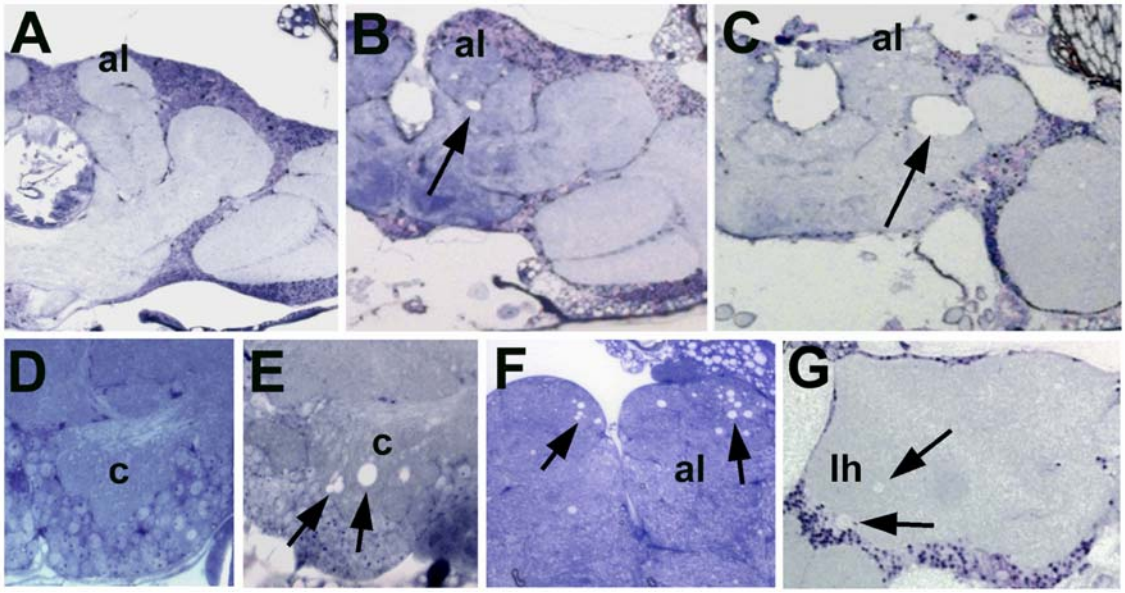

Figure 27: Anatomical phenotype of the *olk* mutant

Progressive neurodegeneration can be observed in the *olk*^{1} mutant. (A and D) 1 day after eclosion *olk*^{1} mutant fly head show no degeneration. (E) First signs of abnormalities can be found in 6-day-old mutants, specifically in the calyx (c). (B) At 10 days of age vacuoles can be found in the mechanosensory neuropil of the lateral protocerebrum and (F) the antennal lobes (al). With further aging (20d) (C) the lesion in the mechanosensory neuropil enlarges dramatically and (G) vacuoles can also be found in the region of the lateral horn (lh) of the protocerebrum. 1µm horizontal plastic head sections stained with toluidine blue.

Dying cells displayed signs of necrosis such as swelling and lysis of the somata without resorbtion of the nuclei. Electron microscopy (EM) pictures showing a vacuole in the neuropil (Figure 28A) and the cortical cell layer (Figure 28B) revealed degeneration of nerve fibers as well as neuronal cell bodies. The presence of an intact nucleus together

with the swelling and lysis of the affected cells in semi-thin plastic sections suggests that these neurons undergo necrotic cell death (Figure 28C).

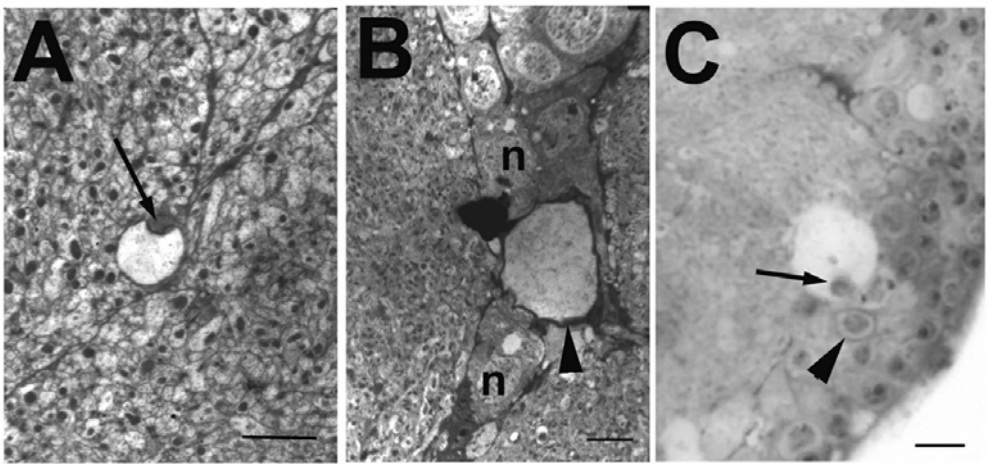

Figure 28: Necrotic cell death in *olk*

(A) Electron micrograph of a vacuole that formed in the neuropil of the antennal lobe of a 6 day old *olk* fly. A residual fragment of the degenerated fiber is still localized within the vacuole (arrow). (B) EM of a 14 day old *olk* fly brain, showing a vacuole surrounded by a prominent glial sheath that was found near the antennal lobe in the cortical region occupied by neuronal cell bodies. (C) A plastic section of a 15 day old *olk* mutant brain show that a residual nucleus (arrow) could still be detected within the vacuole, suggesting necrotic cell death. The arrowhead points to the thick glial sheath surrounding an adjacent neuron. n: nucleus. Scale bars: A= 1 µm, B= 2 µm, C= 5 µm.

B.1.2- Selective degeneration of projection neurons

To study what kind of cells where involved in this specific degeneration process, the GAL4/ UAS system was used to express GFP in several specific cell types. Considering the localized nature of anatomical defects it was expected to find specific cells that are more affected by the cell death. Using the D52H, 2384 and MB244-36y drivers for expression of GFP in Kenyon cells of the mushroom bodies as well as C232-GAL4 for the ring neurons of the central complex showed no unusual loss of GFP expression or the respective GFP expressing cells.

The GH146-GAL4 line (Stocker et al. 1997) drives expression in the projection neurons (PNs). In *olk* mutants the GFP intensity decreases with age in the GH146 driven lines

(Figure 29). This is not a general phenomena throughout the brain as other cell types, e.g. Kenyon cells and ring neurons, do not show loss of GFP staining as mentioned above. Therefore the cell death appears to be limited to a subpopulation of cells that includes the PNs.

PNs connect the antennal lobes to the mushroom bodies, the center for olfactory memory (Heisenberg 2003) and the lateral horn. PNs have their dendrites in the antennal glomeruli, where they form synapses with axons from olfactory receptor neurons and local interneurons. The axons of the PNs run in at least two tracts, the larger inner antennocerebral tract (iACT) and the smaller medial antennocerebral tract (mACT)(Figure 29A). In *olk* flies the PNs initially appear to develop normally and make appropriate connections in their target areas (Figure 29B). However in 10-d-old olk^1 flies GFP expression in the PN dendritic fields within the antennal lobes was noticeably weaker and the inner antennocerebral tract appeared both thinner and more weakly stained than in wild-type animals of the same age (Figure 29C). GFP labeling also appeared weaker in the lateral horn and calyx although the size of the terminal field in these regions appeared unchanged or possibly even slightly enlarged. In contrast, the medial antennocerebral tract (which bypasses the mushroom body calyx) and its terminal field seemed not to be affected at this age. After 23 days only a faint staining was still visible in the olk^1 flies (Figure 29D), apparently because of the loss of all GFP-expressing neurons.

B.1.3- Olfactory memory defects in the *olk* mutant

Most of the affected areas described above, mushroom bodies, PNs, and antennal lobes are involved in receiving and processing olfactory input. Therefore an olfactory learning and/ or memory defect seemed to be a likely effect of this mutation. To study this hypothesis associative and nonassociative olfactory learning performance was tested at different ages. The following behavioral experiments were performed by Martin Schwärzel, the methods are described in Bettencourt da Cruz et. al (2005). For the sake of completeness the results are mentioned below.

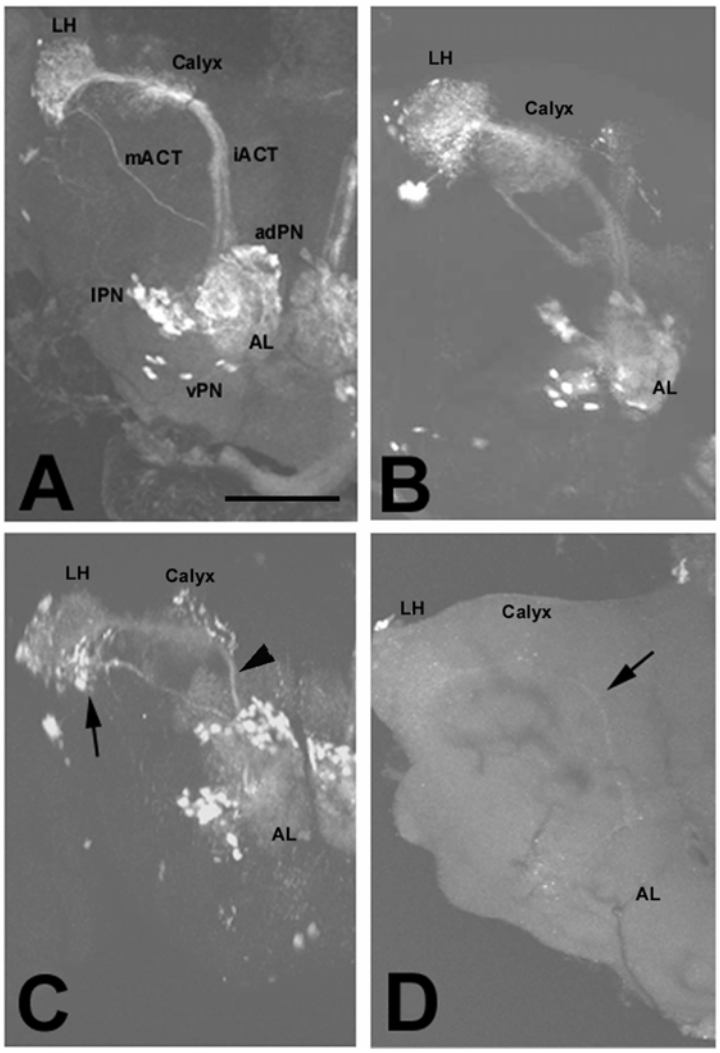

Figure 29: Degeneration of projection neurons

Degeneration of projection neurons in *olk*[1] mutants (visualized by GFP expression). (A) Wild-type, 10 d. The PNs send their dendrites into the antennal lobe (AL) and their axons into the calyx via the inner antennocerebral tract (iACT) and into the lateral horn (LH) via the medial antennocerebral tract (mACT). (B) In 1-d-old mutants, the PNs appear normal. (C) In a 10-d-old mutant, the staining of the dendritic field in the antennal lobe was noticeably weaker, and the iACT appeared both thinner and more weakly stained (arrowhead). The staining of the mACT (arrow) and its termination field and of the cell bodies of all three types of PNs was not noticeably altered at this age. (D) Further aging (23 d) resulted in severely reduced staining in all of these regions, suggesting that most or all of the PNs had undergone cell death. Images show whole-mounts using GH146-GAL4 and UAS-GFP. adPN, vPN, and lPN: anterodorsal, ventral, and lateral projection neurons, respectively. Scale bar, 50 µm.

Although young (3 d old) *olk* flies did not exhibit detectable signs of degeneration, they already displayed significant impairment in their olfactory learning compared with wild-type Canton-S control flies (Figure 30A). In *olk*[1] flies the performance index (PI) was reduced by about 50% and in *olk*[3] by ~80% at this age. These results show that the

affected neurons are measurably dysfunctional well before the onset of overt degeneration. By day 5, an age where first signs of degeneration become evident, olfactory learning was completely disrupted in *olk*^{3} flies. In *olk*^{1} flies a more gradual age-dependent decline in the PI was observed, reaching a PI of 25% of control by day 5 and 10% by day 8, whereas aging in wild-type flies did not significantly change performance. This age-dependent effect on learning ability in *olk* mutants was accompanied by additional deficits in their response to task-relevant stimuli. In *olk*^{1} mutants reactivity to the olfactory stimuli (benzaldehyde and octanol) was significantly reduced in 8-d-old flies (Figure 30B and C), possibly the result of the onset of degeneration in their antennal lobes at this age. This decrement was not apparent in *olk*^{3} mutants. However, these alleles did show a significantly reduced response to electric shock as early as day 3, an effect that was not influenced by aging (Figure 30D). These results reveal that olfactory-associated behavioral defects precede overt degeneration of olfactory lobe-associated structures in the brain. This is obvious in young *olk*^{3} flies, which show a severe reduction of their performance index long before the onset of degeneration. Also an effect of aging on the associative learning phenotype is seen in this allele because the reactivity to odors and shock does not change significantly with age. In *olk*^{1} effects of aging on perception of the olfactory stimuli could add to the decrease of the learning index in aged flies. In young *olk*^{1} flies, however, learning is clearly affected because the PI is reduced to ~50% without a significant change in olfactory perception.

B.2- Molecular characterization of the *olk* mutant

B.2.1- Mapping and identification of the *olk* mutation

Classical deletion mapping revealed that deficiencies deleting region 1E3-2B12 were not able to complement the *olk* phenotype (Figure 31C and D). Heterozygous *olk* flies show no phenotype (Figure 31A and B) therefore the deletion must cover the region of the *olk* mutation. The *futsch* gene is localized in this region (2A2-3) and the viable *futsch*^{N94} mutant was provided to us by Christian Klämbt. Heterozygous *futsch*^{N94}/ *olk* flies revealed that *olk* is allelic to *futsch* because they showed a degenerative phenotype comparable to homozygous *olk* flies (Figure 31E).

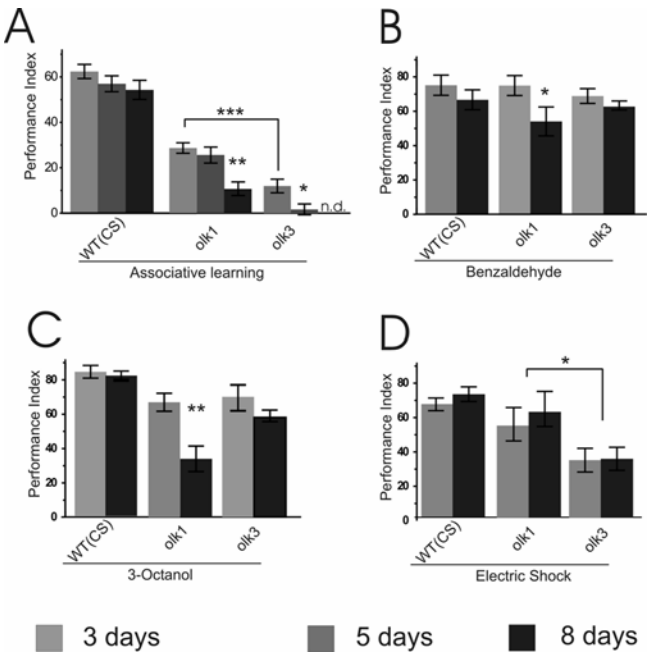

Figure 30: Olfactory learning in *olk* mutants

Progressive loss of olfactory learning ability in *olk* mutants. Associative and nonassociative olfactory behavior was tested at the age of 3, 5, and 8 d. (A) Performance of olfactory short-term memory progressively declines in *olk* mutant flies. Already by day 3, performance was significantly impaired ($p < 0.001$ for both olk^1 and olk^3 compared with wild-type Canton-S). Performance indices (PIs) were near zero by day 5 in olk^3 ($p < 0.05$) and by day 8 in olk^1 ($p < 0.01$). Day 8 was not measured in olk^3 mutants. (B–D) Response to the task-relevant stimuli was measured for the associated odorants (B and C) and the behavioral reinforcer electric shock (D). Olfactory acuity was also affected in an age-dependent manner in olk^1 mutant flies ($p < 0.05$ for benzaldehyde and $p < 0.01$ for 3-octanol, respectively), whereas there was no progressive effect on acuity of response to electric shock. However, overall sensitivity was significantly reduced in *olk3* mutants ($p < 0.05$). Histograms show means ± SEM of six experiments with 100 flies each.

$futsch^{N94}$ homozygous flies also display a neurodegenerative phenotype, showing vacuoles in the same areas as seen in *olk* mutants (Figure 31F).

The futsch allele P158 isolated by Hummel et al. (2000) seems to be an anamorphic allele. Considering that $futsch^{P158}$ is lethal it seems likely that the isolated olk alleles are hypomorphs or retain part of their function in order to allow viability.

B.2.2- Genomic sequencing of the mutant *futsch* gene

Genomic sequencing of PCR amplified DNA showed a substitution of a guanine to a thymine at position 4783 of the *futsch* cDNA as recorded in the Gadfly annotation. This truncates the protein to about a third of its predicted 5412 amino acids, by creating a stop codon instead of an glutamic acid.

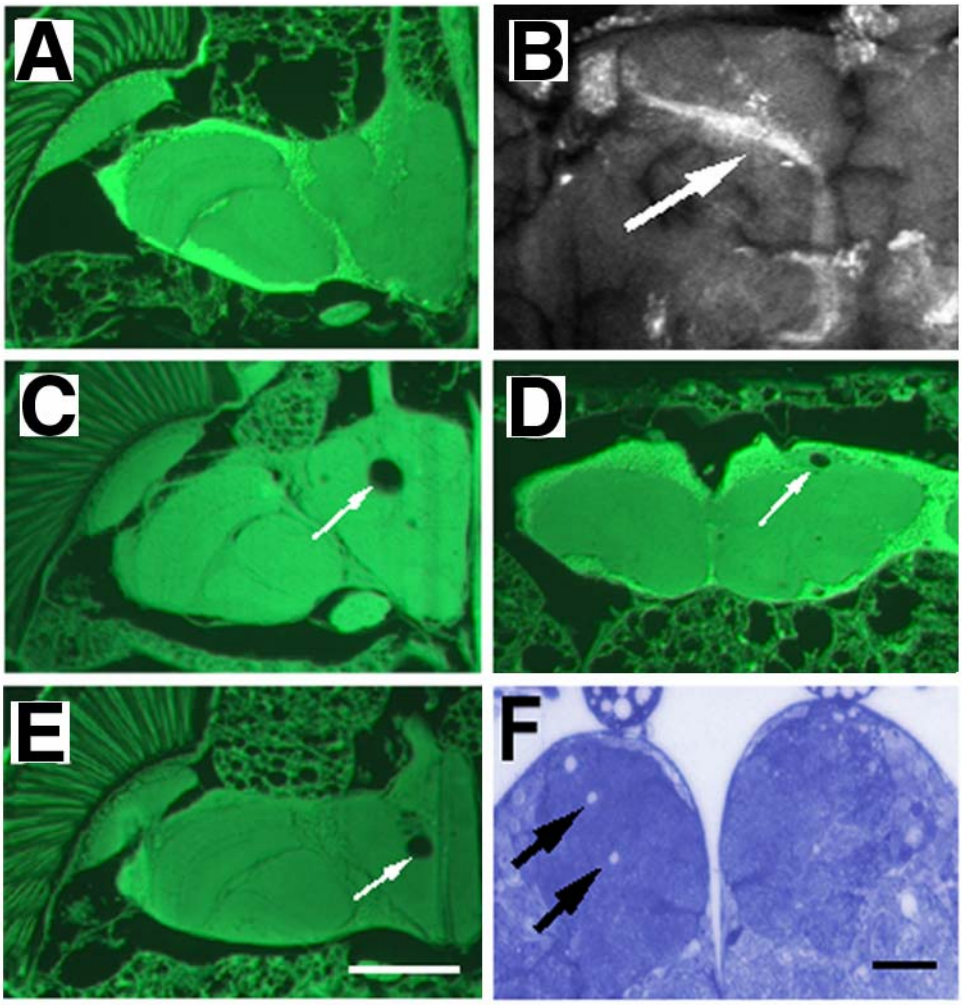

Figure 31: Mapping of *olk* to the *futsch* locus

olk is allelic to *futsch*. (A) Brain section of a 17 day old heterozygous olk^1 fly did not show a degenerative phenotype. (B) The pattern of PNs (labeled with GH146-GAL4 and UAS-GFP) in a 28 day old heterozygous olk^1 fly was not different from wild type. (C and D) Deficiencies deleting the region 1E3-2B12 uncovered the *olk* phenotype. (C) The brain of a 5 day old olk^1 /Df(1)S39 fly showing the large vacuoles in the mechanosensory neuropil. (D) Section from the brain of a 10 day old olk^1/Df(1)A94 fly showing the vacuoles in the calyx. (E) A 12 day old olk^1/$futsch^{N94}$ fly exhibited the *olk* phenotype (F) Brain sections from a 7 day old $futsch^{N94}$ fly also exhibited the *olk* phenotype. Scale bar = 20 µm

B.2.3- Western blot analysis of the *olk* mutant

To further confirm the identity of the *olk* mutation a western blot was performed using the monoclonal 22C10 antibody which was shown to recognize the *futsch* gene (Hummel et al. 2000). Futsch levels are diminished in olk^{2+3} and the truncated Futsch protein produced by olk^1 mutants cannot be detected because the epitope recognized by the 22C10 lies at the C-terminal end of the protein (Hummel et al. 2000).

Nevertheless this truncated protein contains the highly conserved N-terminus and most likely retains a partial function. In contrast *olk*^{2} and *olk*^{3} are most likely regulatory mutants because low amounts of the full-length protein were detected in western blots. The residual function and/ or amounts of Futsch protein would explain the hypomorphic character of these alleles. As mentioned above futsch null mutants are most likely lethal (Hummel et al. 2000).

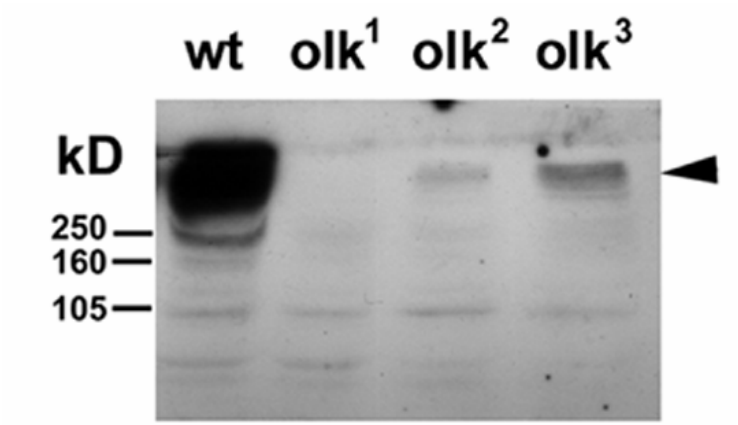

Figure 32: Western blot of *olk* mutants
Western blot using the anti-*futsch* antibody 22C10. The amount of Futsch protein (arrowhead) is significantly reduced in *olk*^{2} and *olk*^{3} mutants compared with wild-type controls. In *olk*^{1} flies, no protein was detected.

B.3- Alterations in the cytoskeletal structure of *olk* mutants

B.3.1- Tubulin organization differences between *olk* and wt

As already noted, silver staining of *olk* mutant brains suggest that these animals exhibit defects in the organization of their neuronal cytoskeleton. To study the integrity of the mutant cytoskeleton brain sections were stained with an antibody against tubulin. Surprisingly, overall antitubulin staining was noticeably more intense in 14-d-old *olk*^{1} flies than in age matched wild-type flies (Figure 33A and B). Confocal microscopy of

tubulin-stained brain sections revealed that this effect was due to a more densely localized pattern of staining in neurites of the mutant brains, including neurites in the calyx (Figure 33D), compared with the more dispersed distribution of tubulin in wt animals (Figure 33C).

This altered pattern of tubulin staining in *olk* mutants might be due to structural differences in the microtubule network of CNS neurons and/ or an upregulation of tubulin in the mutant antennal lobes. To investigate this issue in more detail electron microscopic studies were performed on 14-d-old olk^1 and wild-type flies. When comparing microtubule distributions in neuronal fibers within wild-type versus *olk* mutant brains, a noticeable increase in microtubule number was observed in the mutant animals, an alteration that was detectable both in longitudinal sections (Figure 34A and B) and cross sections (Figure 34C and D). In addition microtubules within the axons of olk^1 brains often exhibited abnormalities in their organization, including uneven spacing, bending, and in some instances actually crossing of adjacent microtubules (Figure 34E and F).

B.3.2- Upregulation of tubulin in *olk*

To find out if the denser appearance of the nerve fibers was due to the tighter spacing of microtubules or if there is increase in total amount of tubulin a western blot was performed. Western blots from head homogenates of 1-4 day-old flies confirmed an increase of about 40% in tubulin expression compared to wt (Figure 35). This result strongly suggests that the more intense tubulin staining in the mutant brains is a consequence of both, an increase in the overall amount of tubulin as well as its assembly into microtubules in *olk* mutant neurons. This upregulation would result in a greater number of microtubules in neurons, but reduced microtubule spacing and this ultrastructural abnormality would also explain the more compact appearance of the microtubule distributions seen in immunostained brain sections. These experiments confirm an important role of Futsch in the organization and dynamics of the cytoskeleton, not only during development (as previously reported (Roos et al. 2000)) but also into adulthood.

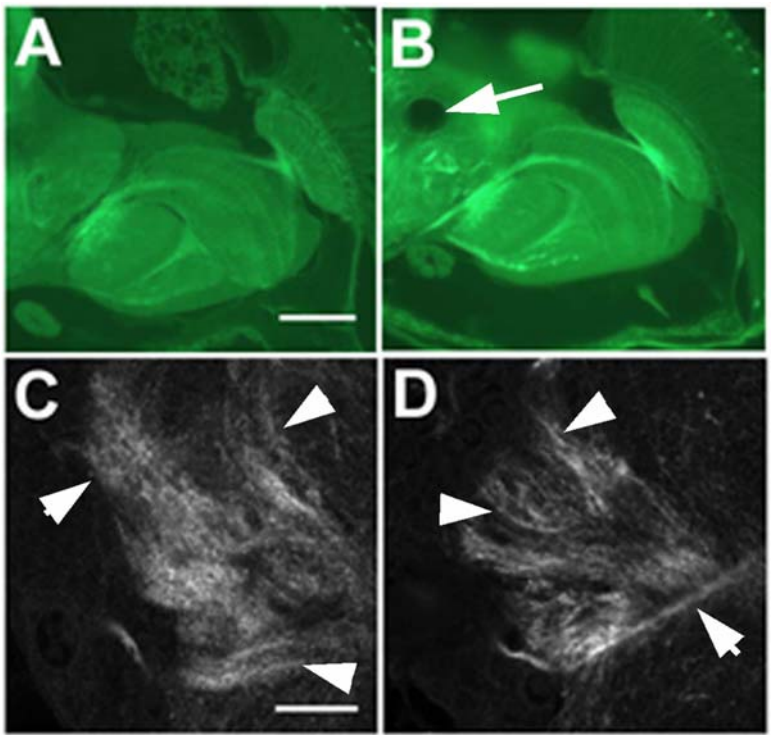

Figure 33: Differing tubulin organization in *olk* mutants

(A) Tubulin staining in a paraffin section of a 14-d-old wild-type fly. (B) Overall tubulin staining appeared stronger in an age-matched *olk*[1] mutant animal. (C and D) Confocal microscopic images taken from the calyx of these sections from (C) wild-type and (D) *olk*[1] animals reveal a more densely localized pattern of staining in the mutant (arrowheads).

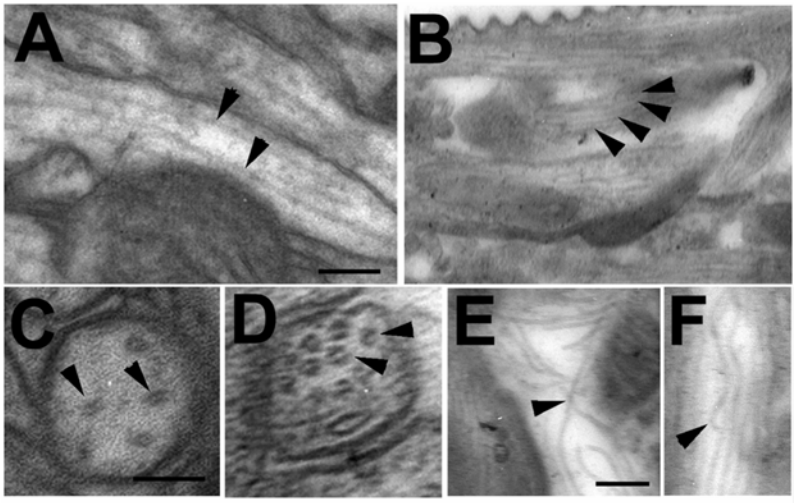

Figure 34: Antennal lobes of *olk*[1] show disorganized microtubule in electron microscopy

Disorganized microtubule in the antennal lobes of *olk*[1]. (A) Microtubules (arrowheads) in a 14-d-old wild-type antennal lobe are straight and evenly spaced. (B) In an age-matched *olk*[1] mutant, a noticeable increase in the number of microtubules was apparent (arrowheads), leading to reduced spacing between microtubules. This difference in density could also be seen in cross sections from wild-type (C) and *olk*[1] mutant flies (D). (E and F) In addition, microtubules in the mutant were seen to bend, touch, or cross each other (arrowheads), a phenotype not observed in wild-type brains. Scale bar, 0.05 µm.

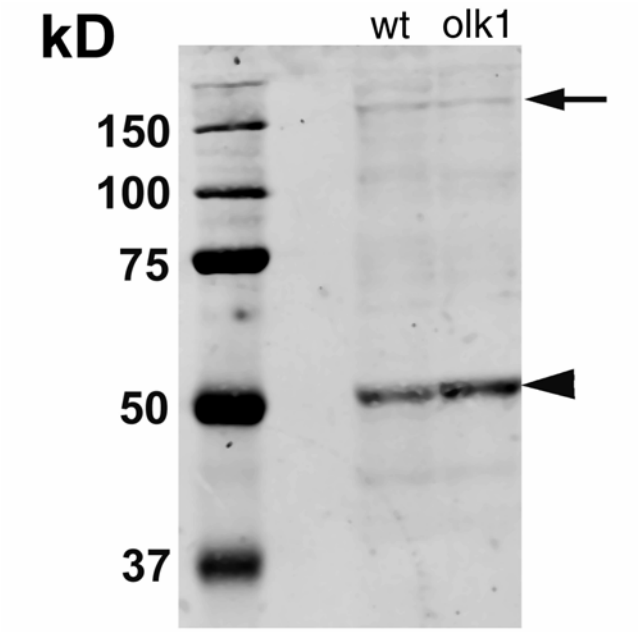

Figure 35: Enhanced tubulin levels in *olk*[1] mutant

Tubulin expression is increased in *olk*[1]. A stronger tubulin band (arrowhead) is detectable in *olk* mutant flies. Staining with an anti-SWS antibody (arrow) shows equal loading in both lanes. Statistics on six Western Blots showed an increase in tubulin staining in *olk*[1] to 139%±12 after normalization to the SWS loading control.

B.3.3- Reduced rate of transport in *olk* mutants

To assess the possible consequences of the alterations seen in the microtubule network of *olk*[1] flies, various aspects of outgrowth were examined and transport in primary neuronal cultures from wild-type and mutant brains. Neurons derived from *olk*[1] flies did not show any obvious defects in general outgrowth in vitro, developing a neuritic network indistinguishable to that of wild-type neurons (Figure 36A and B). To determine whether *olk* mutations induce defects in cellular transport, time-lapse imaging was used to analyze the movements of mitochondria within the growing neurites. Mitochondria were grouped into three categories: mitochondria that did not change their position during the entire observation time, mitochondria that did not exhibit net changes in their position but wobbled back and forth (covering not more than 2 µm in distance) and mitochondria that moved 2 µm either retrograde or anterograde within the neurites. Although the number of mitochondria undergoing small wobbling movements was not significantly different between wt and *olk*[1] neurons, significant differences were detected in the two other categories of motion (Figure

36C). In *olk*[1] neurons almost twice as many mitochondria showed no changes in their positions (33 vs. 18% in wild-type, $p < 0.05$), whereas the number of actively moving mitochondria was reduced by half (18 vs. 37% in wild-type, $p < 0.01$). These results indicate that the abnormalities seen in the microtubule network of *olk*[1] mutant flies corresponds with measurable disruptions in mitochondrial transport within the axons and dendrites of neuronal cells (Figure 36).

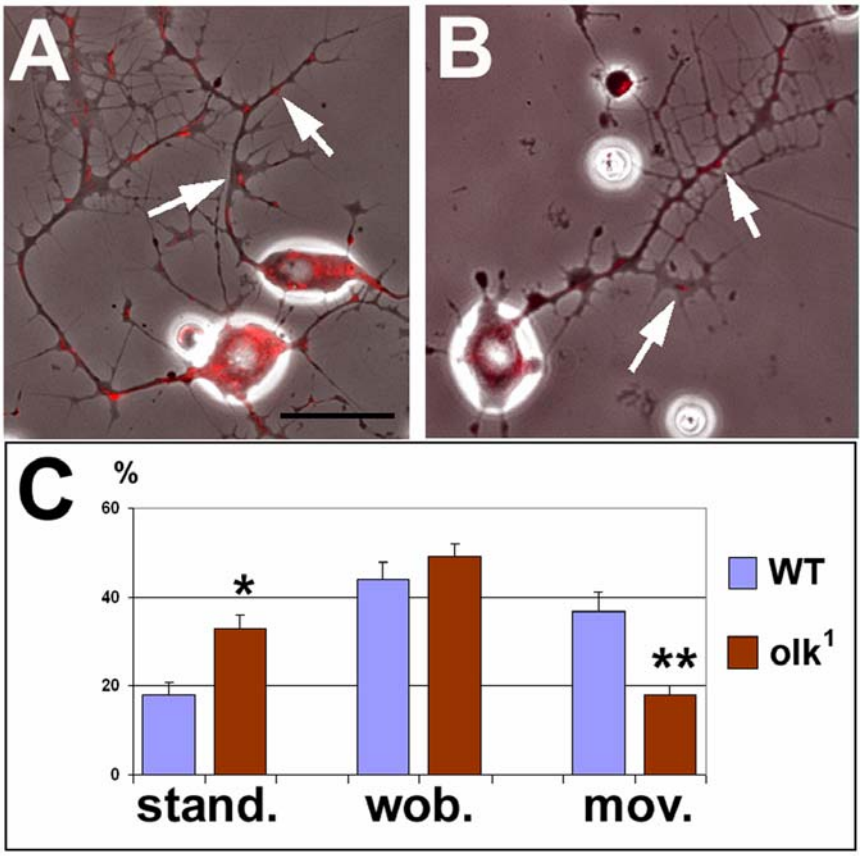

Figure 36: Mitochondrial transport

Neurons cultured for 24 h from (A) wild-type and (B) *olk*[1] pupae show similar patterns of outgrowth and branching. (C) To analyze axonal transport, the movement of labeled mitochondria (red, arrows in A and B) was observed for 98 s with pictures taken every 2 s. During this interval, significantly more mitochondria in *olk*[1] did not change their position (stand.) and fewer mitochondria showed active movement within the neurites (mov.). The number of mitochondria exhibiting small back-and-forth movements (<2 µm; wob.) was not significantly changed in *olk*[1] neurons. Histograms show means ± SEMs. Scale bar, (A and B) 10 µm.

B.4- Interactions of *futsch* with other genes

B.4.1- Expression pattern of *futsch*

Futsch is expressed widely throughout the brain with stronger expression in the antennal lobes (Figure 37A) and the calyx (Figure 37B). Vacuoles are only present in defined parts of the brain and develop in a specific spatial manner. This effect might be due to redundancy of MAPs in other cells. Alternatively the most affected cells might be more susceptible to the lack of intact Futsch. The stronger expression of Futsch in the antennal lobes also suggests that these cells require higher levels of Futsch for normal function.

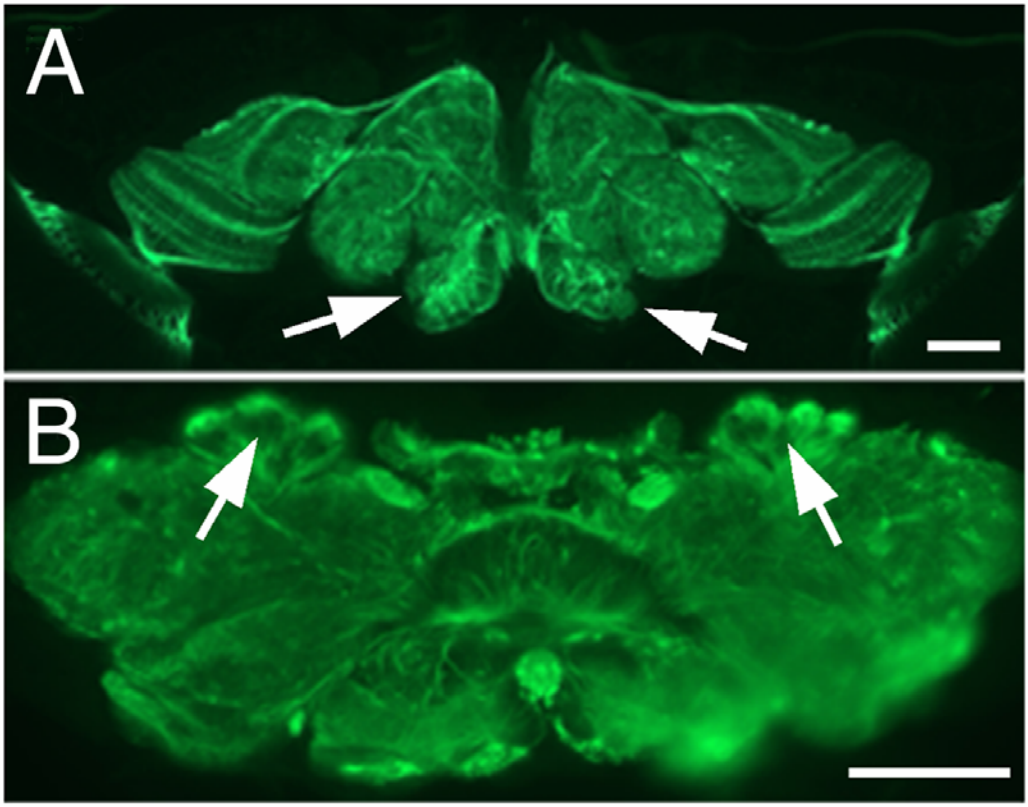

Figure 37: Expression pattern of Futsch

Immunohistochemistry of wild-type brain sections using 22C10 (anti- Futsch). Futsch is widely distributed in the brain, with strong expression in the antennal lobes (arrows in A) and calyx (arrows in B). Scale bar 50 µm.

B.4.2- Interaction of *futsch* with *dfmr1*

Futsch is negatively regulated by the *Drosophila Fragile X mental retardation* gene (*dfmr1* (Zhang et al. 2001)). Mutations in *dfmr1* show a similar synaptic phenotype as *futsch* in the larval neuromuscular junction, whereas the combined mutations of both genes restores normal synaptic structure (Zhang et al. 2001). DFMR1 is highly expressed in the larval mushroom bodies (Schenck et al. 2002) and in most, if not all, neurons in the adult brain (Morales et al. 2002). Using an α-DFMR1 antibody (red) to immunostain PNs expressing GFP (via the GAL4-GH146/ UAS-GFP construct; green), it was shown that these neurons also specifically express the DFMR1 protein (Figure 38A and B). To investigate whether mutations in *dfmr1* suppresses the degenerative phenotype of *olk,* the olk^1 mutants were crossed with flies carrying a homozygous lethal genomic deletion in *dfmr1* (kindly provided by C. Klämbt, University Münster). Comparisons between olk^1 flies carrying one copy of the *dfmr1* deletion and control flies coming out of the same cross, a dramatic suppression of the *olk* degenerative phenotype was observed. The size of vacuoles in the mechanosensory neuropil of the ventrolateral protocerebrum was reduced by approximately one third at day 14, compared with olk^1 mutants of the same age (Figure 38C).

To determine whether *dfmr1* similarly affects the microtubule phenotype seen in *olk* mutants, sections of fly brains from both strains were immunostained with α-tubulin antibodies. In contrast to the abnormally condensed pattern of tubulin staining seen in the calyx of olk^1 mutants (Figure 38D), *olk* flies carrying the *dfmr1* deletion showed a noticeable reversion to a more diffuse pattern of staining seen in wild-type animals (Figure 38E). These results substantiate the hypothesis that Futsch and DFMR1 interact in CNS neurons, demonstrating that the degenerative phenotype of the *olk* mutants (hypomorphic alleles of *futsch*) can be suppressed by a reduction of the negative regulator *dfmr1*.

The synaptic defects in *dfmr1* mutants can be attributed to an upregulation of *futsch* expression in the absence of DFMR1 (Zhang et al. 2001). Thus, both underexpression and overexpression of functional Futsch protein may result in similar (though subtly different) abnormalities in synaptic function. This model predicts that an increase in

DFMR1 function might be sufficient to create an *olk*-like phenotype. To test this hypothesis DFMR1 was overexpressed, but unfortunately both pan-neuronal expression and expression specifically in the PNs induced lethality during development (as has also been reported when DFMR1 was over-expressed in the eye and wing)(Wan et al. 2000)).

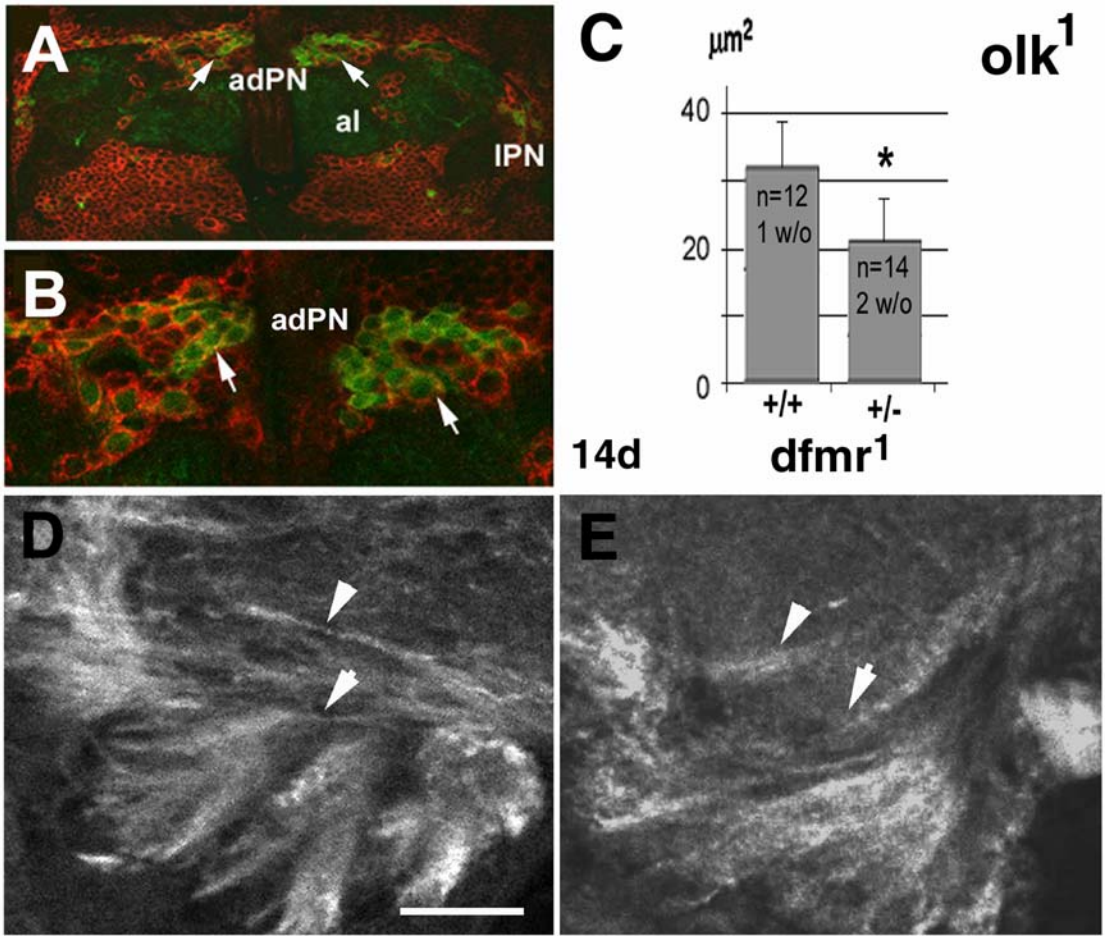

Figure 38: Interaction of *olk* with *dfmr1*

(A) Double staining using a α-DFMR1 antibody (red) and GFP staining of PNs (green). (B) A higher magnification view shows that the anterodorsal PNs (adPN; arrows) express DFMR1. Al, antennal lobes; lPN, lateral projection neurons. (C) The average size of vacuoles in the mechanosensory neuropil of the lateral protocerebrum was significantly reduced in day 14 *olk*[1] flies carrying the *dfmr1* deletion (+/-), compared with age-matched *olk*[1] flies from the same cross but carrying a balancer chromosome (+/+). Average vacuole size was reduced by approximately one-third compared with control *olk* flies ($p < 0.01$). Histograms show means ± SEM, and the number of flies measured in each strain are indicated. (D and E) Anti-tubulin immunostaining of brain sections from 14-d-old *olk*[1] flies without the *dfmr1* deficiency (D) and with the *dfmr1* deficiency (E). Removing one copy of *dfmr1* restored the overall pattern of tubulin staining pattern toward the more diffuse pattern seen in wild-type flies (compare with Figure 33). Scale bar, (A) 15 µm; (B) 6 µm; (D and E) 10 µm.

B.4.3- Tau has partially overlapping functions with *futsch*

Experiments in vertebrates have suggested that different members of the MAP family may have overlapping functions (DiTella et al. 1996; Teng et al. 2001). In flies, previous reports have shown that endogenous TAU, another MAP protein, is normally highly expressed in the eye but not in the brain (Heidary and Fortini 2001). To investigate the possibility of similar compensatory or redundant functions in *Drosophila*, either fly or bovine tau (driven by the neuronal-specific GAL4-*ELAV*) was expressed in *olk*^{1} mutant flies. In comparison with *olk* flies carrying the UAS-tau, constructs but lacking the GAL4-*ELAV* driver, flies expressing either *Drosophila* or vertebrate tau showed an ~25% reduction in the size of vacuoles that developed in the mechanosensory neuropil (Figure 39). However, no effect of exogenously expressed *tau* on the microtubule phenotype induced by the *olk* mutants (as seen at the light microscopic level) was detected. This suggests that the neurodegenerative effects of defective Futsch protein may include additional functions or result from more subtle effects on microtubule. The suppression of the degenerative phenotype of *olk* suggests that ectopic Tau expression can partially substitute for the loss of Futsch in the projection neurons. Thus, different members of the MAP family share overlapping functional activity that has been evolutionarily conserved.

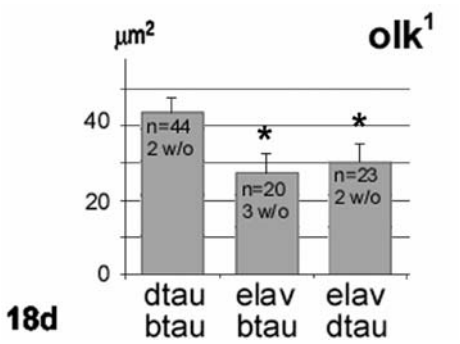

Figure 39: Interaction with *tau*

Eighteen-day-old *olk*^{1} flies that also expressed either fly *tau* (*dtau*) or bovine *tau* (*btau*) in all neurons (driven by the *ELAV* promoter) had significantly fewer vacuoles than in *olk*^{1} flies ($p < 0.05$). Histograms show means ± SEM, and the number of flies measured in each strain are indicated.

Discussion

sws

Subcellular SWS localization

Stainings with the obtained α-SWS antibody revealed a subcellular organization of SWS that is similar to that visualized for NTE in mice. SWS is found in vesicles that co-immunostain with the ER marker Grp78. Localization is disturbed in the N-terminally truncated form of SWS (SWSΔ1-80). GFP-tagged constructs of NTE are found to be localized to the cytoplasmic face of the ER (Li et al. 2003) and endogenous NTE is found in the ER in cultured hippocampal mouse neurons (Akassoglou et al. 2004).

Unusual distribution of Calnexin, also an ER marker, was observed in COS cells expressing NTE-GFP constructs at high levels (Li et al. 2003). Constructs lacking the catalytic domain as well as overexpression of full length NTE showed aberrant Calnexin distribution, however NTE-GFP constructs lacking the first TM did not (Li et al. 2003).

Functional domains of SWS

In vitro modulation of NTE activity by cAMP was not observed under standard assay conditions (Glynn 2000). Analysis of SWS constructs with a defective cAMP binding domain however showed a less deleterious overexpression effect in the eye than wt SWS overexpression (Figure 17 & Figure 18). One of the models of interaction of the subunits for PKA suggests that the regulatory subunit binds to the catalytic subunit using amino acids from both, the cAMP binding and the protein interaction domain (Figure 40) and that this is regulated by cAMP (Herberg et al. 1994). Mutating the cAMP binding domain might therefore also have consequences on the binding of SWS to its interaction partners. If cAMP initiates dissociation of an inhibitory unit from SWS then abolishing this function should lead to constitutive binding of the inhibitor. Since the SWS overexpression phenotype is probably due to excessive SWS activity the constitutively inhibited construct would lead to a less severe overexpression phenotype. Consistent with this model the construct with the modified protein interaction

domain displayed an increased deleterious effect compared to wt SWS (Figure 16). Modifying the protein interaction domain should abolish binding of an inhibitor altogether, therefore allowing SWS to be constitutively active (Figure 40). However, this model is based on the assumption that only the enzymatic properties of SWS are modulating the degeneration.

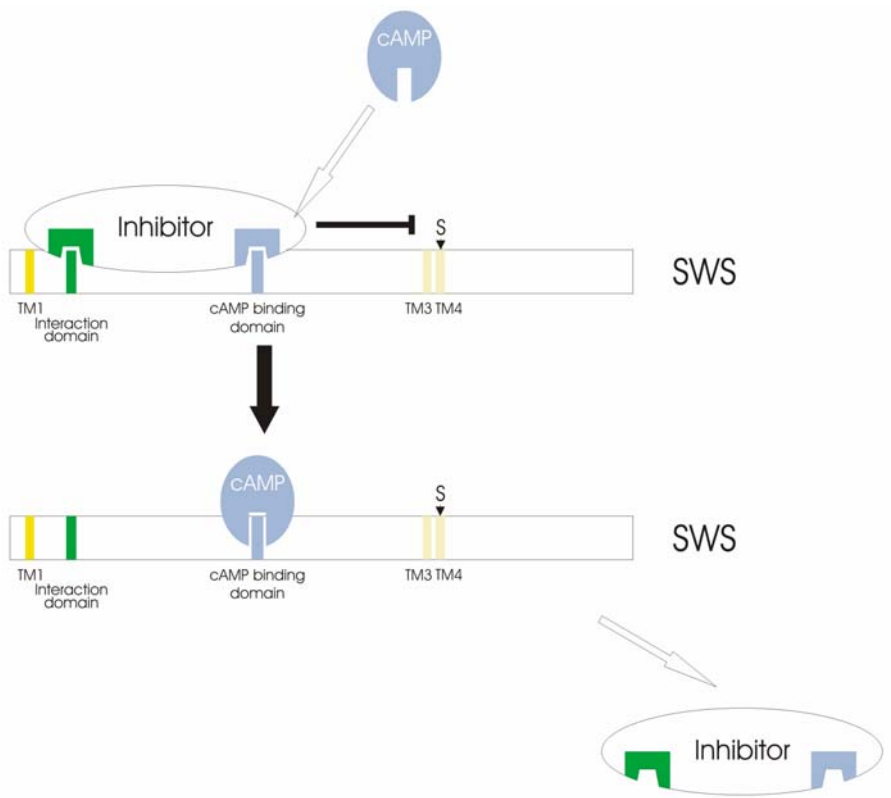

Figure 40: Model for cAMP influence on SWS.
Based on knowledge from the interaction between the regulatory and catalytic subunit of PKA this model suggests that an inhibitor is keeping SWS in an inactive state. This interaction occurs via the interaction domain and the cAMP binding domain. Binding of cAMP displaces the inhibitor and allows SWS to become catalytically active. Therefore preventing cAMP binding by mutating the binding site should result in constitutive inhibition in this model. For labeling see Figure 16

It is possible that other proteins are involved in causing the deleterious effect or that SWS has a function besides its known serine esterase properties. SWS could regulate another protein, for example PKA-C3, with the deregulation of that protein leading to degeneration. PKA-C3 has been isolated in yeast two hybrid screens using SWS and

SWS fragments as bait. If the protein or proteins that bind to SWS (PKA-C3 or other proteins) cause the deleterious phenotype independently of the SWS esterase activity, this should be visible in mutants affecting these SWS binding partners. Currently a mutant allele of the *pka-c3* gene, one of the best candidates for an interaction partner for SWS identified so far, is being created.

A SWS construct lacking the first 80 amino acids (SWS∆1-80) shows severe deleterious effects when expressed in *Drosophila*. Despite an untouched catalytic domain it shows no activity in a standard esterase essay (Muhlig-Versen et al. 2005). A SWS construct lacking the catalytic site serine also shows no in vitro catalytic activity but no overexpression phenotype. This suggests that an additional function is involved in producing the deleterious effect in SWS∆1-80. To confirm this hypothesis SWS∆1-80 was modified to mutate the catalytic site serine. Although the deleterious effect of this construct might be due to different mechanism than the degeneration seen with over-expression of full length SWS or OPIDN, this gave us insights into whether esterase activity is the only method for SWS to achieve a deleterious effect. The severe effect of SWS∆1-80 is slightly attenuated by a mutation substituting its catalytic site serine with an aspartate. This suggests that although the esterase function might contribute to the degeneration it is not the primary cause. This shows that there is a non-esterase dependent function of SWS as it was proposed for intoxication of NTE with neuropathic OPs.

The classical mechanism of the aging reaction (Figure 3) involves the translocation of a side-group derived from the bound OP onto NTE (Johnson 1982). However, recent results have suggested that although this reaction is present in most aging agents it is not causal for the development of OPIDN. Instead a proton loss from the active site serine bound to the OP, resulting in a negative charge, seems to cause a similar effect (Kropp et al. 2004). However, a mutant form of SWS containing a negatively charged aspartate instead of the catalytically active serine was catalytically inactive and unable to produce any type of deleterious phenotype in *Drosophila* (Muhlig-Versen 2001). It has to be taken into account that, although degeneration can be observed in *Drosophila* with loss- and gain-of function forms of SWS, it has not been shown that

any of the mechanisms that cause the degeneration are related to the mechanisms that cause OPIDN. It is possible that *Drosophila* is unable to develop symptoms comparable to those of OPIDN in mammals, although it appears likely that SWS can be intoxicated by neuropathic OPs (D. Kretzschmar, personal communication). However it is not yet known if non-neuropathic OPs show the same effect and therefore if the intoxication is dependent on the aging reaction.

This set of experiments shows that SWS contains a function that is different from the esterase function. However, it is unclear if the non-esterase function observed in SWS∆1-80 and in OPIDN are identical.

Physiological function of SWS in vivo

Phosphatidylcholine (PtdCho) is the major phospholipid of eukaryotic cell membranes. PtdCho is synthesized by the Kennedy CDP-choline pathway and in hepatocytes by methylation of phosphatidylethanolamine (PtdEtn) (Cui and Houweling 2002). The degradation of PtdCho, necessary to control the PtdCho levels in the cell membrane, have not been studied as intensely (Glynn 2005).

Levels of PtdCho are increased in *sws* mutants and decreased in *sws* overexpressing flies, suggesting that SWS is involved in the degradation of phophatidylcholine (PtdCho). Inversely triacylglycerol (TAG) levels were decreased in *sws* mutants and increased when SWS is overexpressed. Considering that diacylglycerol has been shown to be the immediate precursor for both PtdCho and TAG this is consistent with a redirecting of the pathway to the production of the alternative product (Allan 2000; Jackowski et al. 2000).

During the course of this work several studies in other systems have given hints as to the function of SWS/ NTE. Evidence has been presented that NTE catalyzes the deacylation of PtdCho in yeast and in mammalian cells (Zaccheo et al. 2004). The deacylation of PtdCho produces glycerophosphocholine (GroPCho). This molecule is not present in the yeast *nte*^{1} mutants indicating that in yeast NTE1 is the only enzyme responsible for the deacylation of PtdCho (Zaccheo et al. 2004). However, in *nte*^{1} yeast PtdCho levels are not increased and the cells show no obvious phenotypes suggesting

that unlike metazoan cells, yeast is able to control its PtdCho levels by down regulating the synthesis rate.

Depletion of PtdCho in membranes has been shown to lead to apoptotic cell death (Wright et al. 2004) and induction of ER-stress-related protein GADD153 (growth arrest and DNA-damage-inducible protein), which has been shown to have proapoptotic activity (van der Sanden et al. 2003). If SWS is truly responsible for PtdCho degradation, excessive SWS present in flies overexpressing SWS would lead to a reduction in PtdCho levels which in turn would lead to the apoptotic cell death observed in *sws*. Reduction of PtdCho levels has been observed in several neurodegenerative diseases although it is not clear if this downregulation is causing the detrimental effects to the cell or if membrane breakdown is a result of prior deficits (Klein 2000).

Accumulation of PtdCho has also been reported to have deleterious effects on cell integrity and neuronal signaling. Excess PtdCho is intrinsically toxic to Golgi secretory function (Xie et al. 2001) and elevated PtdCho levels can be found in specific brain regions of Alzheimer`s patients (Soderberg et al. 1992). PtdCho and related choline compounds are also an important source for signaling molecules (Billah and Anthes 1990; Exton 1994) and have been found to have a neuronal-specific function consisting of promoting synthesis and transmission of neurotransmitters (McDaniel et al. 2003). Thus, in addition to defects associated with membrane integrity, excess PtdCho in neurons may also result in the misregulation of transmitter synthesis and release. Such an effect might further contribute to the degeneration of neurites and subsequent neuronal death, an effect that is compatible with the progressive appearance of vacuoles in the neuropil of *sws* mutant flies.

In addition to the alteration in PtdCho levels due to *sws* mutations a severe decrease in sterol ester levels in *sws* mutants was also observed. Cholesterol ester, a sterol ester, can be synthesized by transacylation from PtdCho to cholesterol. This reaction is catalyzed by lecithin acyltransferase (LCAT), a serum enzyme that acts on the surface of high-density lipoproteins (reviewed in Jonas 2000). Although LCAT is primarily synthesized in the liver, smaller amounts can be found in the brain and cultured glial cells secrete significant amounts into the surrounding culture medium (Collet et al.

1999). The role of LCAT in the brain is not yet understood. SWS shows no significant sequence homology to LCAT and an LCAT orthologue can be found in the *Drosophila* genome. Therefore SWS presumably does not act directly as an LCAT-like enzyme, but might influence brain LCAT via an alternative pathway.

These results support the hypothesis that SWS plays an important role in the lipid metabolism of the ER by controlling the PtdCho degradation and possibly cholesterol ester synthesis.

olk

The characterization of the *olk*$^{1-3}$ mutants revealed that they are hypomorphic alleles of the *futsch* gene, which encodes a protein with substantial sequence similarity to vertebrate MAP1B.

In the embryo, *futsch* is required for axonal pathfinding and transgenic rescue experiments have shown that a short fragment of the protein (containing the first 618 amino acids) partially restores embryonic viability (Hummel et al. 2000). Similarly in mice, the N-terminus of MAP1B is vital for the function of this protein because animals expressing only the first 571 aa are also viable (Takei et al. 1997). However, these results are still controversial, as other groups reported that expression of this truncated MAP1B does not rescue lethality (Edelmann et al. 1996; Gonzalez-Billault et al. 2000). The characterization of *futsch*^{olk1} shows that the N-terminal third of Futsch is sufficient to support normal development into adulthood. However, the progressive degeneration seen in adults in all three *olk* alleles demonstrates that the structural and functional maintenance of the nervous system requires additional domains of the protein and/ or increased protein levels.

Experiments performed in this thesis have shown that the PNs of the olfactory system undergo cell death in *futsch*^{olk} mutants, apparently due to necrotic cell death. The first signs of degeneration appear within the calyx regions, well before any signs of cell death, indicating that axonal degeneration precedes neuronal death of the PNs. Moreover, the results of this work support the conclusion that defects in the cytoskeleton of these neurons lead to a progressive disruption in their axonal and dendritic integrity, ultimately culminating in the death of the neurons.

In vertebrates mitral cells are analogous to insect PNs, connecting the olfactory bulb with the olfactory cortex (Marin et al. 2002). Innervation of the olfactory bulb continues to be modified throughout adult life, corresponding with the persistent expression of juvenile MAP isoforms in the mitral cells (Viereck et al. 1989). Interestingly, olfactory dysfunctions have been described as one of the first signs of both Parkinson's and Alzheimer's disease (Kovacs et al. 2001; Hawkes 2003) and mitral cell degeneration is

a common feature in Alzheimer patients (Kovacs et al. 1999). The results from this work suggest that as in humans, the olfactory centers of the brain in *Drosophila* are particularly susceptible to disruptions in MAP proteins, an effect that corresponds with the need of these neurons for continuous, experience-dependent remodeling throughout adult life.

The role of Futsch in regulating tubulin assembly in neurons was confirmed by the marked changes seen in the organization and distribution of microtubules in the *futsch*^{olk} mutants. This suggests that the lack of functional Futsch protein results in a destabilization of the cytoskeleton, which induces a compensatory upregulation of tubulin expression. A similar defect has been shown in mice lacking both MAP1B and MAP2, in which the spacing of microtubules was significantly diminished (Teng et al. 2001). Alternatively, the *futsch*^{olk} mutations might disrupt the dynamics of tubulin assembly/ disassembly, resulting in an abnormal accumulation of microtubules.

In primary neuronal cultures prepared from the *futsch*^{olk} mutants a significant reduction in mitochondrial movement compared with wild-type neurons was observed, which most likely reflects a general reduction in axonal and dendritic transport due to disruptions in the microtubule network. Recently, it was shown that regenerating neurons in MAP1B-deficient mice exhibited defects in axonal branching and growth cone motility, also apparently due to a disruption of normal cytoskeletal dynamics (Bouquet et al. 2004). The results of this work show that mutations in *futsch*^{olk} affect the ability of neurons to execute normal aspects of transport and motility required to maintain them through adult life.

Alterations in the microtubule network were detected throughout the brains of *futsch*^{olk} mutants, concordant with the widespread expression of Futsch in most neurons. Neurodegeneration, however, was restricted to the olfactory system. The specificity of this degenerative phenotype could be due in part to the relatively long axons and extensive termination fields of the PNs, which might render them more sensitive to partial reductions in Futsch function. Similar observations of cell-specific sensitivities have been made in a number of human diseases. For example Huntingtin protein (Tobin and Signer 2000), several spinocerebellar ataxia proteins (Ross 2002) and the

Amyloid Precursor Protein (Selkoe 2001) are expressed in many neurons but only specific subsets of cells are affected and undergo cell death in the associated diseases.

Alternatively, cell type-specific expression of different MAPs might account for the sensitivities of specific brain regions to defects in a particular MAP. In vertebrates, several MAPs have been shown to have overlapping functions: MAP2 can substitute MAP1B in dendrites, whereas tau may substitute for MAP1B in axons (DiTella et al. 1996; Takei et al. 2000; Teng et al. 2001). A similar redundancy in *Drosophila* MAPs might preclude more widespread neurodegeneration in the *futsch*^{olk} mutants. Notably, suppression of the *futsch*^{olk} phenotype by ectopic expression of tau showed that another MAP can partially substitute for Futsch. Two other MAPs have also been described in *Drosophila* (Pereira et al. 1992; Kellogg et al. 1995) but their expression patterns in the adult brain are not yet known. Thus, the potential role of functional compensation by endogenously expressed MAP proteins in *Drosophila* merits further investigation.

Futsch is negatively regulated by the *Drosophila fragile X mental retardation* (*dfmr1*) gene. The neurodegeneration and learning deficiencies seen in *futsch*^{olk} mutants are caused by a decrease in Futsch function and a deletion in *dfmr1* partially suppressed this phenotype. This suggests that this effect is due to a reduction in *dfmr1*-mediated inhibition of Futsch expression, resulting in a net increase in Futsch activity. Disease-associated mutations in the human FraX gene also result in transcriptional silencing and loss of FraX function (Jin and Warren 2003). In combination with results obtained in this work, these observations suggest that the functional relationship between MAP1B and FraX-related proteins has been maintained across phylogenetic lines, whereby the function of FraX proteins is fundamentally linked to the regulation of MAP1B/Futsch expression.

Altered MAP protein expression and disruptions in the cytoskeleton are associated with a number of neurodegenerative diseases but whether defective MAPs actually cause neurodegenerative phenotypes is still in dispute (Brandt 2001). As already noted, the overlapping or complementary functions of different vertebrate MAPs have hindered an

analysis of their importance to neuronal viability in the adult brain. In this regard the relative simplicity of cytoskeletal associated proteins in *Drosophila* provides a means of deciphering their authentic roles in the nervous system. The results presented here show that Futsch, the MAP1B orthologue of *Drosophila*, plays an essential role in the maintenance of the adult nervous system and that defects in this protein result in progressive behavioral and neurodegenerative defects. Thus, the *futsch*^{olk} mutants reveal that also other MAPs besides tau can be involved in neurodegeneration. Although MAP1B has yet to be implicated in a human neurodegenerative disease, mutations in gigaxonin, a binding partner of MAP1B, result in axonal degeneration and cell death in humans (Ding et al. 2002). Besides providing new insight into the endogenous function of MAP-related proteins in vivo, these results demonstrate the potential value of a model systems approach for investigating the molecular mechanisms underlying neurodegenerative disorders in more complex organisms, including humans.

Bibliography

Adams, M. D., Celniker, S. E., Holt, R. A., Evans, C. A., Gocayne, J. D., Amanatides, P. G., Scherer, S. E., Li, P. W., Hoskins, R. A., Galle, R. F., George, R. A., Lewis, S. E., Richards, S., Ashburner, M., Henderson, S. N., Sutton, G. G., Wortman, J. R., Yandell, M. D., Zhang, Q., Chen, L. X., Brandon, R. C., Rogers, Y. H., Blazej, R. G., Champe, M., Pfeiffer, B. D., Wan, K. H., Doyle, C., Baxter, E. G., Helt, G., Nelson, C. R., Gabor, G. L., Abril, J. F., Agbayani, A., An, H. J., Andrews-Pfannkoch, C., Baldwin, D., Ballew, R. M., Basu, A., Baxendale, J., Bayraktaroglu, L., Beasley, E. M., Beeson, K. Y., Benos, P. V., Berman, B. P., Bhandari, D., Bolshakov, S., Borkova, D., Botchan, M. R., Bouck, J., Brokstein, P., Brottier, P., Burtis, K. C., Busam, D. A., Butler, H., Cadieu, E., Center, A., Chandra, I., Cherry, J. M., Cawley, S., Dahlke, C., Davenport, L. B., Davies, P., de Pablos, B., Delcher, A., Deng, Z., Mays, A. D., Dew, I., Dietz, S. M., Dodson, K., Doup, L. E., Downes, M., Dugan-Rocha, S., Dunkov, B. C., Dunn, P., Durbin, K. J., Evangelista, C. C., Ferraz, C., Ferriera, S., Fleischmann, W., Fosler, C., Gabrielian, A. E., Garg, N. S., Gelbart, W. M., Glasser, K., Glodek, A., Gong, F., Gorrell, J. H., Gu, Z., Guan, P., Harris, M., Harris, N. L., Harvey, D., Heiman, T. J., Hernandez, J. R., Houck, J., Hostin, D., Houston, K. A., Howland, T. J., Wei, M. H., Ibegwam, C., Jalali, M., Kalush, F., Karpen, G. H., Ke, Z., Kennison, J. A., Ketchum, K. A., Kimmel, B. E., Kodira, C. D., Kraft, C., Kravitz, S., Kulp, D., Lai, Z., Lasko, P., Lei, Y., Levitsky, A. A., Li, J., Li, Z., Liang, Y., Lin, X., Liu, X., Mattei, B., McIntosh, T. C., McLeod, M. P., McPherson, D., Merkulov, G., Milshina, N. V., Mobarry, C., Morris, J., Moshrefi, A., Mount, S. M., Moy, M., Murphy, B., Murphy, L., Muzny, D. M., Nelson, D. L., Nelson, D. R., Nelson, K. A., Nixon, K., Nusskern, D. R., Pacleb, J. M., Palazzolo, M., Pittman, G. S., Pan, S., Pollard, J., Puri, V., Reese, M. G., Reinert, K., Remington, K., Saunders, R. D., Scheeler, F., Shen, H., Shue, B. C., Siden-Kiamos, I., Simpson, M., Skupski, M. P., Smith, T., Spier, E., Spradling, A. C., Stapleton, M., Strong, R., Sun, E., Svirskas, R., Tector, C., Turner, R., Venter, E., Wang, A. H., Wang, X., Wang, Z. Y., Wassarman, D. A., Weinstock, G. M., Weissenbach, J., Williams, S. M., WoodageT, Worley, K. C., Wu, D., Yang, S., Yao, Q. A., Ye, J., Yeh, R. F., Zaveri, J. S., Zhan, M., Zhang, G., Zhao, Q., Zheng, L., Zheng, X. H., Zhong, F. N., Zhong, W., Zhou, X., Zhu, S., Zhu, X., Smith, H. O., Gibbs, R. A., Myers, E. W., Rubin, G. M. and Venter, J. C. (2000). "The genome sequence of Drosophila melanogaster." Science **287**(5461): 2185-95.

Akassoglou, K., Malester, B., Xu, J., Tessarollo, L., Rosenbluth, J. and Chao, M. V. (2004). "Brain-specific deletion of neuropathy target esterase/swisscheese results in neurodegeneration." Proc Natl Acad Sci U S A **101**(14): 5075-80.

Allan, D. (2000). "Lipid metabolic changes caused by short-chain ceramides and the connection with apoptosis." Biochem J **345 Pt 3**: 603-10.

Ashburner, M. (1989). Drosophila- Laboratory Manual, Cold Spring Harbor Laboratory Press.

Atkins, J. and Glynn, P. (2000). "Membrane association of and critical residues in the catalytic domain of human neuropathy target esterase." J Biol Chem **275**(32): 24477-83.

Ausubel, F. M., Brent, R., Kingston, R. E., Moore, D. D., Seidman, J. G. and Struhl, K. (1988). Current Protocols in Molecular Biology, Wiley.

Avila, J., Ulloa, L., Diez-Guerra, J. and Diaz-Nido, J. (1994). "Role of phosphorylated MAPlB in neuritogenesis." Cell Biol Int **18**(5): 309-14.

Bettencourt da Cruz, A., Schwarzel, M., Schulze, S., Niyyati, M., Heisenberg, M. and Kretzschmar, D. (2005). "Disruption of the MAP1B-related protein FUTSCH leads to changes in the neuronal cytoskeleton, axonal transport defects, and progressive neurodegeneration in Drosophila." Mol Biol Cell **16**(5): 2433-42.

Bilen, J. and Bonini, N. M. (2005). "Drosophila as a model for human neurodegenerative disease." Annu Rev Genet **39**: 153-71.

Billah, M. M. and Anthes, J. C. (1990). "The regulation and cellular functions of phosphatidylcholine hydrolysis." Biochem J **269**(2): 281-91.

Bouquet, C., Soares, S., von Boxberg, Y., Ravaille-Veron, M., Propst, F. and Nothias, F. (2004). "Microtubule-associated protein 1B controls directionality of growth cone migration and axonal branching in regeneration of adult dorsal root ganglia neurons." J Neurosci **24**(32): 7204-13.

Brand, A. H. and Perrimon, N. (1993). "Targeted gene expression as a means of altering cell fates and generating dominant phenotypes." Development **118**(2): 401-15.

Brandt, R. (2001). "Cytoskeletal mechanisms of neuronal degeneration." Cell Tissue Res **305**(2): 255-65.

Brown, R. C., Lockwood, A. H. and Sonawane, B. R. (2005). "Neurodegenerative diseases: an overview of environmental risk factors." Environ Health Perspect **113**(9): 1250-6.

Cavanagh, J. B. (1954). "The toxic effects of triortho-cresyl phosphate on the nervous system; an experimental study in hens." J Neurol Neurosurg Psychiatry **17**(3): 163-72.

Cavanagh, J. B. and Patangia, G. N. (1965). "Changes in the Central Nervous System in the Cat as the Result of Tri-O-Cresyl Phosphate Poisoning." Brain **88**: 165-80.

Collet, X., Francone, O., Besnard, F. and Fielding, C. J. (1999). "Secretion of lecithin:cholesterol acyltransferase by brain neuroglial cell lines." Biochem Biophys Res Commun **258**(1): 73-6.

Cui, Z. and Houweling, M. (2002). "Phosphatidylcholine and cell death." Biochim Biophys Acta **1585**(2-3): 87-96.

Davis, C. S. and Richardson, R. J. (1987). "Neurotoxic esterase: characterization of the solubilized enzyme and the conditions for its solubilization from chicken brain microsomal membranes with ionic, zwitterionic, or nonionic detergents." Biochem Pharmacol **36**(9): 1393-9.

De Jonghe, P., Mersivanova, I., Nelis, E., Del Favero, J., Martin, J. J., Van Broeckhoven, C., Evgrafov, O. and Timmerman, V. (2001). "Further evidence that neurofilament light chain gene mutations can cause Charcot-Marie-Tooth disease type 2E." Ann Neurol **49**(2): 245-9.

Ding, J., Liu, J. J., Kowal, A. S., Nardine, T., Bhattacharya, P., Lee, A. and Yang, Y. (2002). "Microtubule-associated protein 1B: a neuronal binding partner for gigaxonin." J Cell Biol **158**(3): 427-33.

DiTella, M. C., Feiguin, F., Carri, N., Kosik, K. S. and Caceres, A. (1996). "MAP-1B/TAU functional redundancy during laminin-enhanced axonal growth." J Cell Sci **109 (Pt 2)**: 467-77.

Edelmann, W., Zervas, M., Costello, P., Roback, L., Fischer, I., Hammarback, J. A., Cowan, N., Davies, P., Wainer, B. and Kucherlapati, R. (1996). "Neuronal abnormalities in microtubule-associated protein 1B mutant mice." Proc Natl Acad Sci U S A **93**(3): 1270-5.

Exton, J. H. (1994). "Phosphatidylcholine breakdown and signal transduction." Biochim Biophys Acta **1212**(1): 26-42.

Figlewicz, D. A., Krizus, A., Martinoli, M. G., Meininger, V., Dib, M., Rouleau, G. A. and Julien, J. P. (1994). "Variants of the heavy neurofilament subunit are associated with the development of amyotrophic lateral sclerosis." Hum Mol Genet **3**(10): 1757-61.

Foster, N. L., Wilhelmsen, K., Sima, A. A., Jones, M. Z., D'Amato, C. J. and Gilman, S. (1997). "Frontotemporal dementia and parkinsonism linked to chromosome 17: a consensus conference. Conference Participants." Ann Neurol **41**(6): 706-15.

Glynn, P. (1997). "Neuropathy target esterase (NTE): molecular characterisation and cellular localisation." Arch Toxicol Suppl **19**: 325-9.

Glynn, P. (2000). "Neural development and neurodegeneration: two faces of neuropathy target esterase." Prog Neurobiol **61**(1): 61-74.

Glynn, P. (2005). "Neuropathy target esterase and phospholipid deacylation." Biochim Biophys Acta **1736**(2): 87-93.

Glynn, P., Read, D. J., Lush, M. J., Li, Y. and Atkins, J. (1999). "Molecular cloning of neuropathy target esterase (NTE)." Chem Biol Interact **119-120**: 513-7.

Gonzalez-Billault, C., Avila, J. and Caceres, A. (2001). "Evidence for the role of MAP1B in axon formation." Mol Biol Cell **12**(7): 2087-98.

Gonzalez-Billault, C., Demandt, E., Wandosell, F., Torres, M., Bonaldo, P., Stoykova, A., Chowdhury, K., Gruss, P., Avila, J. and Sanchez, M. P. (2000). "Perinatal lethality of microtubule-associated protein 1B-deficient mice expressing alternative isoforms of the protein at low levels." Mol Cell Neurosci **16**(4): 408-21.

Gonzalez-Billault, C., Jimenez-Mateos, E. M., Caceres, A., Diaz-Nido, J., Wandosell, F. and Avila, J. (2004). "Microtubule-associated protein 1B function during normal development, regeneration, and pathological conditions in the nervous system." J Neurobiol **58**(1): 48-59.

Guo, A., Li, L., Xia, S. Z., Feng, C. H., Wolf, R. and Heisenberg, M. (1996). "Conditioned visual flight orientation in Drosophila: dependence on age, practice, and diet." Learn Mem **3**(1): 49-59.

Hammarback, J. A., Obar, R. A., Hughes, S. M. and Vallee, R. B. (1991). "MAP1B is encoded as a polyprotein that is processed to form a complex N-terminal microtubule-binding domain." Neuron **7**(1): 129-39.

Harada, A., Oguchi, K., Okabe, S., Kuno, J., Terada, S., Ohshima, T., Sato-Yoshitake, R., Takei, Y., Noda, T. and Hirokawa, N. (1994). "Altered microtubule organization in small-calibre axons of mice lacking tau protein." Nature **369**(6480): 488-91.

Hasan, G. (1990). "Molecular cloning of an olfactory gene from Drosophila melanogaster." Proc Natl Acad Sci U S A **87**(22): 9037-41.

Hawkes, C. (2003). "Olfaction in neurodegenerative disorder." Mov Disord **18**(4): 364-72.

Heidary, G. and Fortini, M. E. (2001). "Identification and characterization of the Drosophila tau homolog." Mech Dev **108**(1-2): 171-8.

Heisenberg, M. (2003). "Mushroom body memoir: from maps to models." Nat Rev Neurosci **4**(4): 266-75.

Heisenberg, M. and Böhl, K. (1979). "Isolation of anatomical brain mutants of Drosophila by histological means." Z Naturforsch **C**(34): 143-147.

Herberg, F. W., Dostmann, W. R., Zorn, M., Davis, S. J. and Taylor, S. S. (1994). "Crosstalk between domains in the regulatory subunit of cAMP-dependent protein kinase: influence of amino terminus on cAMP binding and holoenzyme formation." Biochemistry **33**(23): 7485-94.

Himmler, A. (1989). "Structure of the bovine tau gene: alternatively spliced transcripts generate a protein family." Mol Cell Biol **9**(4): 1389-96.

Hofmann, K. and Stoffel, W. (1993). "TMbase- A database of membrane spanning protein segmens." Biol. Chem. Hoppe Seyler **34**: 166.

Hummel, T., Krukkert, K., Roos, J., Davis, G. and Klambt, C. (2000). "Drosophila Futsch/22C10 is a MAP1B-like protein required for dendritic and axonal development." Neuron **26**(2): 357-70.

Hutton, M., Lendon, C. L., Rizzu, P., Baker, M., Froelich, S., Houlden, H., Pickering-Brown, S., Chakraverty, S., Isaacs, A., Grover, A., Hackett, J., Adamson, J., Lincoln, S., Dickson, D., Davies, P., Petersen, R. C., Stevens, M., de Graaff, E., Wauters, E., van Baren, J., Hillebrand, M., Joosse, M., Kwon, J. M., Nowotny, P., Che, L. K., Norton, J., Morris, J. C., Reed, L. A., Trojanowski, J., Basun, H., Lannfelt, L., Neystat, M., Fahn, S., Dark, F., Tannenberg, T., Dodd, P. R., Hayward, N., Kwok, J. B., Schofield, P. R., Andreadis, A., Snowden, J., Craufurd, D., Neary, D., Owen, F., Oostra, B. A., Hardy, J., Goate, A., van Swieten, J., Mann, D., Lynch, T. and Heutink, P. (1998). "Association of missense and 5'-splice-site mutations in tau with the inherited dementia FTDP-17." Nature **393**(6686): 702-5.

Jackowski, S., Wang, J. and Baburina, I. (2000). "Activity of the phosphatidylcholine biosynthetic pathway modulates the distribution of fatty acids into glycerolipids in proliferating cells." Biochim Biophys Acta **1483**(3): 301-15.

Jackson, G. R., Wiedau-Pazos, M., Sang, T. K., Wagle, N., Brown, C. A., Massachi, S. and Geschwind, D. H. (2002). "Human wild-type tau interacts with wingless pathway components and produces neurofibrillary pathology in Drosophila." Neuron **34**(4): 509-19.

Jamal, G. A. (1997). "Neurological syndromes of organophosphorus compounds." Adverse Drug React Toxicol Rev **16**(3): 133-70.

Jin, P. and Warren, S. T. (2003). "New insights into fragile X syndrome: from molecules to neurobehaviors." Trends Biochem Sci **28**(3): 152-8.

Johnson, M. K. (1969). "The delayed neurotoxic effect of some organophosphorus compounds. Identification of the phosphorylation site as an esterase." Biochem J **114**(4): 711-7.

Johnson, M. K. (1977). "Improved assay of neurotoxic esterase for screening organophosphates for delayed neurotoxicity potential." Arch Toxicol **37**(2): 113-5.

Johnson, M. K. (1982). "Initiation of organophosphate-induced delayed neuropathy." Neurobehav Toxicol Teratol **4**(6): 759-65.

Johnson, M. K. and Richardson, R. J. (1983). "Biochemical endpoints: neurotoxic esterase assay." Neurotoxicology **4**(2): 311-20.

Jonas, A. (2000). "Lecithin cholesterol acyltransferase." Biochim Biophys Acta **1529**(1-3): 245-56.

Kellogg, D. R., Oegema, K., Raff, J., Schneider, K. and Alberts, B. M. (1995). "CP60: a microtubule-associated protein that is localized to the centrosome in a cell cycle-specific manner." Mol Biol Cell **6**(12): 1673-84.

Kirschner, M. and Mitchison, T. (1986a). "Beyond self-assembly: from microtubules to morphogenesis." Cell **45**(3): 329-42.

Kirschner, M. W. and Mitchison, T. (1986b). "Microtubule dynamics." Nature **324**(6098): 621.

Klein, J. (2000). "Membrane breakdown in acute and chronic neurodegeneration: focus on choline-containing phospholipids." J Neural Transm **107**(8-9): 1027-63.

Kovacs, T., Cairns, N. J. and Lantos, P. L. (1999). "beta-amyloid deposition and neurofibrillary tangle formation in the olfactory bulb in ageing and Alzheimer's disease." Neuropathol Appl Neurobiol **25**(6): 481-91.

Kovacs, T., Cairns, N. J. and Lantos, P. L. (2001). "Olfactory centres in Alzheimer's disease: olfactory bulb is involved in early Braak's stages." Neuroreport **12**(2): 285-8.

Kretzschmar, D., Hasan, G., Sharma, S., Heisenberg, M. and Benzer, S. (1997). "The swiss cheese mutant causes glial hyperwrapping and brain degeneration in Drosophila." J Neurosci **17**(19): 7425-32.

Kropp, T. J., Glynn, P. and Richardson, R. J. (2004). "The mipafox-inhibited catalytic domain of human neuropathy target esterase ages by reversible proton loss." Biochemistry **43**(12): 3716-22.

Kutschera, W., Zauner, W., Wiche, G. and Propst, F. (1998). "The mouse and rat MAP1B genes: genomic organization and alternative transcription." Genomics **49**(3): 430-6.

Kuznetsov, S. A., Rodionov, V. I., Nadezhdina, E. S., Murphy, D. B. and Gelfand, V. I. (1986). "Identification of a 34-kD polypeptide as a light chain of microtubule-associated protein-1 (MAP-1) and its association with a MAP-1 peptide that binds to microtubules." J Cell Biol **102**(3): 1060-6.

Lane, M. E. and Kalderon, D. (1993). "Genetic investigation of cAMP-dependent protein kinase function in Drosophila development." Genes Dev **7**(7A): 1229-43.

Li, Y., Dinsdale, D. and Glynn, P. (2003). "Protein domains, catalytic activity, and subcellular distribution of neuropathy target esterase in Mammalian cells." J Biol Chem **278**(10): 8820-5.

Lindsley, D. L. and Zimm, G. G. (1992). The genome of Drosophila melanogaster, Academic Press.

Lush, M. J., Li, Y., Read, D. J., Willis, A. C. and Glynn, P. (1998). "Neuropathy target esterase and a homologous Drosophila neurodegeneration-associated mutant protein contain a novel domain conserved from bacteria to man." Biochem J **332 (Pt 1)**: 1-4.

Maleszka, R., de Couet, H. G. and Miklos, G. L. (1998). "Data transferability from model organisms to human beings: insights from the functional genomics of the flightless region of Drosophila." Proc Natl Acad Sci U S A **95**(7): 3731-6.

Mann, S. S. and Hammarback, J. A. (1994). "Molecular characterization of light chain 3. A microtubule binding subunit of MAP1A and MAP1B." J Biol Chem **269**(15): 11492-7.

Marin, E. C., Jefferis, G. S., Komiyama, T., Zhu, H. and Luo, L. (2002). "Representation of the glomerular olfactory map in the Drosophila brain." Cell **109**(2): 243-55.

Matthews, K. A., Kaufman, T. C. and Gelbart, W. M. (2005). "Research resources for Drosophila: the expanding universe." Nat Rev Genet **6**(3): 179-93.

McDaniel, M. A., Maier, S. F. and Einstein, G. O. (2003). ""Brain-specific" nutrients: a memory cure?" Nutrition **19**(11-12): 957-75.

McDowell, I. (2001). "Alzheimer's disease: insights from epidemiology." Aging (Milano) **13**(3): 143-62.

Meek, P. D., McKeithan, K. and Schumock, G. T. (1998). "Economic considerations in Alzheimer's disease." Pharmacotherapy **18**(2 Pt 2): 68-73; discussion 79-82.

Meixner, A., Haverkamp, S., Wassle, H., Fuhrer, S., Thalhammer, J., Kropf, N., Bittner, R. E., Lassmann, H., Wiche, G. and Propst, F. (2000). "MAP1B is required for axon guidance and Is involved in the development of the central and peripheral nervous system." J Cell Biol **151**(6): 1169-78.

Melendez, A., Li, W. and Kalderon, D. (1995). "Activity, expression and function of a second Drosophila protein kinase A catalytic subunit gene." Genetics **141**(4): 1507-20.

Mersiyanova, I. V., Perepelov, A. V., Polyakov, A. V., Sitnikov, V. F., Dadali, E. L., Oparin, R. B., Petrin, A. N. and Evgrafov, O. V. (2000). "A new variant of Charcot-Marie-Tooth disease type 2 is probably the result of a mutation in the neurofilament-light gene." Am J Hum Genet **67**(1): 37-46.

Miklos, G. L., Yamamoto, M., Burns, R. G. and Maleszka, R. (1997). "An essential cell division gene of Drosophila, absent from Saccharomyces, encodes an unusual protein with tubulin-like and myosin-like peptide motifs." Proc Natl Acad Sci U S A **94**(10): 5189-94.

Morales, J., Hiesinger, P. R., Schroeder, A. J., Kume, K., Verstreken, P., Jackson, F. R., Nelson, D. L. and Hassan, B. A. (2002). "Drosophila fragile X protein, DFXR, regulates neuronal morphology and function in the brain." Neuron **34**(6): 961-72.

Moser, M., Li, Y., Vaupel, K., Kretzschmar, D., Kluge, R., Glynn, P. and Buettner, R. (2004). "Placental failure and impaired vasculogenesis result in embryonic lethality for neuropathy target esterase-deficient mice." Mol Cell Biol **24**(4): 1667-79.

Moser, M., Stempfl, T., Li, Y., Glynn, P., Buttner, R. and Kretzschmar, D. (2000). "Cloning and expression of the murine sws/NTE gene." Mech Dev **90**(2): 279-82.

Muhlig-Versen, M. (2001). Histologische und funktionelle Untersuchung des swiss-chesse-Proteins und seines Orthologs aus Vertebraten in transgenen Drosophila melanogaster. Naturwissenschaftliche Fakultät III- Biologie und vorklinische Medizin. Regensburg, Universität Regensburg.

Muhlig-Versen, M., da Cruz, A. B., Tschape, J. A., Moser, M., Buttner, R., Athenstaedt, K., Glynn, P. and Kretzschmar, D. (2005). "Loss of Swiss cheese/neuropathy target esterase activity causes disruption of phosphatidylcholine homeostasis and neuronal and glial death in adult Drosophila." J Neurosci **25**(11): 2865-73.

Myers, E. W., Sutton, G. G., Delcher, A. L., Dew, I. M., Fasulo, D. P., Flanigan, M. J., Kravitz, S. A., Mobarry, C. M., Reinert, K. H., Remington, K. A., Anson, E. L., Bolanos, R. A., Chou, H. H., Jordan, C. M., Halpern, A. L., Lonardi, S., Beasley, E. M., Brandon, R. C., Chen, L., Dunn, P. J., Lai, Z., Liang, Y., Nusskern, D. R., Zhan, M., Zhang, Q., Zheng, X., Rubin, G. M., Adams, M. D. and Venter, J. C. (2000). "A whole-genome assembly of Drosophila." Science **287**(5461): 2196-204.

O`Kane, C. J. and in: Roberts, D. B. (1998). Drosophila: A practical approach. New York, Oxford university press.

Pereira, A., Doshen, J., Tanaka, E. and Goldstein, L. S. (1992). "Genetic analysis of a Drosophila microtubule-associated protein." J Cell Biol **116**(2): 377-83.

Petroianu, G., Hardt, F., Toomes, M., Bergler, W. and Rufer, R. (2001). "High-dose intravenous paraoxon exposure does not cause organophosphate-induced delayed neuropathy (OPIDN) in mini pigs." J Appl Toxicol **21**(4): 263-8.

Poorkaj, P., Bird, T. D., Wijsman, E., Nemens, E., Garruto, R. M., Anderson, L., Andreadis, A., Wiederholt, W. C., Raskind, M. and Schellenberg, G. D. (1998). "Tau is a candidate gene for chromosome 17 frontotemporal dementia." Ann Neurol **43**(6): 815-25.

Pope, C. N. and Padilla, S. (1989). "Modulation of neurotoxic esterase activity in vitro by phospholipids." Toxicol Appl Pharmacol **97**(2): 272-8.

Poteet-Smith, C. E., Shabb, J. B., Francis, S. H. and Corbin, J. D. (1997). "Identification of critical determinants for autoinhibition in the pseudosubstrate region of type I alpha cAMP-dependent protein kinase." J Biol Chem **272**(1): 379-88.

Robertson, H. M., Preston, C. R., Phillis, R. W., Johnson-Schlitz, D. M., Benz, W. K. and Engels, W. R. (1988). "A stable genomic source of P element transposase in Drosophila melanogaster." Genetics **118**(3): 461-70.

Roos, J., Hummel, T., Ng, N., Klambt, C. and Davis, G. W. (2000). "Drosophila Futsch regulates synaptic microtubule organization and is necessary for synaptic growth." Neuron **26**(2): 371-82.

Ross, C. A. (2002). "Polyglutamine pathogenesis: emergence of unifying mechanisms for Huntington's disease and related disorders." Neuron **35**(5): 819-22.

Rubin, G. M., Yandell, M. D., Wortman, J. R., Gabor Miklos, G. L., Nelson, C. R., Hariharan, I. K., Fortini, M. E., Li, P. W., Apweiler, R., Fleischmann, W., Cherry, J. M., Henikoff, S., Skupski, M. P., Misra, S., Ashburner, M., Birney, E., Boguski, M. S., Brody, T., Brokstein, P., Celniker, S. E., Chervitz, S. A., Coates, D., Cravchik, A., Gabrielian, A., Galle, R. F., Gelbart, W. M., George, R. A., Goldstein, L. S., Gong, F., Guan, P., Harris, N. L., Hay, B. A., Hoskins, R. A., Li, J., Li, Z., Hynes, R. O., Jones, S. J., Kuehl, P. M., Lemaitre, B., Littleton, J. T., Morrison, D. K., Mungall, C., O'Farrell, P. H., Pickeral, O. K., Shue, C., Vosshall, L. B., Zhang, J., Zhao, Q., Zheng, X. H. and Lewis, S. (2000). "Comparative genomics of the eukaryotes." Science **287**(5461): 2204-15.

Ruffer-Turner, M. E., Read, D. J. and Johnson, M. K. (1992). "Purification of neuropathy target esterase from avian brain after prelabelling with [3H]diisopropyl phosphorofluoridate." J Neurochem **58**(1): 135-41.

Schenck, A., Van de Bor, V., Bardoni, B. and Giangrande, A. (2002). "Novel features of dFMR1, the Drosophila orthologue of the fragile X mental retardation protein." Neurobiol Dis **11**(1): 53-63.

Segel, L. (2002). "Ginger Jake blues." The Medical Post **38**(34).

Selkoe, D. J. (2001). "Alzheimer's disease: genes, proteins, and therapy." Physiol Rev **81**(2): 741-66.

Senanayake, N. (1981). "Tri-cresyl phosphate neuropathy in Sri Lanka: a clinical and neurophysiological study with a three year follow up." J Neurol Neurosurg Psychiatry **44**(9): 775-80.

Smith, H. V. and Spalding, J. M. (1959). "Outbreak of paralysis in Morocco due to ortho-cresyl phosphate poisoning." Lancet **2**: 1019-21.

Smith, M. I., Elove, E. and Frazier, W. H. (1930). "The pharmacological action of certain phenol esters with special reference to the etiology of the so-called Ginger paralysis." Public Health Rep **45**(2509-2524).

Soderberg, M., Edlund, C., Alafuzoff, I., Kristensson, K. and Dallner, G. (1992). "Lipid composition in different regions of the brain in Alzheimer's disease/senile dementia of Alzheimer's type." J Neurochem **59**(5): 1646-53.

Spillantini, M. G., Murrell, J. R., Goedert, M., Farlow, M. R., Klug, A. and Ghetti, B. (1998). "Mutation in the tau gene in familial multiple system tauopathy with presenile dementia." Proc Natl Acad Sci U S A **95**(13): 7737-41.

Stocker, R. F., Heimbeck, G., Gendre, N. and de Belle, J. S. (1997). "Neuroblast ablation in Drosophila P[GAL4] lines reveals origins of olfactory interneurons." J Neurobiol **32**(5): 443-56.

Takei, Y., Kondo, S., Harada, A., Inomata, S., Noda, T. and Hirokawa, N. (1997). "Delayed development of nervous system in mice homozygous for disrupted microtubule-associated protein 1B (MAP1B) gene." J Cell Biol **137**(7): 1615-26.

Takei, Y., Teng, J., Harada, A. and Hirokawa, N. (2000). "Defects in axonal elongation and neuronal migration in mice with disrupted tau and map1b genes." J Cell Biol **150**(5): 989-1000.

Taylor, S. S., Buechler, J. A. and Yonemoto, W. (1990). "cAMP-dependent protein kinase: framework for a diverse family of regulatory enzymes." Annu Rev Biochem **59**: 971-1005.

Teng, J., Takei, Y., Harada, A., Nakata, T., Chen, J. and Hirokawa, N. (2001). "Synergistic effects of MAP2 and MAP1B knockout in neuronal migration, dendritic outgrowth, and microtubule organization." J Cell Biol **155**(1): 65-76.

Tobin, A. J. and Signer, E. R. (2000). "Huntington's disease: the challenge for cell biologists." Trends Cell Biol **10**(12): 531-6.

Triebig, G. (1990). "[Toxic encephalopathy as an occupational disease]." Dtsch Med Wochenschr **115**(34): 1287-90.

Tucker, R. P., Binder, L. I. and Matus, A. I. (1988). "Neuronal microtubule-associated proteins in the embryonic avian spinal cord." J Comp Neurol **271**(1): 44-55.

Tucker, R. P., Garner, C. C. and Matus, A. (1989). "In situ localization of microtubule-associated protein mRNA in the developing and adult rat brain." Neuron **2**(3): 1245-56.

Ulloa, L., Ibarrola, N., Avila, J. and Diez-Guerra, F. J. (1994). "Microtubule-associated protein 1B (MAP1B) is present in glial cells phosphorylated different than in neurones." Glia **10**(4): 266-75.

van der Sanden, M. H., Houweling, M., van Golde, L. M. and Vaandrager, A. B. (2003). "Inhibition of phosphatidylcholine synthesis induces expression of the endoplasmic reticulum stress and apoptosis-related protein CCAAT/enhancer-binding protein-homologous protein (CHOP/GADD153)." Biochem J **369**(Pt 3): 643-50.

van Tienhoven, M., Atkins, J., Li, Y. and Glynn, P. (2002). "Human neuropathy target esterase catalyzes hydrolysis of membrane lipids." J Biol Chem **277**(23): 20942-8.

Viereck, C., Tucker, R. P. and Matus, A. (1989). "The adult rat olfactory system expresses microtubule-associated proteins found in the developing brain." J Neurosci **9**(10): 3547-57.

Wan, L., Dockendorff, T. C., Jongens, T. A. and Dreyfuss, G. (2000). "Characterization of dFMR1, a Drosophila melanogaster homolog of the fragile X mental retardation protein." Mol Cell Biol **20**(22): 8536-47.

Williams, D. G. (1983). "Intramolecular group transfer is a characteristic of neurotoxic esterase and is independent of the tissue source of the enzyme. A comparison of the aging behaviour of di-isopropyl phosphorofluoridate-labelled proteins in brain, spinal cord, liver, kidney and spleen from hen and in human placenta." Biochem J **209**(3): 817-29.

Williams, D. W., Tyrer, M. and Shepherd, D. (2000). "Tau and tau reporters disrupt central projections of sensory neurons in Drosophila." J Comp Neurol **428**(4): 630-40.

Winrow, C. J., Hemming, M. L., Allen, D. M., Quistad, G. B., Casida, J. E. and Barlow, C. (2003). "Loss of neuropathy target esterase in mice links organophosphate exposure to hyperactivity." Nat Genet **33**(4): 477-85.

Wittmann, C. W., Wszolek, M. F., Shulman, J. M., Salvaterra, P. M., Lewis, J., Hutton, M. and Feany, M. B. (2001). "Tauopathy in Drosophila: neurodegeneration without neurofibrillary tangles." Science **293**(5530): 711-4.

Wright, M. M., Howe, A. G. and Zaremberg, V. (2004). "Cell membranes and apoptosis: role of cardiolipin, phosphatidylcholine, and anticancer lipid analogues." Biochem Cell Biol **82**(1): 18-26.

Xie, Z., Fang, M. and Bankaitis, V. A. (2001). "Evidence for an intrinsic toxicity of phosphatidylcholine to Sec14p-dependent protein transport from the yeast Golgi complex." Mol Biol Cell **12**(4): 1117-29.

Xiong, W. C., Okano, H., Patel, N. H., Blendy, J. A. and Montell, C. (1994). "repo encodes a glial-specific homeo domain protein required in the Drosophila nervous system." Genes Dev **8**(8): 981-94.

Zaccheo, O., Dinsdale, D., Meacock, P. A. and Glynn, P. (2004). "Neuropathy target esterase and its yeast homologue degrade phosphatidylcholine to glycerophosphocholine in living cells." J Biol Chem **279**(23): 24024-33.

Zhang, Y. Q., Bailey, A. M., Matthies, H. J., Renden, R. B., Smith, M. A., Speese, S. D., Rubin, G. M. and Broadie, K. (2001). "Drosophila fragile X-related gene regulates the MAP1B homolog Futsch to control synaptic structure and function." Cell **107**(5): 591-603.

Figures

Figure 1: *sws* mutant phenotype ... 13
Figure 2: Reaction mechanism of serine esterases ... 18
Figure 3: Alternative mechanisms for the aging reaction ... 19
Figure 4: SWS protein with the designated fusion protein fragment ... 32
Figure 5: α-SWS antibody staining on SWS overexpressing flies ... 33
Figure 6: Western blot of *sws* overexpressing, wild-type and sws deficient flies ... 35
Figure 7: Expression pattern of DSWS ... 36
Figure 8: Vesicles in higher magnification α-SWS stainings ... 37
Figure 9: Double staining with α-SWS and ER-marker ... 38
Figure 10: Diagram of the CytoTrap system ... 39
Figure 11: Fragments used as yeast two hybrid bait ... 40
Figure 12: SWS proteins with potential functional domains ... 44
Figure 13: Neurodegeneration in *sws* mutant flies and rescue of *sws* phenotype ... 45
Figure 14: GMR-GAL4 control flies ... 46
Figure 15: Amino acid line-up of SWS and PKA-RI ... 47
Figure 16: GMR overexpression of SWS-R^{133}A (protein interaction domain mutant) ... 49
Figure 17: GMR overexpression of SWS-G^{557}Q (cAMP binding domain mutant) ... 50
Figure 18: Ectopic expression of wt and mutated SWS in the eye ... 52
Figure 19: α-SWS stainings on different, overexpressed SWS constructs ... 53
Figure 20: GMR overexpression of SWSΔ1-80/ S^{985}D ... 55
Figure 21: Map of the SWS Protein and all mutated constructs ... 56
Figure 22: GMR overexpression of SWSΔ33-55 ... 58
Figure 23: GMR overexpression of SWSΔ33-55/ S^{985}D ... 59
Figure 24: Different lipid content in *sws* deficient and *sws* overexpressing flies ... 61
Figure 25: Reaction mechanism of LCAT ... 62
Figure 26: Fiber structure defects visible in silver stainings ... 64
Figure 27: Anatomical phenotype of the *olk* mutant ... 65
Figure 28: Necrotic cell death in *olk* ... 66
Figure 29: Degeneration of projection neurons ... 68
Figure 30: Olfactory learning in *olk* mutants ... 70
Figure 31: Mapping of *olk* to the *futsch* locus ... 71
Figure 32: Western blot of *olk* mutants ... 72
Figure 33: Differing tubulin organization in *olk* mutants ... 74
Figure 34: Antennal lobes of olk^1 show disorganized microtubule in electron microscopy ... 74
Figure 35: Enhanced tubulin levels in olk^1 mutant ... 75
Figure 36: Mitochondrial transport ... 76
Figure 37: Expression pattern of Futsch ... 77
Figure 38: Interaction of *olk* with *dfmr1* ... 79
Figure 39: Interaction with *tau* ... 80
Figure 40: Model for cAMP influence on SWS ... 82

Abbreviations

aa	Amino acid
AChE	Acetylcholine esterase
cAMP	Cyclic adenosine mono-phosphate
d	Day
dfmr1	*Drosophila fragile X mental retardation*
EM	Electron microscopy
ER	Endoplasmic reticulum
GFP	Green fluorescent protein
GroPCho	Glycerophosphocholine
LC	Light chain
LCAT	Lecithin cholesterol acyl-transferase
MAP	Microtubule associated protein
NTE	Neuropathy target esterase
olk	*omb-like*
OP	Organophosphate
OPIDN	Organophosphate induced delayed neuropathy
PI	Performance index
pka-c3	*Protein kinase A, catalytic subunit 3*
PN	Projection neuron
PtdCho	Phosphatidylcholine
PtdEtn	Phosphatidyl-ethanolamine
PV	Phenyl valerate
SE	Sterol ester
sws	*swiss cheese*
TAG	Triacylglycerol
TM	Transmembrane domain
TOCP	Tri-ortho-crescyl-phosphate
UAS	Upstream activating sequence
wt	Wild-type

Acknowledgement

Like in many acknowledgements of dissertations I would like to thank my advisor, Doris Kretzschmar, for excellent scientific guidance, fruitful discussions and enthusiasm for my work as well as for the very friendly and uncomplicated way of transmitting scientific and unscientific knowledge. Unlike in many dissertations in my case the mentioned merits are actually real!!!

Many thanks to Erich Buchner who did not hesitate a second, to be my "Doktorvater" in Würzburg and to assure me that it would be no problem to do my lab work in Portland.

Also to Martin Heisenberg for cooperation on my first paper and the good scientific atmosphere in his lab, were we started out before moving to Portland.

The Kretzschmar lab has always provided a friendly and scientifically stimulating environment, I would like to specially mention Laura for help with countless head sections and Thomas for his microscopy expertise. Also a hearty meh to Sarah (M-E-H: Meh!) and a thumbs up to Simone, who both produced excellent results in their short internships.

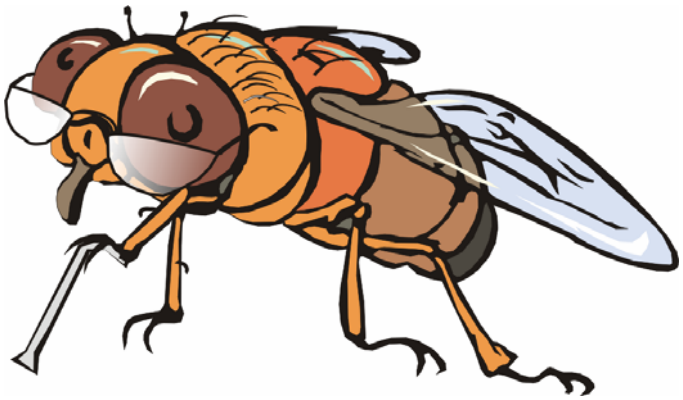

A special honorable mention to Jill, the upcoming star in the *sws* field, not only for good work and having the courage to be the first to read and improve this thesis, but specially for a good friendship despite occasional turmoil.

Martin, thanks for collaboration on my paper, exciting rowing lessons on last minute avoidance of towboats and many good conversations about science, the United States and lots of other topics.

Many thanks to my new friends outside of science in Würzburg and Portland who made life enjoyable in the two new environments. Specially Jason, Jenny, Catherine, Anna, Christine, Angie, Gudrun, Chris & Heather, Sandra and Lara.

To my old friends Christian, Milos, Carla, Pedro, Max, Sonja and Stephan thanks for keeping up contact throughout space and time.

Thank you very much, Sinje, for ongoing efforts to keep me sane, specially during this time, with a continent, an ocean and most of old Europe in between….

Last but not least special thanks to my family, who made it possible for me to pursue the career of my choice.

List of publications

Publications relevant to this thesis

Bettencourt da Cruz, A., Schwarzel, M., Schulze, S., Niyyati, M., Heisenberg, M. and Kretzschmar, D. (2005). "Disruption of the MAP1B-related protein Futsch leads to changes in the neuronal cytoskeleton, axonal transport defects, and progressive neurodegeneration in *Drosophila*." Mol Biol Cell **16**(5): 2433-42.

Muhlig-Versen, M., **da Cruz, A. B.**, Tschape, J. A., Moser, M., Buttner, R., Athenstaedt, K., Glynn, P. and Kretzschmar, D. (2005). "Loss of Swiss cheese/ neuropathy target esterase activity causes disruption of phosphatidylcholine homeostasis and neuronal and glial death in adult *Drosophila*." J Neurosci **25**(11): 2865-73.

Further publications

Kretzschmar, D., Tschape, J., **Bettencourt da Cruz, A.**, Asan, E., Poeck, B., Strauss, R. and Pflugfelder, G. O. (2005). "Glial and neuronal expression of polyglutamine proteins induce behavioral changes and aggregate formation in *Drosophila*." Glia **49**(1): 59-72.

Tschape, J. A., **Bettencourt da Cruz, A.** and Kretzschmar, D. (2003). "Progressive neurodegeneration in *Drosophila*: a model system." J Neural Transm Suppl(65): 51-62.

Streit, A., Bernasconi, L., Sergeev, P., **Cruz, A.** and Steinmann-Zwicky, M. (2002). "mgm 1, the earliest sex-specific germline marker in *Drosophila*, reflects expression of the gene esg in male stem cells." Int J Dev Biol **46**(1): 159-66.

Alexandre Bettencourt da Cruz

geboren am: 19. August 1975 in München

Schulbesuche

1981-1985	Grundschule in Kümmersbruck
1984-1985	Gregor-Mendel-Gymnasium in Amberg
1985-1993	Deutsche Schule Lissabon
Mai 1993	Abschluss Allgemeine Hochschulreife

Hochschulbesuche

Diplomstudiengang Biologie

1993-1998	Universität Regensburg
1997-1998	Diplomarbeit in der Arbeitsgruppe von Prof. Dr. S. Schneuwly, Lehrstuhl für Entwicklungsbiologie: Molekulare und genetische Analyse der *Vam*-Mutation in *Drosophila melanogaster*
27. 12. 1998:	Abschluss:Diplom Biologe

Promotionsstudium

1999-2001	Universität Zürich, Promotionsstudium
seit 2002	Julius-Maximilians Universität, Würzburg/ Oregon Health & Science university, Portland, Oregon, USA Promotion in der Arbeitsgruppe von Prof. Dr. Kretzschmar

Portland, den 27. Februar 2006

Alexandre B. da Cruz